

**THE REACTIONS OF OZONE WITH COMPOUNDS
RELEVANT TO DRINKING-WATER PROCESSING:
PHENOL AND ITS DERIVATIVES**

A dissertation submitted to the University of Namibia in fulfilment of the requirements
for the degree of Doctor of Philosophy (PhD) in Chemistry

By

Eino Natangwe Mvula

B.Sc.(University of Namibia), B.Sc.(Honours)(University of Cape Town),
M.Sc.(University of Cape Town)

Mülheim an der Ruhr/Leipzig/Windhoek

2002

To my parents

This work was carried out from October 1999 to September 2001 at the Max-Planck Institut für Strahlenchemie in Mülheim an der Ruhr and from November 2001 to June 2002 at the Institut für Oberflächenmodifizierung in Leipzig under the supervision of Prof. Clemens von Sonntag.

I Eino Natangwe Mvula, declare that this dissertation embodies my own work, except where acknowledgement indicates otherwise and that no part of this work has been or is being submitted for any other degree at this or any other University.

ACKNOWLEDGEMENTS

I would like to thank the following people for their valuable help in making this dissertation a success:

Prof. Dr. Clemens von Sonntag, first of all for giving me the opportunity to carry out my work in his research group at **Max-Planck Institut für Strahlenchemie** and at the **Institut für Oberflächenmodifizierung**. I would also like to thank him for excellent supervision, his ability to share his knowledge in ozone and radiation chemistry by means of constructive discussions. From him I have learned a great deal of chemistry. Once more many thanks!

The staff of both the Max-Planck Institut für Strahlenchemie, especially **Ms Ursula Westhof**, and at the Institut für Oberflächenmodifizierung for rendering the analytical services.

My colleagues **Achim Leitzke, Dr. Roman Flyunt, Jacob Theruvathu, Dr. Gertraud Mark**. Special thanks goes to **Achim Leitzke** for assisting with the GC-MS analysis and the stopped-flow apparatus.

I also would express my sincere thanks to **Prof. Dr. Reiner Mehnert** who graciously enabled me to finalise my thesis at the Institut für Oberflächenmodifizierung

The **German Academic Exchange Service (DAAD)** for awarding me the stipend, allowing me to carry out my studies in Germany.

The **University of Namibia** for financial support through the staff development program.

PUBLICATIONS AND CONFERENCES

Published papers:

1. E. Mvula; M. N. Schuchmann; C. von Sonntag, Reactions of phenol-OH-adduct radicals. Phenoxy radical formation by water elimination *vs.* oxidation by dioxygen, *J. Chem. Soc., Perkin Trans. 2*, 2001, 264-268.
2. F. Munoz; E. Mvula; S. E. Braslavsky; C. von Sonntag, Singlet dioxygen formation in the ozone reactions in aqueous solution, *J. Chem. Soc., Perkin Trans. 2*, 2001, 1109-1116.

Papers in preparation:

1. R. Flyunt; G. Mark; E. Mvula; A. Leitzke; R. Schick; E. Reisz; C. von Sonntag, Detection of $\bullet\text{OH}$, $\text{O}_2^{\bullet-}$ and hydroperoxide yields in ozone reactions in aqueous solution.
2. E. Mvula; P. Hörsch; C. von Sonntag, Reactions of ozone with phenols in aqueous solution.
3. J. von Sonntag, E. Mvula, and C. von Sonntag, Photohydration and photoreduction of benzoquinone revisited.

Presentations at Conferences

1. E. Mvula; M. N. Schuchmann and C. von Sonntag, Reactions of phenol with the OH radical and with Ozone in Aqueous Solution. Presented at the Radiation Chemists Meeting (*Strahlenchemiker Treffen*), 15-18 March 2000, Bad Honnef, Germany.
2. E. Mvula; R. Flyunt; A. Leitzke; R. Schick; E. Reisz and C. von Sonntag, Determination of OH radical yields in ozone reactions in aqueous solution. Presented at the Radiation Chemists Meeting (*Strahlenchemiker Treffen*), 17-20 September 2001, Naumburg an der Saale, Germany.

ABSTRACT

Kinetic and mechanistic investigations on the reactions of ozone with phenol and some of its derivatives (hydroquinone, catechol, phloroglucinol, pentachlorophenol, pentabromophenol, 1,2-dimethoxybenzene, 1,4-dimethoxybenzene and 1,3,5-trimethoxybenzene) have been carried out. These compounds were chosen, as they can serve as models for compounds which are abundant in surface waters and wastewater. The scope of the investigation was widened by including dihydrogen sulfide, often a contaminant of ground waters in arid areas, and its organic analogues.

By employing various analytical techniques, such as high performance liquid chromatography (HPLC); ion chromatography (IC); nuclear magnetic resonance spectroscopy (NMR); gas chromatography (GC) and gas chromatography coupled to mass spectroscopy (GC-MS), it was possible to identify and quantify reaction products. The stopped-flow technique was employed to measure rate constants of ozone reactions. When strong substrate absorptions at 240–280 nm prevented the use of this technique, rate constants were measured by competition kinetics. Pulse radiolysis was used for the study of $\bullet\text{OH}$ -induced reactions.

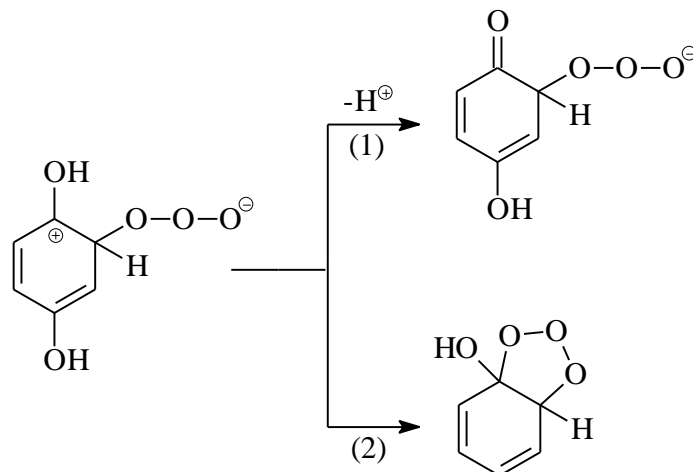
Methods were developed for the detection and quantification of reactive intermediates in ozone reactions such as singlet dioxygen, $\bullet\text{OH}$, $\text{O}_2\bullet^-$ and hydroperoxides. A germanium diode detector was used for the quantification of $\text{O}_2(^1\Delta_g)$ formation. For the detection of $\bullet\text{OH}$ formation, 2-methyl-2-propanol and DMSO were used and tetranitromethane was applied for the detection of $\text{O}_2\bullet^-$.

Based on the products in the reactions of ozone with phenol and its derivatives, various reaction pathways have been identified. Ozone reacts with phenol and its derivatives by ozone addition (Criegee mechanism), electron transfer and O-atom transfer reactions.

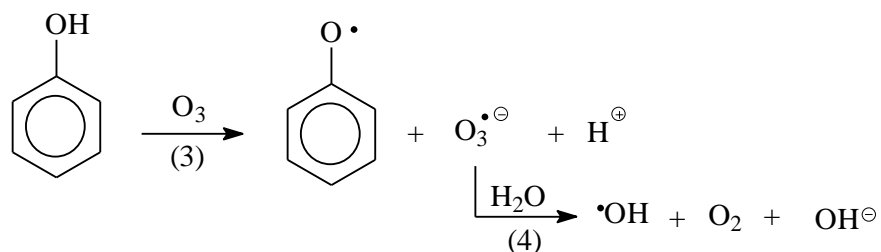
The Criegee mechanism, practically the only reaction with olefins, often occurs to only a small extent here. Instead, $\bullet\text{OH}$ (up to 26%), $\text{O}_2\bullet^-$ and $\text{O}_2(^1\Delta_g)$ are major intermediates.

The occurrence of the Criegee mechanism was confirmed by the yields of hydrogen peroxide and their corresponding carbonyl compounds. The Criegee mechanism is shown to be more pronounced in methoxybenzenes as compared to phenols. For example, in the reaction of ozone with 1,4-dimethoxybenzene, the hydrogen peroxide yield (56%) and that of methyl(2Z,4E)-4-methoxy-6-oxo-hexa-2,4-dienoate (52%), which are the products of the Criegee type reaction, are much higher than that of hydrogen peroxide (5.6%) in the reaction of ozone with hydroquinone. A possible reason for this is that, i.e. the zwitterion formed in the reaction of ozone with hydroquinone may undergo a deprotonation reaction [reaction (1)] which competes with the 1,3- dipolar cycloaddition [reaction (2)]

whereas in the case of the zwitterion formed in the reaction of ozone with 1,4-dimethoxybenzene, the 1,3-dipolar cycloaddition may occur without hindrance.

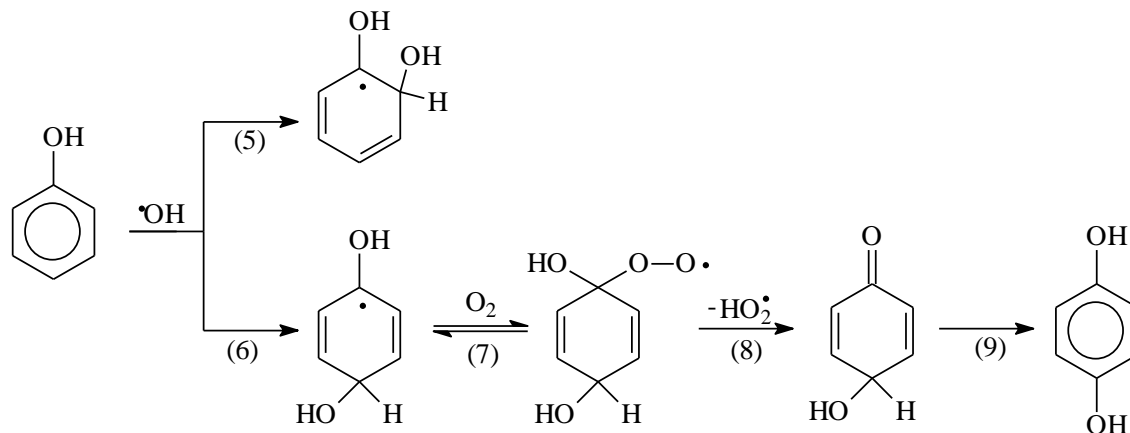


Electron transfer from phenol to ozone leads to the formation of a phenoxyl radical and $\text{O}_3^{\bullet-}$ [reaction (3)]. The latter decays into $\bullet\text{OH}$ [reaction (4)]. The electron transfer reactions were also observed in the reactions of ozone with phenol derivatives studied in this work. In the absence of ozone, phenol-derived phenoxyl radical undergo a bimolecular reaction forming dimers in case of while the catechol- and hydroquinone-derived phenoxyl radicals disproportionate.

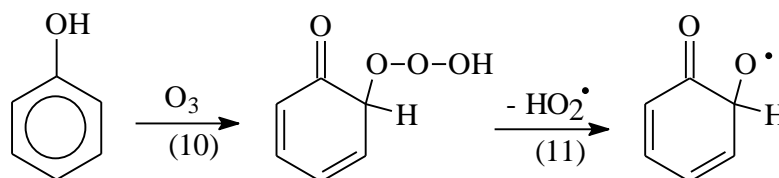


In this work, it is proposed that phenoxyl radicals react very fast with ozone. This helps to explain why destruction of phenol, catechol and hydroquinone by ozone at low conversion accounts for only ~50% of the ozone consumed.

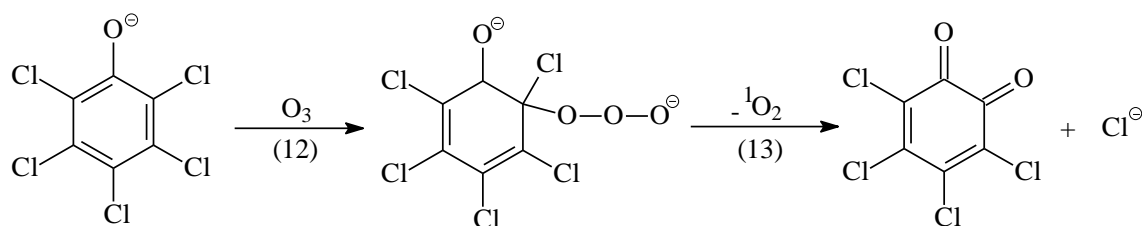
The formation of $\bullet\text{OH}$ in the reaction of ozone with phenols has prompted us to investigate the reaction of $\bullet\text{OH}$ with phenol by pulse radiolysis. Phenol reacts with $\bullet\text{OH}$ by adding preferentially to the *ortho*- [reaction (5), 48 %] and *para*-positions [reaction (6), 36 %]. Catechol and hydroquinone are the main products formed upon dioxygen addition to the dihydroxycyclohexadienyl radicals and subsequent HO_2^{\bullet} -elimination [*e.g.*, reactions (7)–(9)].



Quantification of $\text{HO}_2^\bullet/\text{O}_2^{\bullet-}$ in the reaction of ozone with phenol indicates that $\text{HO}_2^\bullet/\text{O}_2^{\bullet-}$ is exclusively formed as a result of $^\bullet\text{OH}$ attack on phenol. This rules out the possibility of reaction (11) as suggested in the literature.



In the reaction of ozone with phenolic compounds, the formation of $\text{O}_2(^1\Delta_g)$ occurs as a result of ozone addition to the ring. However, only a low yield was observed with phenol (8%), hydroquinone (16%), and catechol (14%) as compared to, *e.g.*, pentachlorophenol (70%) [reaction (13)]. The $\text{O}_2(^1\Delta_g)$ yields in the reaction of methoxybenzene are also low.



The obtained results on $\text{O}_2(^1\Delta_g)$ have revealed the importance of such measurements as it has allowed the detection of very important products that could not be detected using conventional methods.

In case of sulfur-containing compounds *i.e.* 2,3-dihydroxydithiane where up to 100 % $\text{O}_2(^1\Delta_g)$ yield was obtained at pH 7, $\text{O}_2(^1\Delta_g)$ measurements were sufficient to fully elucidate the reaction mechanism. This $\text{O}_2(^1\Delta_g)$ yield is higher than in case of 1,4-dithiothreitol (46%) at pH 4.8 and much higher than in case of H_2S and 1,4-dithiothreitol at pH 7 where $\text{O}_2(^1\Delta_g)$ yields are only 16 and 22%,

respectively. The low $O_2(^1\Delta_g)$ yield in the reaction of ozone with H_2S is observed as a result of ozone reaction with the HS^- where pathways other than O-atom transfer reaction dominate.

Iodide and bromide also react with ozone via O-atom transfer pathway, but the measured $O_2(^1\Delta_g)$ yields are only 56% for Br^- and 12% for I^- . These low yields are due to the relatively long-lived $BrOOO^-/IOOO^-$, the steady state intermediates in this reactions allowing heavy-atom-assisted spin conversion and release of triplet (ground-state) dioxygen.

TABLE OF CONTENTS

1	INTRODUCTION	1
1.1	The ozone molecule	1
1.2	Reactivity of molecular ozone	3
1.2.1	O-atom transfer reactions	3
1.2.2	Electron transfer reactions	4
1.2.3	Ozone addition reactions	4
1.3	Reactions of ozone toward various functional groups.....	4
1.3.1	Reactions of ozone with olefins	4
1.3.2	Reactions with aromatic compounds.....	7
1.3.3	Reactions of ozone with amines.....	10
1.3.4	Reactions of ozone with sulfides and disulfides	12
1.4	Motivation and objectives of this work.....	12
2	EXPERIMENTAL	15
2.1	Substances studied.....	15
2.2	Sample preparation.....	15
2.2.1	γ -Radiolysis and pulse radiolysis.....	15
2.2.2	Ozonation.....	16
2.3	Analytical instrumentation.....	16
2.3.1	Ultraviolet/Visible (UV/VIS) spectroscopy.....	16
2.3.2	High performance liquid chromatography (HPLC)	16
2.3.3	Ion chromatography (IC)	17
2.3.4	Mass spectroscopy (MS)	17
2.3.5	Gas chromatography-mass spectroscopy (GC-MS)	17
2.3.6	Nuclear magnetic resonance (NMR) spectroscopy	17
2.4	Quantitative analysis of stable products by derivatisation.....	18
2.4.1	Hydrogen peroxide measurements	18
2.4.2	Formaldehyde measurements	19
2.5	Quantitative analysis of short-lived products	20
2.5.1	Hydroxyl radical.....	20
2.5.2	Superoxide radical.....	21
2.5.3	Singlet dioxygen.....	21

2.6	Kinetics of ozone reactions.....	22
2.6.1	Stopped-flow method	22
2.6.2	Competition kinetics method	23
2.7	Computation.....	24
2.7.1	Chemical kinetics simulation.....	24
2.7.2	Analysis of HPLC and IC chromatograms.....	24
2.8	Mass spectra of the identified products.....	24
2.8.1	Reaction products of ozone with phenol.....	24
2.8.2	Reaction products of ozone with hydroquinone	26
2.8.3	Reaction products of ozone with anisole.....	27
2.8.4	Reaction products of ozone with 1,2-dimethoxybenzene.....	28
2.8.5	Reaction products of ozone with 1,4-dimethoxybenzene.....	28
2.8.6	Reaction products of ozone with 1,3,5-trimethoxybenzene	29
3	DETECTION OF SINGLET DIOXYGEN IN OZONE REACTIONS	31
3.1	Introduction to singlet dioxygen	31
3.1.1	The singlet dioxygen molecule	31
3.1.2	Generation of singlet dioxygen.....	32
3.1.3	Decay of singlet dioxygen	33
3.2	Singlet dioxygen formation in ozone reactions.....	34
3.3	Mechanism leading to singlet dioxygen formation	36
3.3.1	Phenol and its derivatives.....	36
3.3.2	Methoxybenzenes.....	38
3.3.3	Bromide and iodide ions.....	38
3.3.4	Sulfur-containing compounds	39
4	DETECTION OF HYDROXYL AND SUPEROXIDE RADICALS AS WELL AS HYDROPEROXIDES	44
4.1	Introduction.....	44
4.1.1	The reaction of 2-methyl-2-propanol with the hydroxyl radical	45
4.1.2	The reaction of DMSO with the hydroxyl radical.....	47
4.1.3	The reaction of TNM with the superoxide radical.....	47
4.2	Detection of \bullet OH in the ozone reactions.....	47
4.2.1	The 2-methyl-2-propanol system	47
4.2.2	Factors to be taken into account in the determination of \bullet OH in ozone	

reactions with the 2-methyl-2-propanol / formaldehyde assay	49
4.2.3 The dimethylsulfoxide system	50
4.2.4 Conditions for the formation of $\bullet\text{OH}$ in ozone reactions.....	51
4.3 Detection of superoxide in ozone reactions.....	53
4.3.1 Reaction of tetranitromethane and nitroform anion with ozone	53
4.3.2 The tetranitromethane/nitroform anion system.....	53
4.3.3 Difficulties in the use of tetranitromethane for the detection of superoxide in ozone reactions	55
4.4 Detection of hydroperoxides in ozone reactions.....	57
4.4.1 Hydrogen peroxide and organic hydroperoxides.....	57
4.4.2 Detection of reactive hydroperoxides	62
5 REACTIONS OF OZONE AND HYDROXYL RADICAL WITH PHENOL.....	64
5.1 Reactions of phenol with ozone.....	64
5.1.1 Products yield.....	64
5.1.2 Reactivity of ozone/phenol products with ozone.....	68
5.1.3 Mechanistic considerations	70
5.2 Reactions of phenol with $\text{OH}\bullet$	76
5.2.1 Conversion of the dihydroxycyclohexadienyl radicals into phenoxy radicals	78
5.2.2 Reactions of the dihydroxycyclohexadienyl radicals with dioxygen	80
5.2.3 $\text{HO}_2\bullet$ -elimination reaction of dihydroxycyclohexadienylperoxyl radicals	81
5.2.4 Product studies.....	82
6 REACTIONS OF OZONE WITH DIHYDROXY BENZENES	85
6.1 Reactions of ozone with hydroquinone	85
6.2 Reactions of ozone with catechol	91
7 REACTIONS OF OZONE WITH HALOPHENOLS.....	94
7.1 Kinetics of the reactions of ozone with halophenols.....	94
7.2 Product studies and mechanisms of the reactions of ozone with halophenols.....	96
8 REACTIONS OF OZONE WITH METHOXYBENZENES	99
8.1 Product studies.....	99
8.1.1 Reactions of ozone with anisole.....	99
8.1.2 Reactions of ozone with 1,2-dimethoxybenzene.....	99

8.1.3	Reactions of ozone with 1,4-dimethoxybenzene	100
8.1.4	Reactions of ozone with 1,3,5-trimethoxybenzene	101
8.2	Mechanism of the ozonolysis of methoxy benzenes.....	104
9	SUMMARY AND CONCLUSION	108
9.1	Review of the methodology	108
9.1.1	Kinetics of ozone reactions.....	108
9.1.2	Detection of singlet dioxygen.....	108
9.1.3	Detection of $\bullet\text{OH}$ and $\text{O}_2^{\bullet-}$	108
9.2	General mechanism of the reactions of ozone with phenol and its derivatives.....	110
9.2.1	Reactions of ozone with phenol and dihydroxybenzenes.....	110
9.2.2	Reactions of ozone with halophenols.....	111
9.2.3	Reactions of ozone with methoxybenzenes	112
9.3	Implication of the findings.....	112
10	REFERENCES.....	114
11	APPENDICES	123
12	LIST OF SCHEMES	126
13	LIST OF TABLES	127
14	LIST OF FIGURES	129

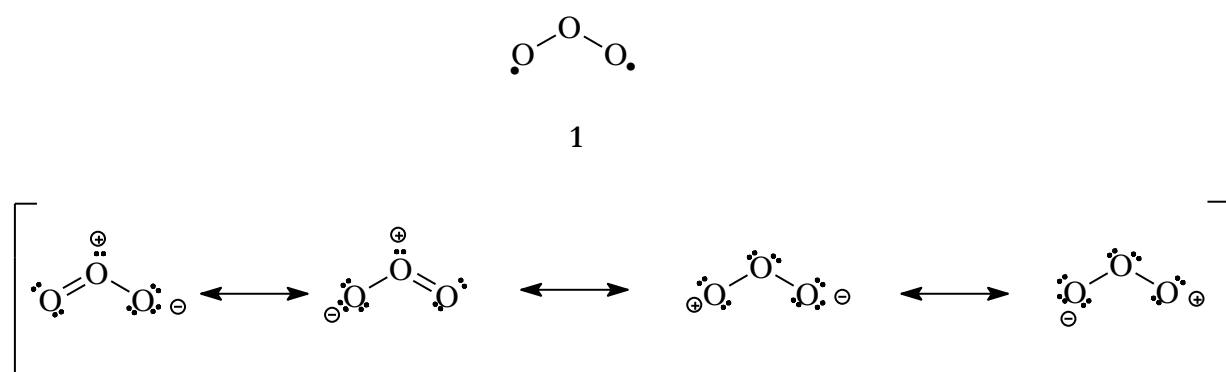
1 INTRODUCTION

The need to improve the quality of drinking water has resulted in a search for new and review of the already existing water treatment methods. Most water sources world-wide contain pollutants which traditional methods are not fully able to remove. Ozonation has proven to be one of the most suitable methods not only for disinfection purposes, but also for the removal of dissolved organic compounds. Chlorination which is the most widely used disinfecting method does not destroy most of the dissolved organic compounds and may result in the formation of trihalomethanes (THM) which are suspected carcinogens.

Investigations of ozone reactions with compounds likely to be found in both natural and waste-water would help understanding how ozone interacts with such compounds. In this Chapter, a brief introduction to ozone, its reactivity towards various compounds and its application in drinking-water treatment is presented.

1.1 The ozone molecule

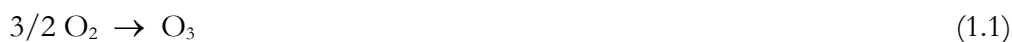
Ozone was discovered in 1840 by Schönbein, who gave it the name ozone derived from the Greek word "*ozein*" meaning to smell.¹ Ozone is an allotrope of dioxygen (O₂). Contemporary calculations have shown that ozone exist as a singlet diradical **1** in its ground state.² Its chemical structure can also be described as a resonance hybrid of four canonical forms of dipolar character as shown in Scheme 1



Scheme 1 Resonance structures of the ozone molecule

The structure of ozone is characterised by a bond angle at the centred oxygen of 116.5° and a O-O bond length of 1.278 Å, according to spectroscopic measurements.³

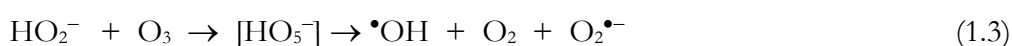
In the laboratory, ozone is produced by passing dry air or dioxygen through a silent electrical discharge consisting of two dielectric separated electrodes which are connected to a high voltage generator. The formation of ozone from dioxygen is an endothermic reaction with the Gibb's free energy of 163.2 kJ mol⁻¹ [reaction (1.1)].

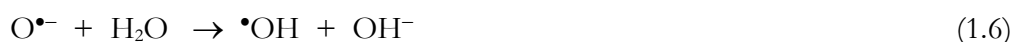


The physical properties of ozone are typically that of a gaseous substance with low melting and boiling points which are -192.5 °C and -111.9 °C respectively.⁴ The solubility of ozone in water increases with decreasing temperature and increasing pressure. At 20°C and 1,013 bar partial pressure, its solubility in water is approximately 1.2×10^{-2} mol dm⁻³.⁴ Ozone has a strong UV absorption in the region 220-300 nm.⁵ In water, the ozone concentration is measured by UV spectrophotometry at $\lambda_{\text{max}} = 260$ nm with absorption coefficient $\epsilon = 3300$ dm⁻³ mol⁻¹ cm⁻¹.^{6,7}

The fate of ozone in aqueous solution depends on the pH as well as on the dissolved substances.^{8,9} Its half life in water is shorter at high pH or high concentration of dissolved organic compounds. The effect of pH on the decomposition of ozone can be rationalised by considering the chemistry of its reaction with OH⁻ and the subsequent radical type chain reaction which accelerates the ozone consumption.

The initial ozone reaction with OH⁻ [reaction (1.2)] is relatively slow with a rate constant of 50-70 dm³ mol⁻¹ s⁻¹ yielding HO₂⁻.^{6,10} The HO₂⁻ reacts with ozone whereby the hydroxyl radical (•OH) and superoxide radical (O₂•⁻) are formed [reaction (1.3), $k = 5.5 \times 10^6$ dm³ mol⁻¹ s⁻¹]. The superoxide radical reacts with ozone yielding O₃•⁻ at a rate constant of 1.6×10^9 dm³ mol⁻¹ s⁻¹ [reaction (1.4)].¹¹ O₃•⁻ is in equilibrium with O₂ and O•⁻. The latter is a strong base [$\text{p}K_{\text{a}}(\text{•OH}) = 11.8$] and rapidly reacts with water yielding •OH and OH⁻ [reaction (1.6)]. The situation become very complex as •OH reacts with O₃ [reaction (1.7), $k = 1 \times 10^8$ dm³ mol⁻¹ s⁻¹] and thus can initiate a chain reaction with HO₂•/O₂•⁻ as intermediates [*cf.* equilibrium (1.8), $\text{p}K_{\text{a}}(\text{HO}_2\bullet) = 4.8$], leading to the self destruction of ozone.





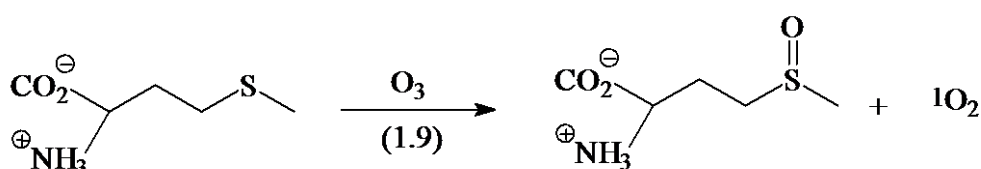
In neutral and acidic solution protonation of $\text{O}_3^{\bullet-}$ may also occur. The ensuing $\text{HO}_3\bullet$ is also very short lived and rapidly loses O_2 yielding $\bullet\text{OH}$.

1.2 Reactivity of molecular ozone

There are three principal reaction pathways which describe the initial ozone attack on organic and inorganic compounds. These reaction pathways are categorised as electron transfer, oxygen-atom transfer and ozone addition reactions. A compound may react with ozone by more than one these pathways.

1.2.1 O-atom transfer reactions

This type of reaction involves the transfer of an oxygen-atom to the reacting substrate forming an substrate-oxide and singlet dioxygen [$\text{O}_2(^1\Delta_g)$]. The factors responsible for oxygen atom transfer are not yet well understood. One might speculate that the strength of the bond formed between oxygen and the substrate functional group is responsible for O-atom transfer. This type of reaction has been observed in the reaction of ozone with sulfur,^{12,13} and nitrogen-containing compounds¹⁴ and bromide and also with iodide (*cf.* Chapter 3). A good example in this regard is the reaction of methionine with ozone which gives rise to $\text{O}_2(^1\Delta_g)$ and methionine sulfoxide in 100% yield [reaction (1.9)].¹² A detailed description of O-atom transfer reactions is given in Chapter 3.



1.2.2 Electron transfer reactions

An electron transfer reaction can be described as a reaction in which an electron moves from one atom or molecule (donor) to another atom or molecule (acceptor). In aqueous solutions, electron transfer reactions are explained in terms of the one electron reduction potentials of the reacting substances. The one-electron reduction potential of ozone is $E(\text{O}_3/\text{O}_3^{\bullet-}) = 1.01 \text{ V}$ at pH 7.¹⁵ This means that only compounds whose reduction potentials are lower than that of ozone can react with ozone by electron transfer (*cf.* Chapter 4).¹⁵⁻¹⁷

Recently, Schank *et al.*¹⁶ have demonstrated the occurrence of electron transfer in the reaction of ozone with 1,1,2,2-tetraphenylethene.

1.2.3 Ozone addition reactions

Two cases of ozone addition reactions have been observed in aqueous solution.

- One of them involves an ozone attack on the A substrate forming an intermediate which dissociates homolytically to yield A-O^{\bullet} and $\text{O}_2^{\bullet-}$ [reaction (1.10)].



- Another case of an ozone addition reaction is that of olefins (*cf.* section 1.3.1). Ozone attacks one of the sp^2 carbon resulting in a formation of a σ -complex or zwitterion which undergoes a 1,3-dipolar cyclisation forming a trioxolane [reaction (1.11), in Scheme 2].

1.3 Reactions of ozone toward various functional groups

1.3.1 Reactions of ozone with olefins

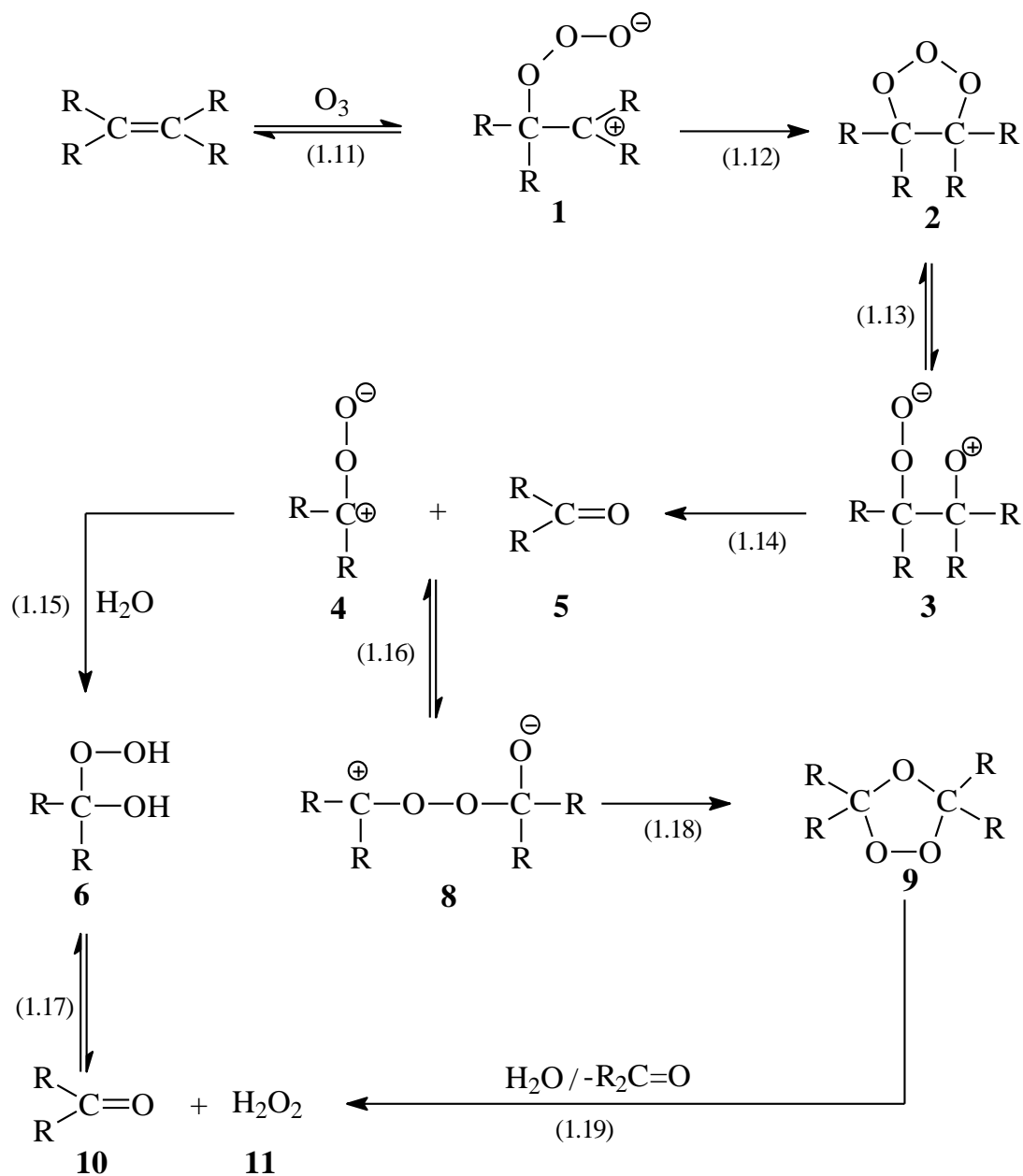
The reaction of ozone with simple olefins has been a subject of various investigations in both organic and aqueous solutions.¹⁸⁻²⁴ This reaction has been categorised as an ozone 1,3-dipolar cycloaddition reaction and is well described in terms of the Criegee mechanism (Scheme 2).²⁵ The initial encounter results in the formation of a π -complex, which gives rise to a zwitterion σ -complex **1** [reaction 1.11] followed by ring closure to form the

primary ozonide **2** also known as 1,2,3-trioxolane [reaction (1.12)]. The primary ozonide **2** decomposes into the zwitterion **3** which decomposes further into another zwitterion **4** and a carbonyl compound **5** [reaction (1.13) and (1.14)]. The zwitterion **4** reacts with water [reaction (1.15)] to give an α -hydroxyalkylhydroperoxide **6** which is in equilibrium with hydrogen peroxide **11** and a carbonyl compound **10** [equilibrium (1.17)]. In water, reaction (1.15) does not compete successfully with reaction (1.16). However, in organic solvents, the zwitterion **4** and carbonyl compound **5** can react to form the Criegee ozonide **8**. In aqueous solution, **9** would hydrolyse yielding two mol of carbonyl compounds **10** and one mol of hydrogen peroxide **11** [reaction (1.19)].

A number of experimental and theoretical studies have been carried out to prove the existence and to characterise the structure of the carbonyloxide **4**.²⁶⁻³⁰ Although most of these theoretical calculations do not take solvent effects into account, the results obtained might be as well useful for aqueous solutions.²⁷ The main focus of these investigations was to show whether the carbonyloxide **4** is a zwitterion or a diradical. Semi-empirical calculations²⁹ suggests that the ground state of the carbonyl compound is a zwitterion while *ab-initio* calculations²⁸ postulate a diradical ground state.

The rate constants of the reaction of ozone with an olefinic compounds decrease with decreasing electron density of the C=C double bond. If the R-group is electron withdrawing, e.g. Cl, the electron density of the C=C double bond decreases hence the rate constant of the reaction. Table 1 shows the rate constants of ozone reactions with various olefins. A similar trend has been observed in carbon tetrachloride.^{22,23} However, in carbon tetrachloride the absolute values are typically one order of magnitude lower than in water.

Error! Use the Home tab to apply Überschrift 1 to the text that you want to appear here.
 Error! Use the Home tab to apply Überschrift 1 to the text that you want to appear here.



Scheme 2 The mechanism of ozone reaction with an olefin²⁴

Table 1 Rate constants of the ozone reactions with various olefins in aqueous solution (taken from ref.²⁴)

Substrate	Rate constant [$\text{dm}^3 \text{mol}^{-1} \text{s}^{-1}$]
Tetramethylethene	$>10^6$
Propene	8.0×10^5
Ethene	1.8×10^5
3-Buten-1-ol	7.8×10^4
Vinyl chloride	1.4×10^4
<i>Trans</i> -1,2-Dichloroethene	6.5×10^3
<i>Cis</i> -1,2-Dichloroethene	540
1,1-Dichloroethene	110
Trichloroethene	14
Tetrachloroethene	0.1

1.3.2 Reactions with aromatic compounds

The reactions of ozone with aromatic compounds in aqueous solution are not yet well understood. This is mainly due to the following factors:

- The rate of initial ozone attack to the substrate may be slower than that of the products. In most cases there is a lack of the material balance and sometimes mechanisms were proposed based on secondary products.
- There is more than one mode of ozone attack on the aromatic ring, and various pathways may lead to the final products.^{31,32}

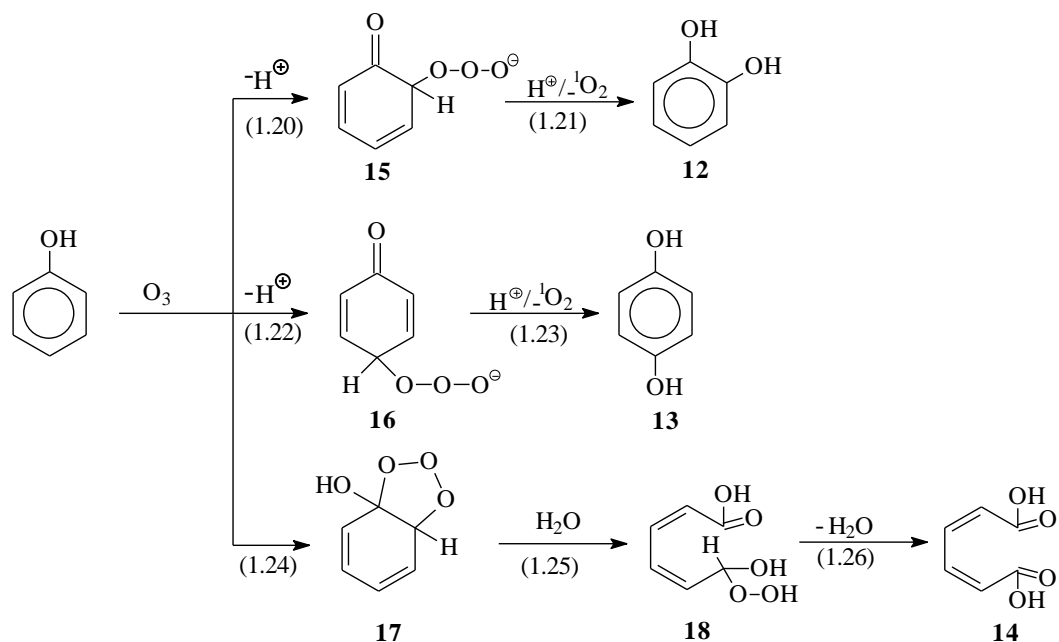
The substituents on the aromatic ring have an effect on its reactivity toward ozone. Hoigné et al.³³ have established a linear relationship between the Hammett-substituent-constant and the logarithm of k/k_0 for aromatic compounds (*cf.* Figure 1, where k is the rate constant of the substrate and k_0 is the rate constant of benzene). A similar relationship was also established by Gurol *et al.*³⁴ It has been concluded from these data that ozone acts as an electrophilic agent.

Figure 1 A plot of the Hammett-substituent-constants *vs.* $\log k/k_0$ for various aromatic compounds according to ref³³.

Phenols are one class of aromatic compounds whose reaction with ozone has been extensively studied, because of the need to purify waste water containing such compounds.³⁴⁻⁵⁸ Despite the fact that a number of studies have been carried out on the reaction of phenol with ozone, most of these studies yielded contradictory results. For example Yamamoto *et al.*⁴² reported the formation of formic acid, glyoxalic acid, oxalic acid and carbon dioxide in the reaction of ozone with phenol. Such products are not primary products and might complicate the elucidation of the reaction mechanism of ozone with phenol.

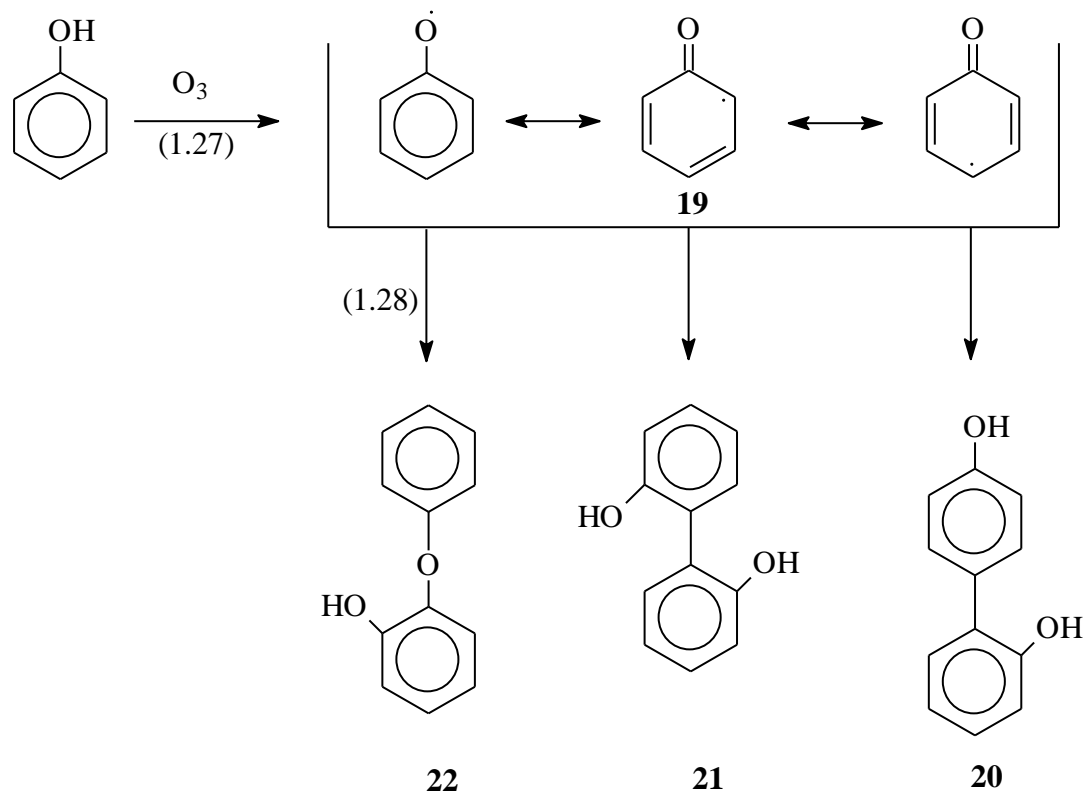
So far, a more comprehensive mechanism for the oxidation of phenol by ozone was proposed by Bailey (*cf.* Scheme 3), based on the formation of catechol **12**, hydroquinone **13** and *cis,cis*-muconic acid **14**.³¹ It was suggested that catechol **12** and hydroquinone **13** are formed as a result of ozone attack at the *ortho*- and *para*-position respectively followed by the O₂ elimination reaction of intermediate **15** and **16** [reactions (1.20)-(1.23)]. The liberated O₂ is supposed to be in its singlet excited state in accordance with the spin conservation rule. However, the yield of singlet oxygen [O₂(¹Δ_g)] formed during the ozonation of phenol

is less than the yield of catechol and hydroquinone (Chapters 3 and 5).⁵³ This suggests that further reaction pathways might be involved in the formation of catechol and hydroquinone. Another possible reaction pathway shown in Scheme 3 is the 1,3 dipolar cycloaddition similar to that of simply olefins [reactions (1.24)-(1.26)] which results in the formation of *cis,cis*-muconic acid **14**.



Scheme 3 Bailey's mechanism for the reaction of ozone with phenol.³¹

It has been reported that the reaction of phenol with ozone might involve oxidation coupling pathways leading to the formation of polymeric compounds.^{43,44,59} Based on gel chromatography, Duguet^{43,44} concluded the formation of compounds with higher molecular weight, but was unable to assign the structure of the products. Konstantinova *et.al.*⁵⁹ have proposed the mechanism which leads to the formation of dimers as shown in Scheme 4. Based on their work done in alkaline media, they identified dimers such as 2,2'-dihydroxybiphenyl **20**, 2,4'-dihydroxybiphenyl **21** and other oligomeric products e.g. **22**. These products are thought to be formed *via* phenoxy radicals [reaction (1.28)].



Scheme 4 Oxidative coupling in the reaction of ozone with phenol.⁴⁸

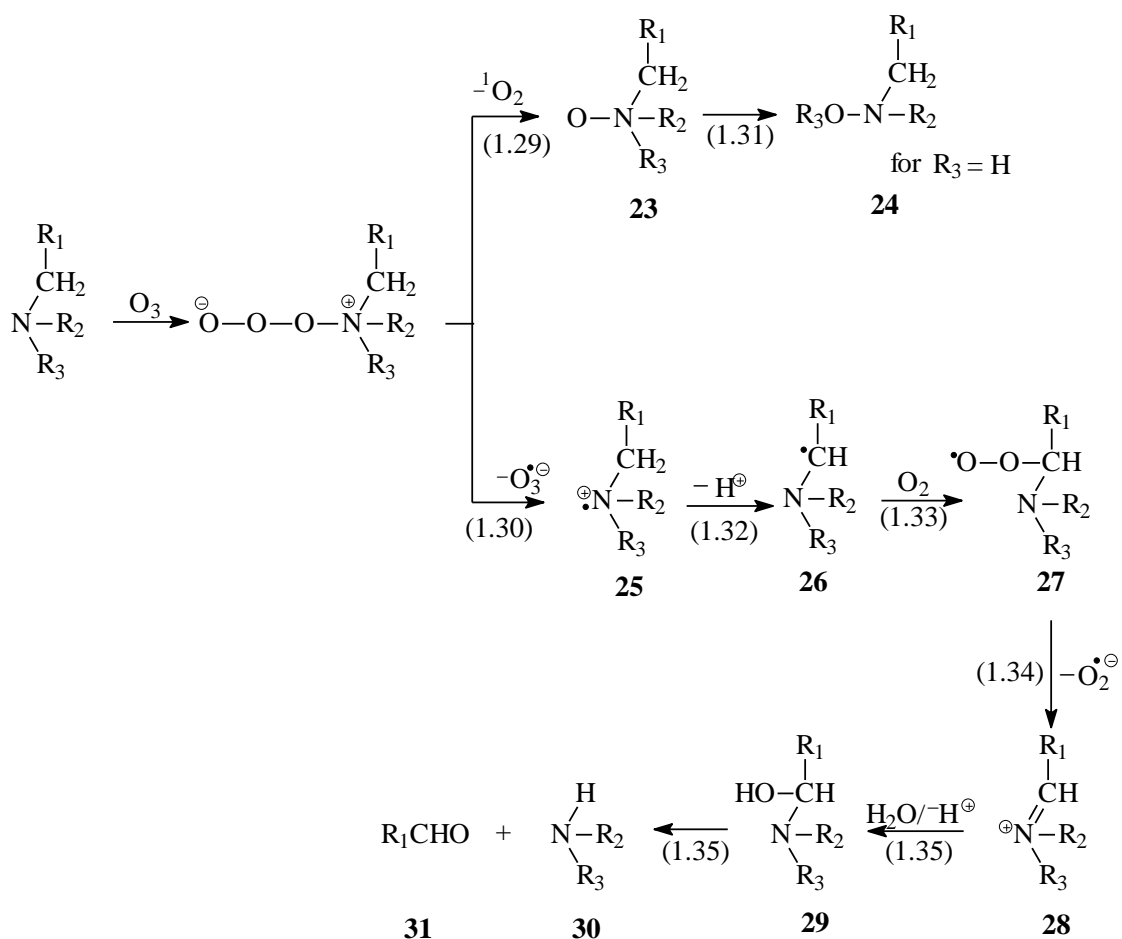
1.3.3 Reactions of ozone with amines

Most of the earlier studies on the reaction of ozone with amines have been carried out in organic solvents such as methanol, chloroform, methylene chloride and cyclohexane.⁶⁰⁻⁶⁴ Recently, Muñoz has carried out these studies in aqueous solution.⁶⁵

A general reaction mechanism of ozone with amines (Scheme 5) involves two different modes of O_3 attack, namely the oxygen atom-transfer [reaction (1.29)] and electron transfer reaction [reaction (1.30)]. The oxygen atom transfer reaction pathway yields singlet dioxygen [$O_2(^1\Delta_g)$] and an aminoxide **23**. In case of primary amines (R_2 and $R_3 = H$) and secondary amines ($R_3 = H$), the aminoxide is unstable and undergoes a hydrogen shift forming the corresponding hydroxylamine [reaction (1.31)].

The electron transfer pathway [reaction (1.30)] gives rise to the radical cation **25** and $O_3^{\bullet-}$. The radical cation **25** deprotonates to yield a carbon-centred radical **26** which in turn reacts with O_2 forming a peroxy radical **27**. The peroxy radical **27** decomposes into an iminium ion **28** and a superoxide radical ($O_2^{\bullet-}$). The iminium ion **28** hydrolyses, producing an amine **30** and an aldehyde **31**.

The aqueous solution studies of amines (trimethylamine, triethylamine, diethylamine and monoethylamine) revealed that the O-atom transfer (80-90%) dominates over electron transfer (10-15%) in the reaction of ozone with tertiary amines.⁶⁵ This is expected in view of the fact that the reduction potential of tertiary amines e.g. $E_o((\text{CH}_3)_3\text{N}^{\bullet+}/((\text{CH}_3)_3\text{N} = 1.04 \text{ V})^{66}$ is very close to that of ozone $E_o(\text{O}_3^{\bullet-}/\text{O}_3 = 1.01 \text{ V})$,¹⁵ allows the electron transfer process to occur, but does not provide much driving force. In the case of secondary amines, the O-atom transfer reaction seems to dominate slightly over electron transfer. The opposite is observed in ozone reactions with primary amines where electron transfer seems to dominate over O-atom transfer. Yet, these systems warrant a more detailed investigation.^{14,65}



Scheme 5 Reaction of ozone with amines ref.⁶⁵

1.3.4 Reactions of ozone with sulfides and disulfides

Most sulfides (disulfides) react with ozone by O-atom transfer producing the corresponding sulfoxides (sulfinic acid thioester) and singlet dioxygen [$O_2(^1\Delta_g)$] [reaction (1.9), on page 3].^{12,31} However, thiols do not react 100% via O-atom transfer. This has been shown in case of dihydrogen sulfide (H_2S) and 1,4-dithiothreitol (*cf.* Chapter 3). Dihydrogen sulfide is of interest in ground-water treatment, but its reaction with ozone is not yet well understood. Contradicting results have been reported on the stoichiometry and reaction mechanism.^{67,68}

1.4 Motivation and objectives of this work

Water is one of the most important natural resources and is a basic requirement for life. Not only is water availability important, but its quality especially for human consumption is equally important. Through scientific research, methods for water quality improvement have been developed. However, most of such methods concentrated mainly on disinfection, *i.e.* the removal of bacteria and viruses. Organic micro-pollutants received comparatively little attention. This is unfortunately still the case in many developing countries.

Traditional physical and chemical methods currently used at many works are only partially able to remove the water contaminants required for safe and high quality drinking water at most water works. Despite the promises that ozone is able to reduce the dissolved organic carbon (DOC) and thus also unwanted contaminants, very little is known about its mode of reaction with dissolved organic substances. Full destruction of dissolved organic substances by ozone is usually not achieved. In order to ensure the safety and quality of drinking water, there is a need to understand the reaction of ozone with compounds likely to be found in natural waters, but also in waste water whenever the latter has to be processed to drinking water (reclamation). This can be useful in predicting the products formed in the ozonated drinking water containing known pollutants and assess their possible environmental and health hazards.

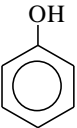
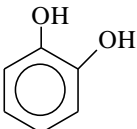
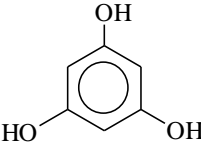
In the ozonolysis of aromatic compounds in aqueous solution some key questions are still unanswered:

(1) What happens at the initial interaction of ozone with the aromatic compounds (van der Waals complexes, direction of site of ozone attack)? (2) Are there radical pathways involved

and to what extent do they occur? (3) What are the effects of substituents on product distribution?

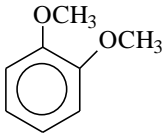
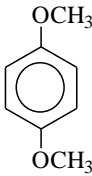
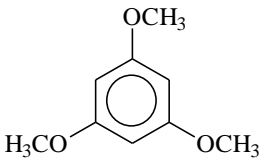
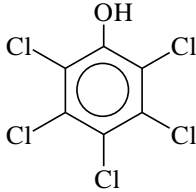
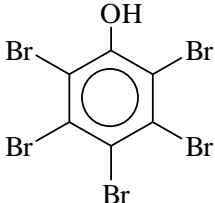
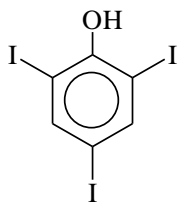
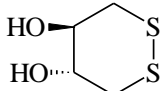
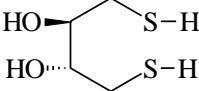
To answer some of these questions and to contribute to the knowledge of ozone reactions in aqueous solutions in general, extensive studies on the reactions of ozone with various phenolic compounds were carried out. The scope of the investigation was widened by including dihydrogen sulfide and its organic analogues (see Table 2). These compounds were chosen as model systems for organic matter containing such functional groups and may be found in both natural and waste water. By employing various analytical techniques, such as high performance liquid chromatography (HPLC); ion chromatography (IC); nuclear magnetic resonance spectroscopy (NMR); gas chromatography (GC) and gas chromatography coupled to mass spectroscopy (GC-MS). The aim of this study was to identify and quantify reaction products in order to elucidate the reaction mechanism. By this way, the predictability of product formation in ozone reactions will be improved.

Table 2 Names, structures, rate constants of ozone reactions and pK_a -values of the compounds investigated in this work.

Name of the substrate	Structure	k (O_3 + substrate) [$dm^3 mol^{-1} s^{-1}$]	PK_a
Phenol		3×10^3 ref. ⁶⁹ 1.3×10^9 (pH 10) ref. ⁶⁹	10
Catechol		3.1×10^5 ref. ³⁴	9.25 12.37 ref. ⁷⁰
Hydroquinone		1.5×10^6 ref. ³⁴	9.91 11.56 ref. ⁷⁰
Phloroglucinol		-	7.97 9.23 ref. ⁷⁰

Error! Use the Home tab to apply Überschrift 1 to the text that you want to appear here.

Error! Use the Home tab to apply Überschrift 1 to the text that you want to appear here.

Table 2 continued			
1,2-Dimethoxybenzene		-	-
1,4-Dimethoxybenzene		1.3×10^5 ref. ⁷¹	-
1,3,5-Trimethoxybenzene		9.4×10^5 ref. ⁷¹	-
Pentachlorophenol			10
Pentabromophenol			10
Triiodophenol			10
Dihydrogen sulfide	H ₂ S	3.4×10^4 (pH 1-4.5) ref. ⁷² 3×10^9 (pH 9) ref. ⁷²	7.0
2,3-Dihydroxydithiane		2.1×10^5	-
1,4-Dithiothreitol		1.7×10^5	9.1 10.5

2 EXPERIMENTAL

2.1 Substances studied

Catechol, hydroquinone and phenol were purchased from Merck, while phloroglucinol; 1,4-dimethoxybenze, 1,2-dimethoxybenze, 1,3,5-trimethoxybenzene, 2,3-dihydroxydithiane and 1,4-dithiothreitol were purchased from Aldrich.

2.2 Sample preparation

2.2.1 γ -Radiolysis and pulse radiolysis

Aqueous solutions of substrates (concentration typically $1 \times 10^{-3} \text{ mol dm}^{-3}$) were saturated with N_2O or $\text{N}_2\text{O}/\text{O}_2(4:1 \text{ v/v})$ prior to irradiation. γ -Radiolysis experiments were carried out in a panoramic ^{60}Co -source (Irradiation unit LCU2, Nuclear Engineering Ltd, England) at a dose rate of 0.1 Gy s^{-1} to total doses of up to 270 Gy (*i.e.* the conversion of the substrate remained below 20%). The dose rate was determined by Fricke dosimetry. Here, an aqueous solution containing $2 \times 10^{-3} \text{ mol dm}^{-3} \text{ FeSO}_4 \cdot 7\text{H}_2\text{O}$, $2 \times 10^{-3} \text{ mol dm}^{-3} \text{ NaCl}$, and $0.4 \text{ mol dm}^{-3} \text{ H}_2\text{SO}_4$ was saturated with dioxygen for 20 min. The samples were then irradiated as a function of time at a fixed position. The concentration of Fe^{3+} was measured by UV-spectrophotometry at 305 nm ($\epsilon = 2097 \text{ dm}^3 \text{ mol}^{-1} \text{ cm}^{-1}$). The G -value of Fe^{3+} which is known to be $16.2 \times 10^{-7} \text{ mol J}^{-1}$ ⁷³ was used to determine the dose rate (D) using equation (2.1).

$$G = \frac{c}{D \times t \times \rho} \quad (2.1)$$

Where G is the number of molecules formed or consumed per ($10^{-7} \text{ mol J}^{-1}$), c is the concentration of Fe^{3+} (mol dm^{-3}), D is the dose rate ($\text{Gy s}^{-1} = \text{J kg}^{-1} \text{ s}^{-1}$) and ρ is the density of the solution (which is 1 kg dm^{-3} for a diluted aqueous solution) and t is the irradiation time.

Pulse radiolysis was carried out with a 2.8 MeV Van-de-Graaf accelerator delivering electron pulses of $0.4 \mu\text{s}$ duration.⁷⁴ Intermediates were monitored by optical detection. For dosimetry, N_2O -saturated $10^{-2} \text{ mol dm}^{-3}$ thiocyanate solution was used for optical detection, taking $G \times \epsilon((\text{SCN})_2^{\bullet-}) = 4.8 \times 10^{-4} \text{ m}^2 \text{ J}^{-1}$ at 480 nm .⁷⁵

2.2.2 Ozonation

Ozone was generated with an oxygen-fed ozonator (Philaqua PiloZ 04, Gladbeck). The exhaust gas containing about 10% ozone was bubbled through Milli-Q-filtered (Millipore) water to make ozone stock solutions. The ozone concentration in the stock solution was measured spectrophotometrically at 260 nm ($\epsilon = 3314 \text{ dm}^3 \text{ mol}^{-1} \text{ cm}^{-1}$).^{6,7} The concentration of the stock solution was usually about $4 \times 10^{-4} \text{ mol dm}^{-3}$. Since ozone is unstable the stock solutions were used immediately after concentration measurement.

For the determination of the product yields, ozone solution was added to the substrate solution by varying its volume in order to vary the ozone concentration. The substrate concentration was always kept in large excess, to avoid reactions of ozone with the primary products.

2.3 Analytical instrumentation

2.3.1 Ultraviolet/Visible (UV/VIS) spectroscopy

UV absorption measurements and spectra recording were performed on a Perkin-Elmer Lambda 16UV/Vis spectrophotometer.

2.3.2 High performance liquid chromatography (HPLC)

HPLC was used as the major tool for identifying and quantifying the products. The analyses were carried out using an HPLC equipment consisting of a Merck/Hitachi L-4500 diode array detector, an L-6200 "Intelligent Pump" and a nucleosil-5 C₁₈-reversed-phase-column (25 cm or 12.5 cm). The following solutions were used as eluent:

- Water was used for post-column derivatisation method to determine H₂O₂ (section 2.4.1).
- An aqueous solution of 50% acetonitrile was used for the analysis of the hydrazone derivative of formaldehyde (section 2.4.2)
- In case of the ozonated solutions of phenol, catechol, hydroquinone and 1,4-dimethoxybenzene an aqueous solution containing 25% methanol and 0.1% phosphoric acid was used as eluent, a 25% aqueous solution of acetonitrile was used for the analysis of ozonated 1,3,5-trimethoxybenzene and 1,2-dimethoxybenzene.

2.3.3 Ion chromatography (IC)

The ionic compounds were measured by ion chromatography using a DIONEX DX 100 or DIONEX 2010i with an ASRSI suppressor. For the measurements of methanesulfinic and methanesulfonic acid, an AS14 column together with an AG 14 guard-column were used and an aqueous solution containing $4.5 \times 10^{-4} \text{ mol dm}^{-3} \text{ Na}_2\text{CO}_3$ and $4.25 \times 10^{-4} \text{ mol dm}^{-3} \text{ NaHCO}_3$ was used as eluent.

2.3.4 Mass spectroscopy (MS)

Isolated products were identified by means of electron spray method using a HP (Hewlett-Packard) 5989 B MS-Engine or by electron ionisation on Finnigan MAT 8200. Spectra of the identified reaction products are given in section 2.8.

2.3.5 Gas chromatography-mass spectroscopy (GC-MS)

For GC-MS, a Hewlett-Packard (5890 Series II) set-up was used. Samples were prepared by adding 70 ml of a $2 \times 10^{-4} \text{ mol dm}^{-3}$ ozone solution to a 30 ml of $2 \times 10^{-3} \text{ mol dm}^{-3}$ substrate solution. The ozonated solutions were usually rotary evaporated to dryness. Dried samples were either dissolved in 0.5 ml diethyl ether and those whose starting material contained OH functionality (e.g. phenol, catechol, hydroquinone) were dissolved in 0.3 ml pyridine and trimethylsilylated with 0.2 ml of *N,N*-bis-trimethylsilyltrifluoroacetamide (BTSEA) and then heated at 70 °C for 30 min to improve their volatility.

2.3.6 Nuclear magnetic resonance (NMR) spectroscopy

^1H -NMR spectra were recorded with a Bruker DRX:500 instrument. The isolated products were either dissolved in D_2O or in CDCl_3 for NMR measurements.

2.4 Quantitative analysis of stable products by derivatisation

2.4.1 Hydrogen peroxide measurements

Hydrogen peroxide was determined with Allen's reagent⁷⁶ using either UV spectroscopy or the technique of post-column derivatisation. The ammoniumheptamolybdate-catalysed reaction of hydrogen peroxide with iodide produces iodine [reaction (2.1)]. An equilibrium is established between I^- and I_2 [reaction (2.2)] forming I_3^- which has a strong absorption at 350 nm.



The following reagents were prepared: Reagent A (0.1 g ammoniumheptamolybdate, 1 g potassium hydroxide, 33 g potassium iodide) in 500 ml water and B (10 g potassium hydrogenphthalate) in 500 ml water.

- UV spectroscopy - 1 ml of sample was poured into the cuvette to which 1 ml of each A and B was added. The solution was mixed and then measured immediately at 350 nm ($\epsilon = 12550 \text{ dm}^3 \text{ mol}^{-1} \text{ cm}^{-1}$).⁷⁶
- Post-column derivatisation - the set-up consist of an HPLC instrument and a reaction pump as shown in Figure 2. Samples were injected onto the HPLC column, which was connected to a reaction pump. In the reaction pump, the HPLC separated sample was mixed with Allen's reagent (A and B) and allowed to react at 50 °C (this is done by using a long loop placed in a water bath) before detection at 350 nm. This method was used to detect H_2O_2 yields in systems where the products cause interference with the direct UV measurements as well as to detect the formation of organic peroxides.

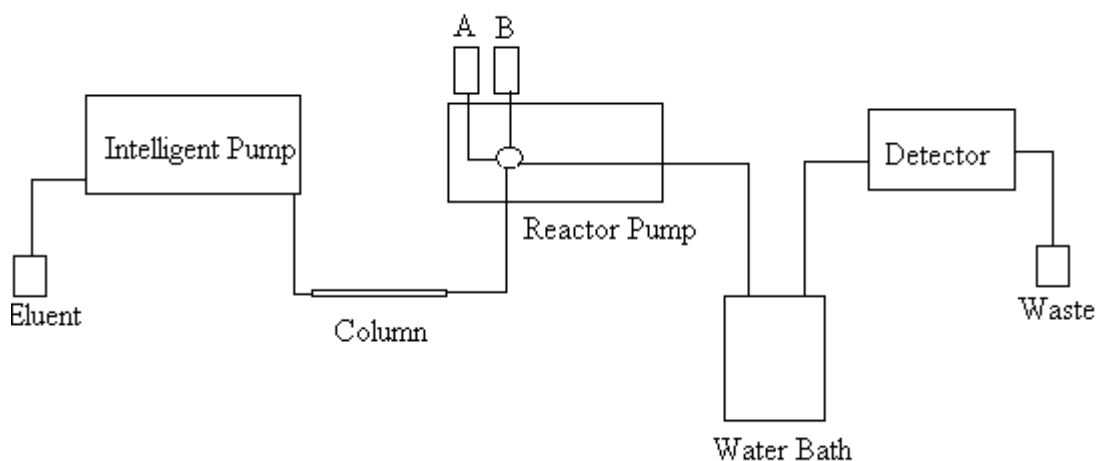


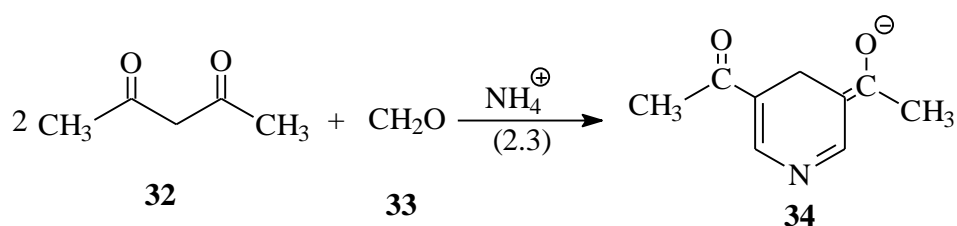
Figure 2 Schematic diagram of the post-column derivatisation instrument.

2.4.2 Formaldehyde measurements

Formaldehyde was detected by either one of the following method:

- Hantzsch method

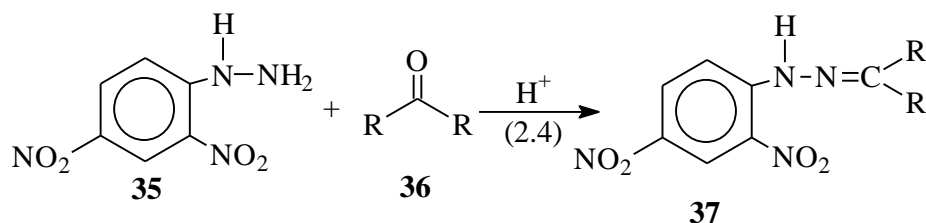
The reaction of acetylacetone **32** with formaldehyde **33** in the presence of an ammonium salt yields a yellow condensation product namely 3,5-diacetyl-1,4-dihydrolutidin **34** [reaction (2.3)]. This product has a strong absorption at 412 nm ($\epsilon = 7530 \text{ dm}^3 \text{ mol}^{-1} \text{ cm}^{-1}$).



In this work, formaldehyde **33** was determined by taking 5 ml of the sample to which 2 ml of the Hantzsch reagent (25 g ammonium acetate, 3 ml acetic acid, and 0.2 ml acetyl acetone filled up to 100 ml) was added and filled up to 10 ml. The mixtures was heated to 50 °C for 30 min and measured by UV spectroscopy at 412 nm after cooling down to room temperature.⁷⁷

- HPLC method

Carbonyl compounds react with 2,4-dinitrophenylhydrazine forming the corresponding hydrazones derivatives [reaction (2.4)]



Formaldehyde was measured as the hydrazone derivative **37** by taking 1.7 ml of the sample, to which 0.2 ml of reagent A (30 mg 2,4-dinitrophenylhydrazine in 25 ml of acetonitrile) and 0.1 ml of reagent B (1 mol dm⁻³ HClO₄ in acetonitrile) was added. The mixture was kept in the dark for at least 30 min at room temperature and then analysed using HPLC. The formaldehyde-2,4-dinitrophenylhydrazone **37** has a strong absorption at 360 nm. This method can also be used for analysing other carbonyl compounds such as acetaldehyde and acetone with good separation.⁷⁸ However, the quantification of acetone proved to be unreliable.⁷⁹

2.5 Quantitative analysis of short-lived products

2.5.1 Hydroxyl radical

OH radical formation was detected by scavenging with 2-methyl-2-propanol or dimethylsulfoxide (DMSO).

- The 2-methyl-2-propanol method

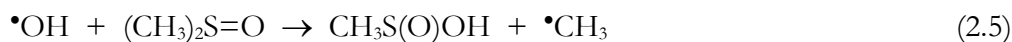
For kinetic reasons, the most ideal method for the detection of •OH in ozone reactions is the 2-methyl-2-propanol method. This is due to the fact that 2-methyl-2-propanol reacts very fast with •OH ($k = 6 \times 10^8 \text{ dm}^3 \text{ mol}^{-1} \text{ s}^{-1}$)⁸⁰ and only very slowly with ozone ($k = 1 \times 10^{-3} \text{ dm}^3 \text{ mol}^{-1} \text{ s}^{-1}$). The hydroxyl radical reacts with 2-methyl-2-propanol by H-abstraction, the subsequent reactions result in the formation of formaldehyde, acetone, 2-methyl-2-hydroxypropanal and 2-methyl-2-hydroxypropanol as major products.⁸¹

In this experiments, formaldehyde was measured either by the Hantzsch method⁷⁷ or by HPLC as 2,4-dinitrophenylhydrazone derivative (section 2.4.2).^{78,79} In order to scavenge

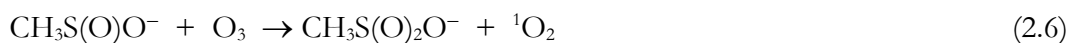
most of $\bullet\text{OH}$ produced, the concentration of 2-methyl-2-propanol used was usually 100 times higher than that of the substrate.

- The dimethylsulfoxide method

In the reaction of $\bullet\text{OH}$ with dimethylsulfoxide (DMSO), methanesulfinic acid is formed in 92% yield [reaction (21)].⁸²

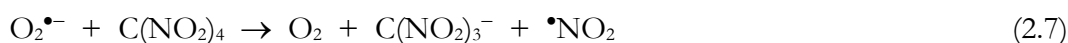


Methanesulfinic acid was detected by ion chromatography (see section 2.3.3). The use of DMSO as $\bullet\text{OH}$ scavenger in ozone reactions has the disadvantage that DMSO reacts reasonably fast with ozone ($k = 8.2 \text{ dm}^3 \text{ mol}^{-1} \text{ s}^{-1}$) and also the product of reaction (2.5), the methanesulfinic acid, is rapidly further oxidised by ozone [reaction (2.6); $k = 2 \times 10^6 \text{ dm}^3 \text{ mol}^{-1} \text{ s}^{-1}$,⁸³ whereby singlet dioxygen $\text{O}_2(^1\Delta_g)$ is the only other product].⁸⁴



2.5.2 Superoxide radical

Superoxide radicals, $\text{O}_2^{\bullet-}$, were determined with tetranitromethane [$\text{C}(\text{NO}_2)_4$]. In the reaction of $\text{C}(\text{NO}_2)_4$ with $\text{O}_2^{\bullet-}$, the nitroform anion is produced [reaction (2.7), $k = 2 \times 10^9 \text{ dm}^3 \text{ mol}^{-1} \text{ s}^{-1}$]. The yield of nitroform anion was determined spectrophotometrically at 350 nm ($\epsilon = 15000 \text{ dm}^3 \text{ mol}^{-1} \text{ cm}^{-1}$).⁸⁵



2.5.3 Singlet dioxygen

Singlet dioxygen, $\text{O}_2(^1\Delta_g)$, was measured by its phosphorescence at 1270 nm using a germanium photodiode (EO-817L, North Coast Scientific Corporation). A Suprasil quartz cell (1 × 1 cm) containing the ozone solution was placed in front of the detector (a schematic representation of the $\text{O}_2(^1\Delta_g)$ detection set-up is shown in Figure 3). The substrate solution was then injected into the cell with the help of a micro-pipette equipped with a trigger system for producing the signal which was recorded on the oscilloscope. As a reference, the formation of $\text{O}_2(^1\Delta_g)$ from the reaction of hydrogen peroxide with hypochlorite [reaction (2.8)] was used and referred to as unity.

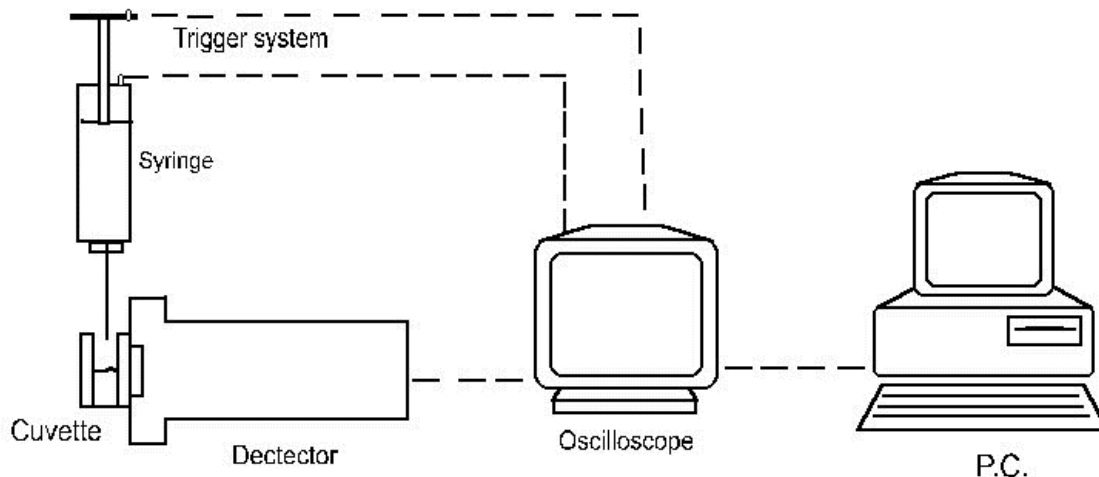
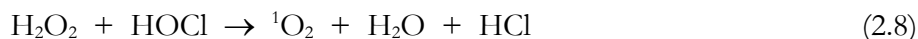


Figure 3 Schematic representation of the $\text{O}_2({}^1\Delta_g)$ detection system.

2.6 Kinetics of ozone reactions

2.6.1 Stopped-flow method

For the measurements of some of the rate constants of reactions investigated in this work, a stopped-flow apparatus (BIOLOGIC SFM-3) was employed. This instrument consists of three syringes (Figure 4) in which the reactants are kept. For the purpose of our investigation, the syringes S1 and S3 were filled with the reactants while S2 was filled with water, which was used for dilution. The components in S1 and S2 are first mixed in M1 and then mixed with the component in S3. The mixture flows in the cuvette where the progress of the reaction was followed spectroscopically. A diode array spectrometer (TIDAS-16, J&M, Analytische Mess-und Regeltechnik) was used to monitor the reaction in the range of 200 to 600nm. An accompanying software (Kinspec, version 2.24, J&M) was used for data collection and analysis.

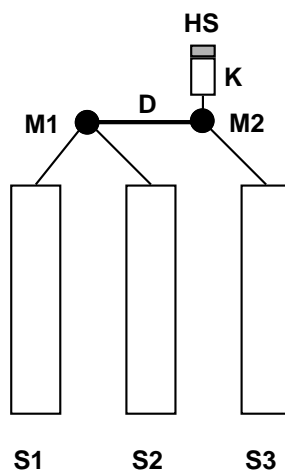


Figure 4 Schematic representation of the BIOLOGIC SFM3 stopped-flow apparatus.

2.6.2 Competition kinetic method

The rate constants of some of the compounds studied in this work were measured by competition kinetics. In order to determine the rate constant of the reaction of ozone with a given substrate R_1 , a competitor R_2 whose reaction details with ozone are known (rate constant and product), is used. The reactions of ozone with the substrate R_1 and the competitor R_2 are given by equations (2.9) and (2.10).



From the rate laws of equations (2.9) and (2.10), the expression (2.11) is derived.

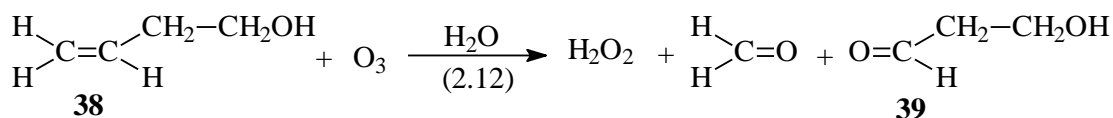
$$\frac{[P_2]}{[P_2]_0} = 1 + \frac{k_1[R_1]}{k_2[R_2]} \quad (2.11)$$

where $[P_2]_0$ is the concentration of P_2 in the absence of the substrate R_1 . The rate constant k_i of the ozone reaction with substrate R_1 can be determined using equation (2.11).

In this work, 3-buten-1-ol **38** was used as the competitor. The reaction of ozone with 3-buten-1-ol **38** yields formaldehyde, H_2O_2 and 3-hydroxypropanal **39** [reaction (2.12), $k = 7.9 \times 10^4 \text{ mol dm}^{-3} \text{ s}^{-1}$].²⁴

Error! Use the Home tab to apply Überschrift 1 to the text that you want to appear here.

Error! Use the Home tab to apply Überschrift 1 to the text that you want to appear here.



A known amount of aqueous solution of ozone was added to solutions containing different ratios of [3-buten-1-ol]/[substrate]. The samples were then quantitatively analysed for formaldehyde (see section 2.4.2). The substrate rate constant was obtained from the slope of the graph [3-buten-1-ol]/[substrate] *vs.* [CH₂O]/[CH₂O]₀. Here, [CH₂O] is the concentration of formaldehyde formed in each [3-buten-1-ol]/[substrate] ratio and [CH₂O]₀ is the concentration of formaldehyde in the absence of a substrate. The concentration of 3-buten-1-ol and that of the substrate were kept ten times higher than that of ozone.

2.7 Computation

2.7.1 Chemical kinetics simulation

Chemical kinetics simulation were performed using the Chemical Kinetics SimulatorTM version 1.01 software (IBM Corp., 1996). This software employs a stochastic method, based on reaction probabilities, to calculate the time evolution of a chemical system using the user specified reaction mechanism and initial conditions.

2.7.2 Analysis of HPLC and IC chromatograms

Since the chromatograms were recorded electronically, the area of the peaks were integrated using the Colarchrom software (Max-Planck-Institut für Kohlenforschung, Mülheim an der Ruhr, Germany).

2.8 Mass spectra of the identified products

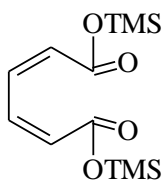
In this section the mass spectra of the products of various ozone reactions, which were identified by either direct MS or GC-MS are presented.

2.8.1 Reaction products of ozone with phenol

Cis,cis-muconic acid [(2*Z*,4*Z*)-hexa-2,4-dienedioic acid] **14** (MW 142); *m/z*(%): 142(6), 124(9), 97(100), 79(16), 51(11), 41(13) was identified by direct MS (*cf.* Figure 5). The *cis,cis*-

Error! Use the Home tab to apply Überschrift 1 to the text that you want to appear here.
Error! Use the Home tab to apply Überschrift 1 to the text that you want to appear here.

muconic acid was also identified by GC-MS after trimethylsilylation **40** (MW 286); m/z (%) 286(3), 271(100), 227(3), 190(2), 169(13), 147(55), 128(4), 107(7), 73(60).



(2Z,4Z)-Bis(trimethylsilyloxy)-hexa-2,4-dienedioate **40**

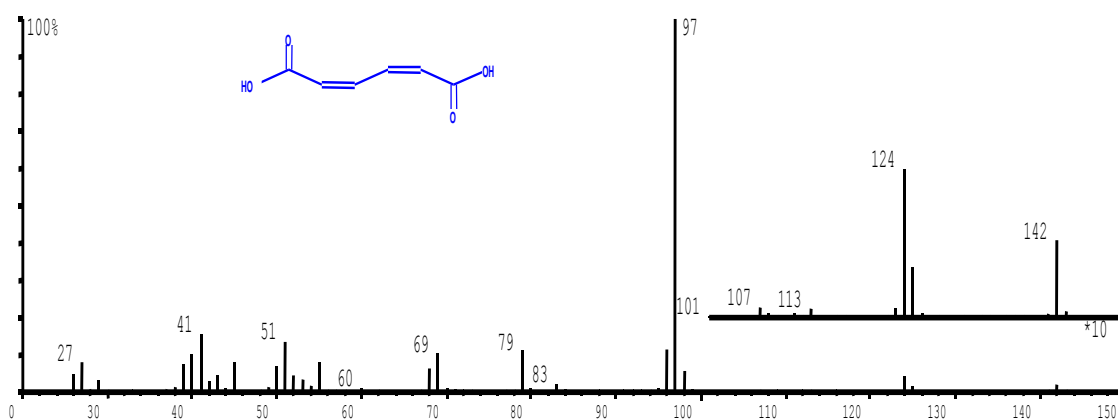


Figure 5 Mass spectrum of (2Z,4Z)-hexa-2,4-dienedioic acid.

In the search for polymeric compounds formed in the reaction of phenol with ozone, two phenol dimers were identified after trimethylsilylation, these are 4,4'-bis(trimethylsilyloxy)biphenyl **41** (MW 330); m/z (%): 330(100), 315(10), 165(3), 150(14), 73(50) and 2,4'-bis(trimethylsilyloxy)biphenyl **42** (MW 330); m/z (%): 330(70), 315(10), 299(3), 142(5), 73(100). The spectra of the two dimers mentioned above are shown graphically in Figure 6 and 7.

Error! Use the Home tab to apply Überschrift 1 to the text that you want to appear here.

Error! Use the Home tab to apply Überschrift 1 to the text that you want to appear here.

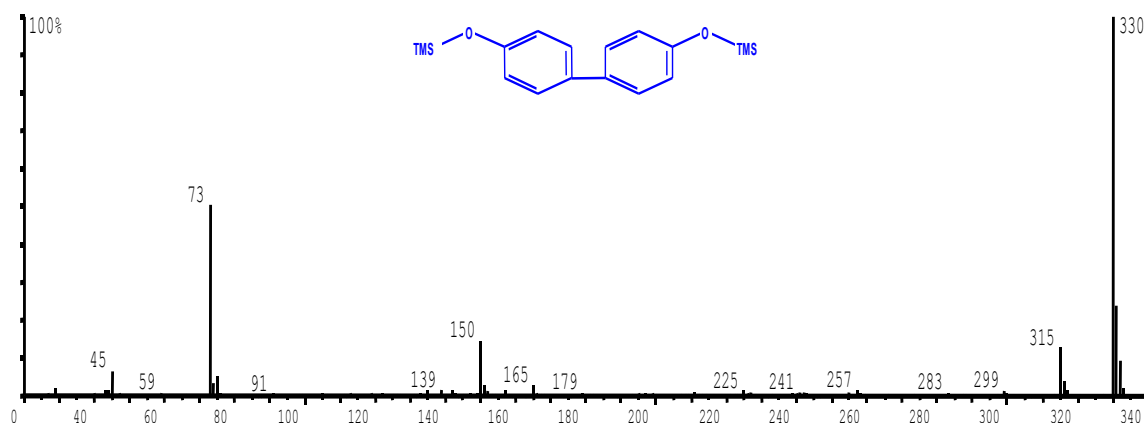


Figure 6 Mass spectrum of 4,4'-bis(trimethylsilyloxy)biphenyl.

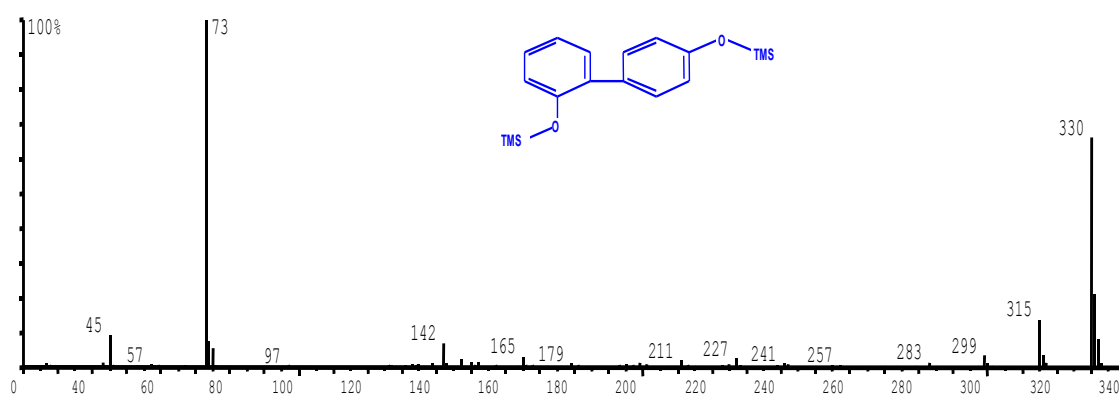
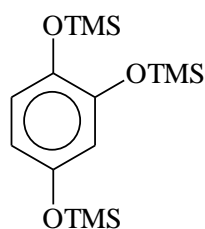


Figure 7 Mass spectrum of 2,4'-bis(trimethylsilyloxy)biphenyl.

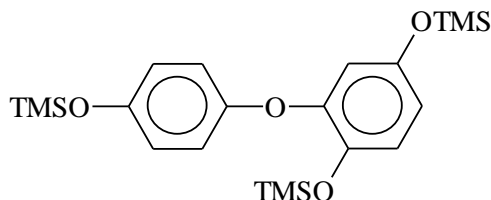
2.8.2 Reaction products of ozone with hydroquinone

A GC-MS analysis of the trimethylsilylated ozonated sample of hydroquinone gave a mass spectrum corresponding to that of the 1,2,4-tris(trimethylsilyloxy)benzene **43** (MW 342) m/z (%): 342(44), 327(4), 254(4), 239(27), 147(7), 73(100).



1,2,4-Tris(trimethylsilyloxy)benzene **43**

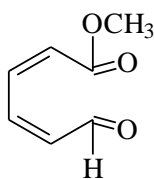
In the same sample, a spectrum was also observed which corresponds to that of the trimethylsilylated 2-(4-hydroxyphenoxy)hydroquinone **44** (MW 430). m/z (%): 430(83), 415(7), 295(13), 58(13), 147(14), 73(100).



1,4-Bis(trimethylsilyloxy)-2-(4-trimethylsilyloxyphenoxy)benzene **44**

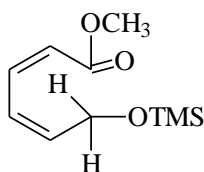
2.8.3 Reaction products of ozone with anisole

A GC-MS analysis of the ozonated anisole reveals the formation of methyl(2*Z*,4*Z*)-6-oxohexa-2,4-dienoate **45** (MW 140) m/z (%): 140(34), 125(12), 111(13), 81(100), 53(63).



Methyl(2*Z*,4*Z*)-6-oxohexa-2,4-dienoate **45**

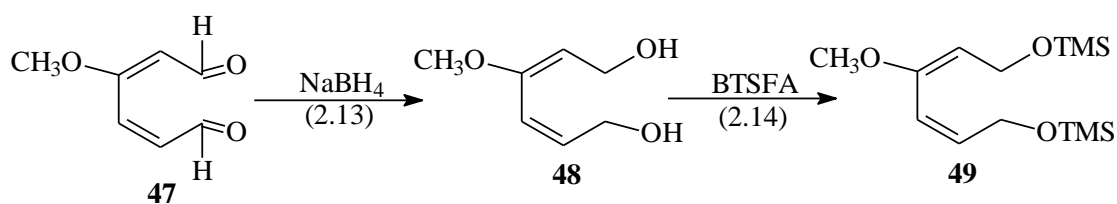
This product was also confirmed after reduction with NaBH₄ followed by trimethylsilylation to give a methyl(2*Z*,4*Z*)-6-trimethylsilyloxyhexa-2,4-dienoate **46** (MW 214) m/z (%): 214(5), 199(5), 155(7), 124(25), 111(10), 98(9), 89(60), 73(100).



Methyl(2*Z*,4*Z*)-6-trimethylsilyloxyhexa-2,4-dienoate **46**

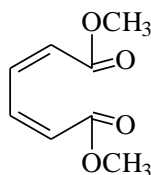
In the same sample described above, a compound whose mass spectrum corresponds to methyl(2*E*,4*Z*)-1,6-bis(trimethylsilyloxy)-3-methoxyhexa-2,4-diene **49** (MW 284) m/z (%): 284(62), 269(8), 254(100), 239(8), 179(3), 147(5), 133(3), 119(7), 112(10), 89(7), 73(57) was identified. This indicates that methyl(2*E*,4*Z*)-3-methoxyhexa-2,4-dienal **47** is formed in the reaction of ozone with anisole.

Error! Use the Home tab to apply Überschrift 1 to the text that you want to appear here.
Error! Use the Home tab to apply Überschrift 1 to the text that you want to appear here.



2.8.4 Reaction products of ozone with 1,2-dimethoxybenzene

A mass spectrum corresponding to that of dimethyl(2*Z*,4*Z*)-hexa-2,4-dienoate **50** (MW 170); m/z (%), 170(13), 155(7), 141(23), 123(12), 111(100), 95(3), 79(15), 69(7), 59(15) was found.



Dimethyl(2*Z*,4*Z*)-hexa-2,4-dienoate **50**

2.8.5 Reaction products of ozone with 1,4-dimethoxybenzene

Mass spectra corresponding to compounds shown below were identified.

Methyl(2*Z*,4*E*)-4-methoxy-6-oxo-hexa-2,4-dienoate **51** (*cf.* Figure 7). (MW 170) m/z (%): 170(6), 155(8), 141(20), 123(6), 111(100), 95(3), 79(6), 69(16), 50(13).

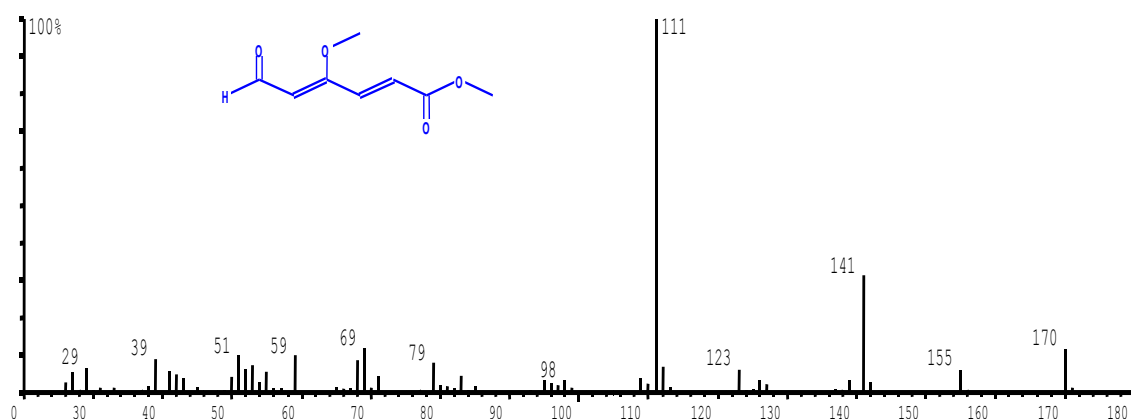
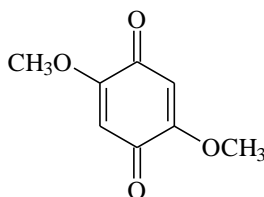


Figure 8 Mass spectrum of methyl(2*Z*,4*E*)-4-methoxy-6-oxo-hexa-2,4-dienoate.

Error! Use the Home tab to apply Überschrift 1 to the text that you want to appear here.

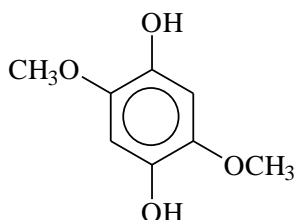
Error! Use the Home tab to apply Überschrift 1 to the text that you want to appear here.

2,5-Dimethoxyl-1,4-benzoquinone **52** (MW 168) m/z (%): 168(10), 153(38), 139(54), 125(19), 95(46), 69(100), 59(20), 53(35).



2,5-Dimethoxyl-1,4-benzoquinone **52**

2,5-Dimethoxyhydroquinone **53** (MW 170) m/z (%): 170(25), 155(33), 139(50), 127(16), 111(13), 95(42), 69(100), 59(42), 53(33).

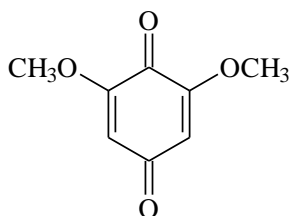


2,5-Dimethoxyhydroquinone **53**

2.8.6 Reaction products of ozone with 1,3,5-trimethoxybenzene

In the reaction of ozone with 1,3,5-trimethoxybenzene the following compounds were identified:

2,6-Dimethoxy-1,4-benzoquinone **54** (MW 168); m/z (%): 168(36), 153(4), 138(11), 125(11), 112(10), 97(11), 80(33), 69(100), 59(13), 53(21) (Figure 9).



2,6-Dimethoxy-1,4-benzoquinone **54**

Error! Use the Home tab to apply Überschrift 1 to the text that you want to appear here.

Error! Use the Home tab to apply Überschrift 1 to the text that you want to appear here.

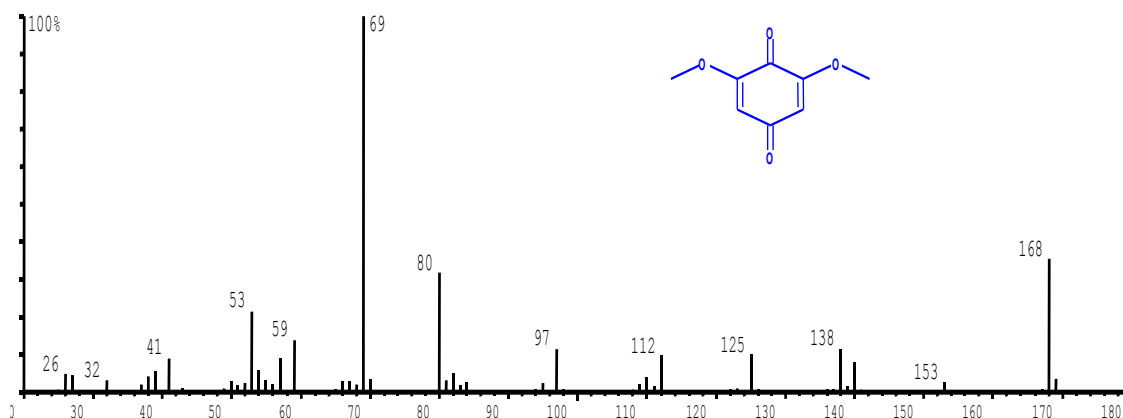
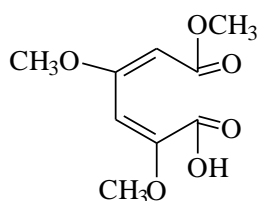


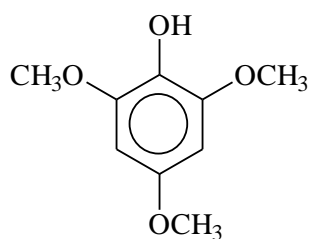
Figure 9 The mass spectrum of 2,6-dimethoxy-*p*-benzoquinone.

(2*E*,4*E*)-2,4,6-Trimethoxy-6-oxo-hexa-2,4-dienoic acid **55** (MW 216): m/z (%): 216(100), 185(24), 157(14), 143(100), 115(35), 10(14), 69(36), 59(34).



(2*E*,4*E*)-2,4,6-Methoxy-6-oxo-hexa-2,4-dienoic acid **55**

2,4,6-Trimethoxyphenol **56** (MW 184): m/z (%); 184(100), 169(64), 154(14), 141(33), 126(17), 109(12), 95(10), 60(17), 53(14).



2,4,6-Trimethoxyphenol **56**

3 DETECTION OF SINGLET DIOXYGEN IN OZONE REACTIONS

3.1 Introduction to singlet dioxygen

3.1.1 The singlet dioxygen molecule

In order to understand the nature and properties of singlet dioxygen, it is important to look at the electronic structure of molecular dioxygen. Dioxygen is unique in that it is the only homonuclear diatomic molecule that has a triplet spin multiplicity in its ground state. From the molecular orbital theory, the ground state electron configuration of dioxygen can be represented as : $(1s\sigma_g)^2 (1s\sigma_u^*)^2 (2s\sigma_g)^2 (2s\sigma_u^*)^2 (2p\sigma_g)^2 (2p\pi_u)^4 (2p\pi_g^*)^2$ (Figure 10), which is a linear combination of O-atomic orbitals.⁸⁶

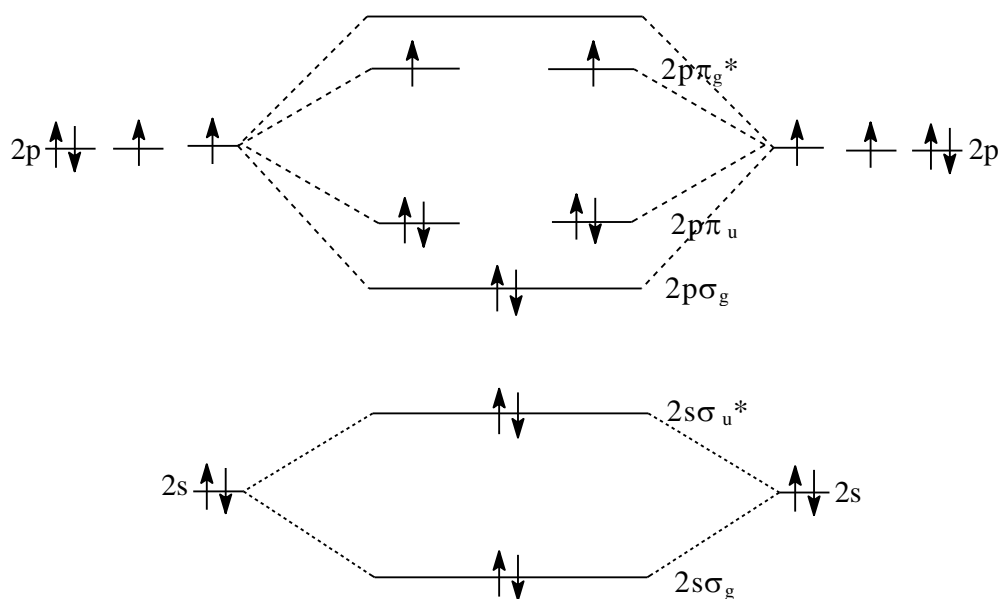


Figure 10 The electron configuration of the O₂ molecule.

The $2p\pi_g^*$ orbitals are doubly degenerate, meaning that electrons can occupy either both orbitals with parallel [triplet ground state ($^3\Sigma_g^+$)], with opposing spin [triplet excited states ($^1\Sigma_g^-$)] or the same orbital with opposing spin [singlet excited state ($^1\Delta_g$)] as shown in Figure 11. According to Hund's rule, the state with the highest multiplicity is the most stable, and this indeed turned out to be the ground state oxygen ($^3\Sigma_g^+$).⁸⁷ The two electronically excited

states, namely the ${}^1\Delta_g$ and ${}^1\Sigma_g^-$ lie about 94 and 157 kJ mol $^{-1}$ above the ground state (${}^3\Sigma_g^+$), respectively. Of these two excited states, the lowest excited state is more stable and longer lived and as a result of this, its properties have been studied more extensively.⁸⁸⁻⁹⁴ The term singlet dioxygen and symbol $O_2({}^1\Delta_g)$ used through out this dissertation designate the lowest excited state of dioxygen.

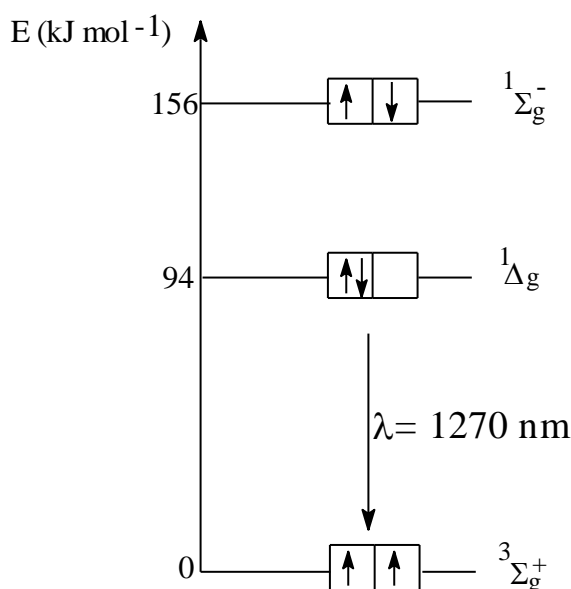


Figure 11 Electronic configuration and energy scheme of three states of dioxygen.

3.1.2 Generation of singlet dioxygen

Singlet dioxygen can be produced by either chemical or physical means. The best-known chemical method of producing $O_2({}^1\Delta_g)$ is the decomposition of hydrogen peroxide by hypochlorite [reaction (2.8)].⁹⁵ This method was also used in this study to generate $O_2({}^1\Delta_g)$ for the calibration by assuming that $O_2({}^1\Delta_g)$ formation is 100% (*cf.* section 2.5.3). The reactions of ozone can also be regarded as one of the chemical methods for the generation of $O_2({}^1\Delta_g)$, especially where up to 100% $O_2({}^1\Delta_g)$ is formed, *e.g.*, the reaction of ozone with sulfides (*cf.* Table 3). However, the high reactivity of ozone may prevent a more general application of this method as a source of $O_2({}^1\Delta_g)$ in $O_2({}^1\Delta_g)$ studies.

There are various physical methods for generating $O_2({}^1\Delta_g)$, *i.e.* photosensitization and gas-phase discharge (microwave generation). The method frequently used for producing $O_2({}^1\Delta_g)$ in the laboratory is photosensitisation. This method involves the use of a sensitizer whose energy (triplet state) is transferred to a dioxygen molecule upon interaction

producing an excited dioxygen molecule. In order for the electron energy exchange to take place, the sensitizer triplet state must be sufficiently energetic ($\geq 94 \text{ kJmol}^{-1}$). However, it should also be taken into account that the energy transfer becomes inefficient at higher sensitizer triplet energy.⁹⁴

3.1.3 Decay of singlet dioxygen

In solution, $\text{O}_2(^1\Delta_g)$ can decay into the ground state by radiative decay (phosphorescence), non-radiative decay due to solvent interaction and non-radiative decay due to the presence of a quencher. The overall rate constant of the decay of $\text{O}_2(^1\Delta_g)$ in solution can be expressed as:

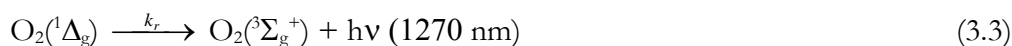
$$k_d = k_r + k_s + k_q[\text{Q}] \quad (3.1)$$

where k_r , k_s and k_q are the rate constants of $\text{O}_2(^1\Delta_g)$ disappearance due to radiative decay, solvent interaction and quencher Q, respectively. In the absence of a quencher, equation (3.1) can be rewritten as:

$$k_d = k_r + k_s = \frac{1}{\tau_o} \quad (3.2)$$

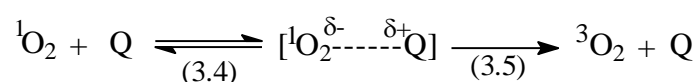
Here, τ_o defines the life time of $\text{O}_2(^1\Delta_g)$ in solution. The life time of $\text{O}_2(^1\Delta_g)$ in water is about 3–4 μs .

- Radiative decay: The radiative decay of $\text{O}_2(^1\Delta_g)$ is the process in which the excited state relaxes into the ground state ($^3\Sigma_g^+$) thereby losing energy equivalent to the difference between the two states (94 kJ mol^{-1}). The energy is lost through light emission with $\lambda = 1270 \text{ nm}$ in the process which is known as phosphorescence [reaction (3.3)].



The applied experimental technique for the detection of $\text{O}_2(^1\Delta_g)$ makes use of the phosphorescence process, whereby the emitted light is measured with the help of a germanium diode detector as described in section 2.5.3. The rate constant of the radiative decay (k_r) depends on the nature of solvent. The effect of the solvent on k_r has been studied extensively, and it has been found to be influenced by the solvent dielectric constant. Water, which has a high dielectric constant shows the lowest k_r followed by alcohols.^{89,93}

- Non radiative decay due to the solvent: The interaction of solvent molecule with $O_2(^1\Delta_g)$ can cause its decay. This involves energy transfer from the excited $O_2(^1\Delta_g)$ to the vibrational levels of the solvent.^{88,90,93,94,96} Since our experiments are carried out using the same solvent (water), solvent induced decay of $O_2(^1\Delta_g)$ does not affect our results.
- Non radiative decay due to quenching: Quenchers are solutes which are capable of deactivating $O_2(^1\Delta_g)$ as a result of either physical or chemical interactions. The physical quenching does not result in loss of the quencher, but can occur either by energy transfer or charge transfer process [reactions (3.4) and (3.5)].



Electron donors such as phenols, thiols and amines are believed to deactivate $O_2(^1\Delta_g)$ by a charge-transfer process.⁹¹ The quenching constants k_q of $O_2(^1\Delta_g)$ by various compounds have been compiled.⁹⁴ The measured $O_2(^1\Delta_g)$ yield in ozone reactions can be affected by the quenching property of the substrate. This has been clearly demonstrated in the reaction of ozone with azide and 1,4-diazabicyclo[2,2,2]octane⁸⁴ In the reaction of ozone with substrates which are good $O_2(^1\Delta_g)$ quenchers, k_q can be useful to calculate the accurate $O_2(^1\Delta_g)$ yield from the measured value. The k_q for compounds studied in this work and appropriate explanation on their effects of the measured $O_2(^1\Delta_g)$ yields are presented in section 3.3.

3.2 Singlet dioxygen formation in ozone reactions

It is well-known that in O_3 reactions singlet dioxygen, $O_2(^1\Delta_g)$, may be formed in high yields.¹² This is always the case when O-transfer reactions dominate. Spin conservation rules then demand that the resulting dioxygen molecule must be in its (excited) singlet state, because the educt and ozone as well as the product are in their singlet (ground) states. A case in point is the reaction of ozone with tertiary amines, whereby aminoxides are generated [reaction (11.29), Scheme 5, on page 11].^{13,14,31,65}

In water, the reactions of ozone may differ considerably from those encountered in the gas phase and in organic solvents.^{24,97} Moreover, the high dielectric constant of water may allow electron-transfer reactions to occur [*e.g.* reaction (1.30), on page 11] which are not

possible in an organic solvent due to the lower solvation energies of the resulting radical ions (*cf.* Chapter 4).

The formation of $O_2(^1\Delta_g)$ may give important information, besides mechanistic aspects, on the formation of potential products that have escaped attention or could not be detected using conventional analytical methods. In the determination of the $O_2(^1\Delta_g)$ yield in aqueous solutions, a number of problems may arise as has been pointed out by Kanofsky and his group in their pioneering work.¹²

There are possible errors which may rise from the instability of the aqueous ozone stock solution. Therefore, repeated measurements of its ozone content were required. The $O_2(^1\Delta_g)$ yields are given in Table 3.

Table 3 $O_2(^1\Delta_g)$ yields in O_3 reactions in % of O_3 consumed at different pH and at various substrate/ O_3 ratios (in parentheses). The data are average values of at least five individual determinations (scatter less than $\pm 15\%$). The O_3 concentrations in these experiments were typically $(1-2) \times 10^{-4} \text{ mol dm}^{-3}$.

Substrate	PH	Yield / % (substrate : ozone)
<i>N,N</i> -Diethylaniline	8.5	7 (17:1)
<i>N,N,N',N'</i> -Tetramethylphenylenediamine	3.5	9 (3:1)
	6	4 (3:1)
Phenol	1.8	No signal (10:1)
	7	6 (10:1)
	9	9 (10:1)
	10	8 (10:1)
1,2-Dihydroxybenzene (Catechol)	7	14 (10:1)
1,4-Dihydroxybenzene (Hydroquinone)	7	16 (10:1)
1,3,5-Trihydroxybenzene (Phloroglucinol)	7	26 (10:1)
2,4,6-Trimethylphenol	7	10 (1:1)
	9	17 (10:1)
Pentachlorophenol	8	58 (1:1), 68 (10:1)
Pentabromophenol	8	48 (1:1), 59 (10:1)
2,4,6-Triiodophenol	9	19 (10:1)
1,2-Dimethoxybenzene		9 (1:1)
1,4-Dimethoxybenzene	7	6 (1:1)
1,3,5-Trimethoxybenzene	7	30 (1:1)

Table 3 continued

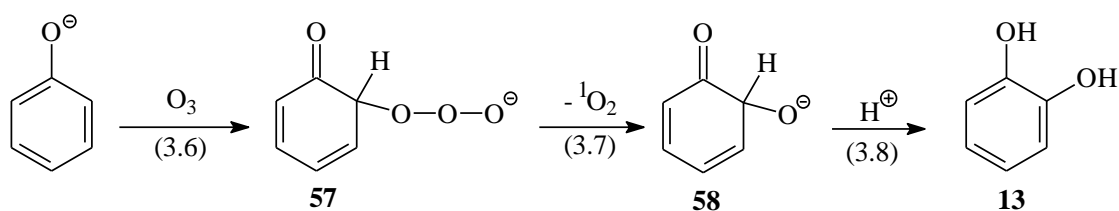
Bromide	7	Weak broad signal (40:1), 56 (400:1)
Iodide	7	12 (3:1)
Dihydrogen sulfide	7	16 (100:1)
	11	15 (100:1)
Methylsulfinate	10	96 (1.4:1)
1,4-Dithiothreitol	4.8	46 (38:1)
	7	22 (38:1)
	9	17 (38:1)
2,3-Dihydroxydithiane	7	105 (31:1)
Methionine	7	104 (42:1)

3.3 Mechanism leading to singlet dioxygen formation

3.3.1 Phenol and its derivatives

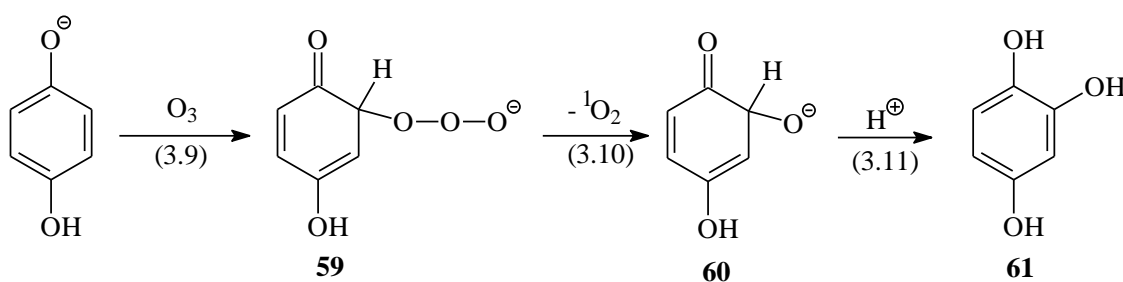
Phenolate reacts as much as six orders of magnitude faster with ozone than phenol.⁶⁹ Thus, even at pH ~7 (especially in the presence of a buffer that re-establishes the equilibrium upon phenolate depletion) the phenolate [$pK_a(\text{phenol}) = 10$] can be the dominating reactant. No $O_2(^1\Delta_g)$ has been observed in the reaction of phenol at pH 1.8, *i.e.* the formation of $O_2(^1\Delta_g)$ at pH 7 is most probable due to a reaction with the phenolate present in the equilibrium.

In view of its importance in water purification, the ozone chemistry of phenol has been widely studied,^{34,41,42,48,51,56,59} but it is not yet fully understood. At present, one can only speculate on the nature of the products that may be formed in the course of $O_2(^1\Delta_g)$ release, although catechol is the most likely ones [reactions (3.6)–(3.8)]. These products are indeed formed, but largely originate from a chain reaction involving $\bullet\text{OH}$ as intermediates (*cf.* Chapter 5)

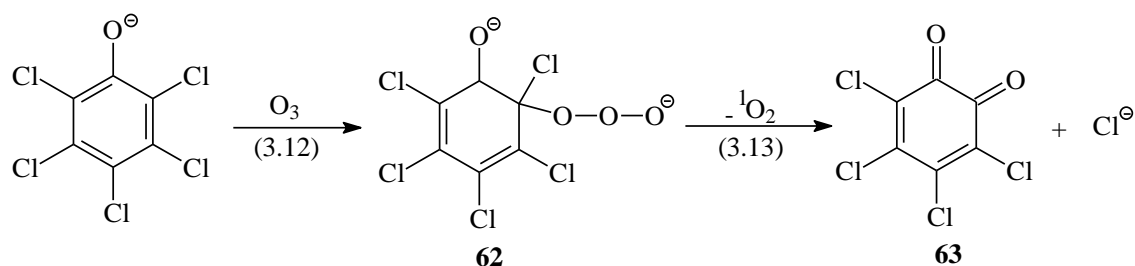


Phenols quench $O_2(^1\Delta_g)$ with rate constants of $\sim 10^6 \text{ dm}^3 \text{ mol}^{-1} \text{ s}^{-1}$. At the phenol concentration used in this experiment, this low quenching rate will not influence our $O_2(^1\Delta_g)$ yield at pH 7. Upon deportation, the resulting quenching rate constant raises to $1.8 \times 10^8 \text{ dm}^3 \text{ mol}^{-1} \text{ s}^{-1}$, *i.e.* quenching still has no effect at pH 9, but may have lowered our pH 10 value slightly.

The $O_2(^1\Delta_g)$ yields in the reaction of ozone with catechol and hydroquinone are higher than that with phenol (from data in Table 3). Apart from kinetic studies of the reaction of ozone with catechol and hydroquinone,³⁴ no mechanistic investigation has been carried out on these systems. Similar to phenol, $O_2(^1\Delta_g)$ release comes as a result of ozone addition to the hydroquinone [reactions (3.9)-(3.11)] in which the corresponding product, 1,2,4-trihydroxybenzene is formed. The fate of 1,2,4-trihydroxybenzene and other products formed in these systems is discussed in Chapter 6.

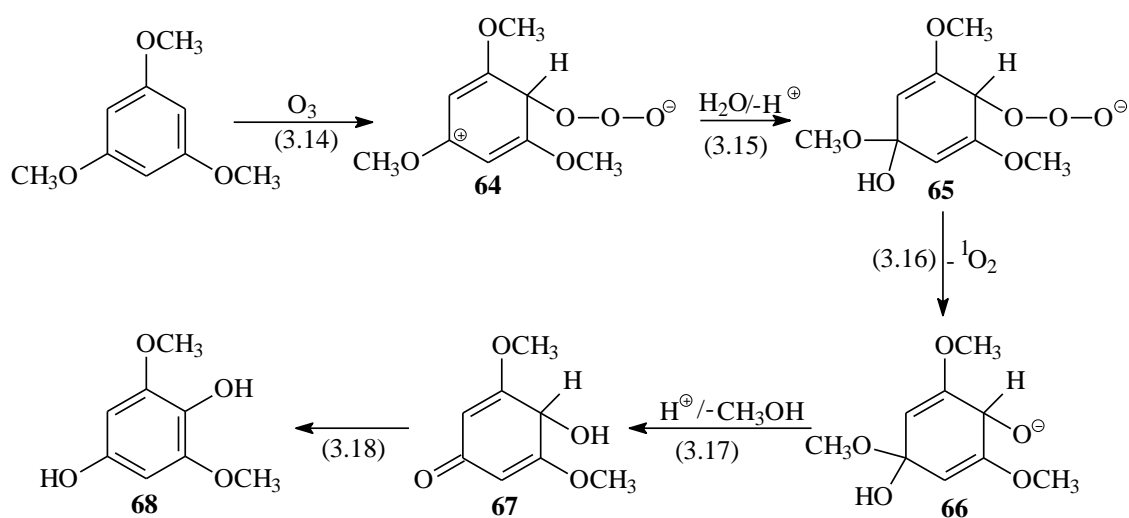


Much higher $O_2(^1\Delta_g)$ yields are observed with halogenated phenolates (Table 3). The electronegative nature of halogens reduces the electron density of the phenyl ring of halogenated phenols as compared to the parent phenol. This makes electron transfer reactions unfavourable, and the ozone addition reactions dominate. In the case of pentachlorophenol, the ozone attack at the *para*- or *ortho*- position, is followed by a Cl^- elimination (note that halogenide ions are good leaving groups) [reaction (3.12) and (3.13)]. The products formed as a result of $O_2(^1\Delta_g)$ released in this reaction are *o*-chloranil **63** and *p*-chloranil (not shown) which has also been identified. However, their subsequent hydrolysis in water releasing Cl^- have prevented their quantitative determination.⁹⁸ A similar reaction pathway is expected in case of pentabromophenol.



3.3.2 Methoxybenzenes

The $O_2(^1\Delta_g)$ yield in the reaction of 1,3,5-trimethoxybenzene (30%) is considerably higher than that of the 1,2-dimethoxybenzene (5%) and 1,4-dimethoxybenzene (6%). The pathway leading to the $O_2(^1\Delta_g)$ formation in the reaction of ozone with 1,3,5-trimethoxybenzene is shown in Scheme 6. Upon ozone addition at the *ortho*-positions, a zwitterion **64** is formed, whose positive charge is preferentially located at the methoxy-substituted carbon due to resonance stabilisation. The zwitterion **64** undergoes fast hydrolysis, forming a hemiacetal function [reaction (3.15), which in turn hydrolyses to a keto-function and methanol [reaction (3.17)]. This lead to the formation of 2,6-dimethoxyhydroquinone which was identified as one of the reaction products.



Scheme 6 The reaction of 1,3,5-trimethoxybenzene with ozone leading to the formation of $O_2(^1\Delta_g)$.

3.3.3 Bromide and iodide ions

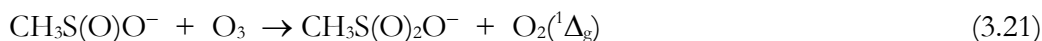
In the reaction of ozone with Br^- , $\text{O}_2(^1\Delta_g)$ is produced in a ~50% yield [reaction (3.19 a, b)], and in the case if I^- the $\text{O}_2(^1\Delta_g)$ yield is only ~18% [reaction (3.20 a, b)].



Reaction (3.19 a, b) is currently considered as the only primary process occurring in the Br^- system.⁹⁹⁻¹⁰² Since Br^- and I^- are poor $\text{O}_2(^1\Delta_g)$ quenchers [$k(\text{Br}^-) = 1 \times 10^6 \text{ dm}^3 \text{ mol}^{-1} \text{ s}^{-1}$; $k(\text{I}^-) = 7.2 \times 10^6 \text{ dm}^3 \text{ mol}^{-1} \text{ s}^{-1}$],⁹⁴ quenching cannot be the reason why the $\text{O}_2(^1\Delta_g)$ yield does not reach 100%. It has been shown by kinetic methods and *ab initio* calculations that the reaction of Br^- with ozone occurs via a steady-state intermediate BrOOO^- , where the first step is even reversible.¹⁰³ This low experimental $\text{O}_2(^1\Delta_g)$ yield is readily explained if the adducts (IOOO^- and BrOOO^-) are sufficiently long-lived to allow heavy-atom-assisted spin conversion and release of triplet (ground-state) dioxygen. This effect would be more pronounced with I^- than with the lighter Br^- , as observed. In the corresponding reaction with I^- , such a heavy atom effect should be even more pronounced. Indeed, the $\text{O}_2(^1\Delta_g)$ yield is even lower in this system. The reaction of ozone with I^- is one of the standard methods for measuring O_3 concentrations. In this assay, I_2 is determined.^{104,105} Its yield has been in dispute, *cf.* ref.¹⁰⁶, although there seems to be now a general agreement that the stoichiometry is 1:1. The low $\text{O}_2(^1\Delta_g)$ yield found in this study may be the basis for studying again mechanistic details of this interesting and certainly complex reaction.

3.3.4 Sulfur-containing compounds

The methanesulfinate ion reacts rapidly with O_3 by O-transfer to methanesulfonate and $\text{O}_2(^1\Delta_g)$ [reaction (3.21); $k = 2 \times 10^6 \text{ dm}^3 \text{ mol}^{-1} \text{ s}^{-1}$].⁸³ An electron transfer reaction that would give rise to a very efficient chain reaction is not observed.⁸³



The sulfide methionine reacts very rapidly with O_3 ($k = 1.8 \times 10^6 \text{ dm}^3 \text{ mol}^{-1} \text{ s}^{-1}$),¹⁰⁷ the $\text{O}_2(^1\Delta_g)$ yield being practically 100% (*cf.* Table 3 and ref.¹²) [reaction (1.9)]. Its sulfoxide has

Error! Use the Home tab to apply Überschrift 1 to the text that you want to appear here.
Error! Use the Home tab to apply Überschrift 1 to the text that you want to appear here.

been reported as the only detected product,¹⁰⁸ and in this work, it was confirmed that the methionine sulfoxide yield is indeed 100% (Figure 12).

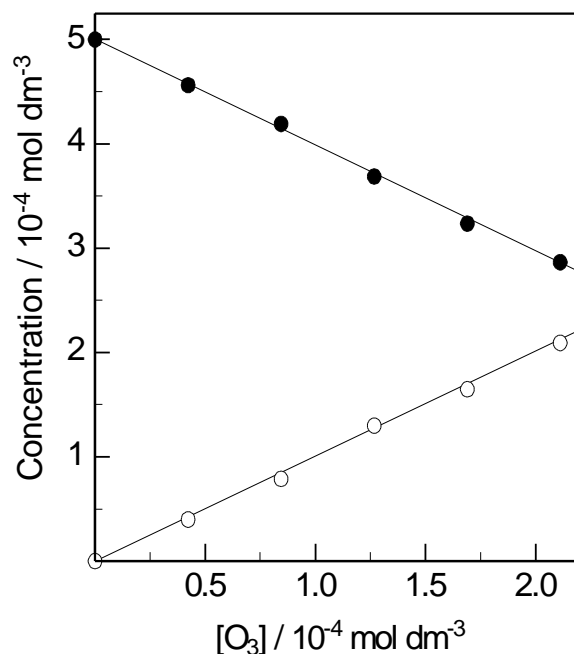


Figure 12 Reaction of ozone with methionine at pH 3. Consumption of methionine and formation of its sulfoxide as a function of the ozone concentration.

The disulfide 2,3-dihydroxydithiane **69** in its reaction with ozone gives also rise to 100% $O_2(^1\Delta_g)$ [reaction (3.22)]. The rate constant of this reaction was determined by competition kinetics as described in section 2.6.2. From the slope of the competition plot (Figure 13) a rate constant of $k = 2.1 \times 10^5 \text{ dm}^3 \text{ mol}^{-1} \text{ s}^{-1}$ is obtained.

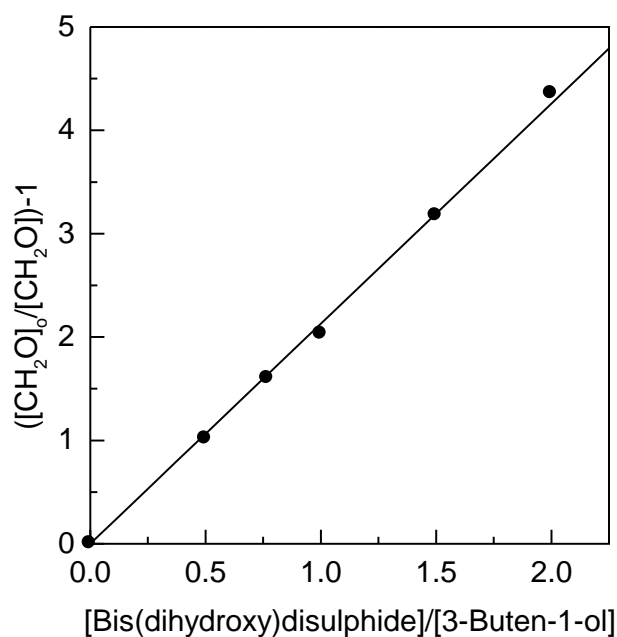
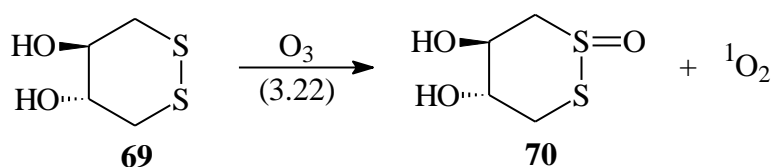


Figure 13 Plot of the competition of 3-buten-1-ol with 2,3-dihydroxydithiane at pH 7 for the reactions of ozone. Formaldehyde yields result from the reaction of ozone with 3-buten-1-ol.



This reaction is notably faster than the rate constant of ozone with cystine for which a value of $550 \text{ dm}^3 \text{ mol}^{-1} \text{ s}^{-1}$ has been reported.⁶⁹ In order to see whether the reaction of 2,3-dihydroxydithiane is unusually high, the rate constant for bis(dihydroxyethyl)sulfide was also determined using the same method, whereby a value of $1.7 \times 10^5 \text{ dm}^3 \text{ mol}^{-1} \text{ s}^{-1}$ for this disulfide was obtained from the slope of the competition plot (Figure 14), *i.e.* we have no explanation for the low rate of reaction reported for cystine. In both cases in our experiment, the final products are the corresponding *S*-alkyl sulfinates, corroborating that the ozone reaction proceeds by O-transfer.

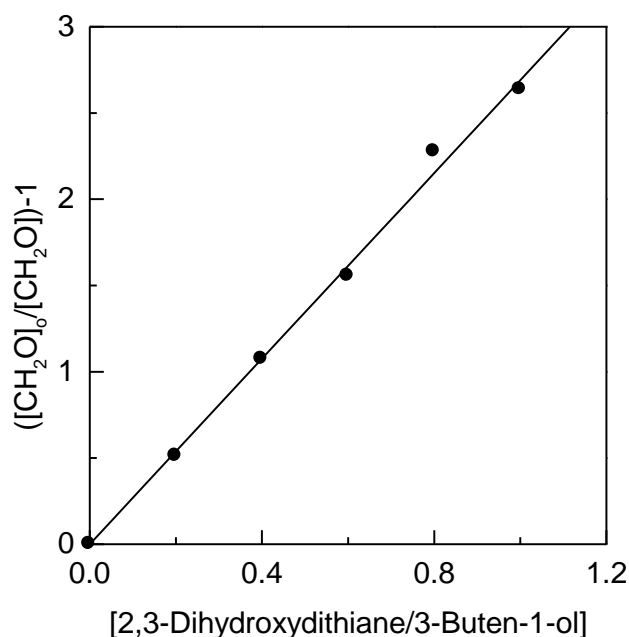


Figure 14 Plot of the competition of 3-buten-1-ol with bis(dihydroxyethyl)sulfide at pH 7 for the reactions of ozone. Formaldehyde yields result from the reaction of ozone with 3-buten-1-ol.

Compared with sulfides and disulfides, thiols show relatively low $O_2(^1\Delta_g)$ yields (< 50%), especially when deprotonated [$pK_a(H_2S) = 7.0$; $pK_a(1,4\text{-dithiothreitol}) = 9.1, 10.5$]. The rate constant of the reaction H_2S with ozone is $3 \times 10^4 \text{ dm}^3 \text{ mol}^{-1} \text{ s}^{-1}$ while that of HS^- is $9 \times 10^9 \text{ dm}^3 \text{ mol}^{-1} \text{ s}^{-1}$.⁷² Thus, thiolates react much more readily with ozone than thiols,⁶⁹ and changes in $O_2(^1\Delta_g)$ yields are already observed in a pH range where the thiol still predominates. A case in point is 1,4-dithiothreitol which shows a strong drop in the $O_2(^1\Delta_g)$ yield on going from pH 4.8 to 7.

For H_2S , this phenomenon can be well explained by using the pK_a values to calculate the extent of dissociation of H_2S [equations (3.23) and (3.24)] as well as the rate constant of the reaction of ozone with H_2S as a function of pH [equation (3.25)]:

$$\alpha_p = \frac{1}{1 + 10^{pH - pK}} \quad (3.23)$$

$$\alpha_d = 1 - \alpha_p \quad (3.24)$$

$$k_{pH} = k_p \alpha_p + k_d \alpha_d \quad (3.25)$$

where, α_p and α_d are the degree of protonation and dissociation, respectively, and the k_p and k_d are rate constants of the direct reactions of ozone with H_2S and HS^- , respectively.

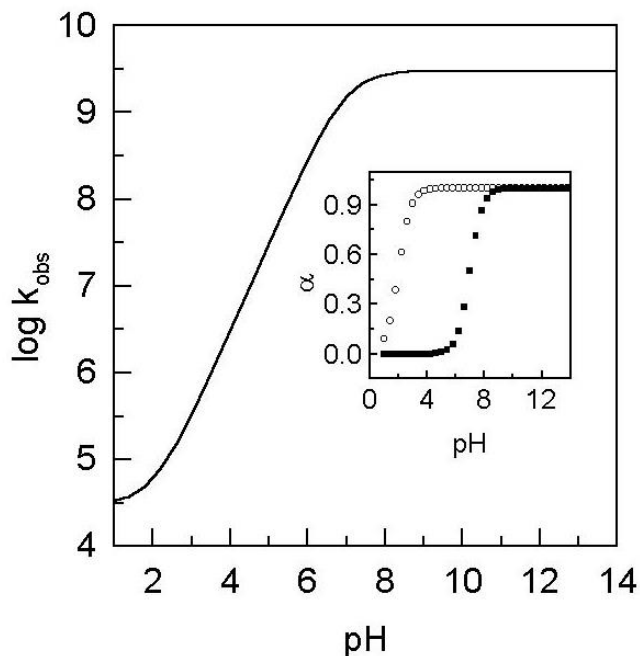


Figure 15 Variation of $\log k(\text{O}_3 + \text{H}_2\text{S})$ with pH. Inset: The pK curve of H_2S , fraction of HS^- in aqueous solution (ν) and the “reactivity pK” curve, the fraction of HS^- reaction with ozone (μ).

As shown in Figure 15, at pH above 4, ozone reacts primarily with the dissociated form of H_2S , namely the HS^- hence the yield of $\text{O}_2(^1\Delta_g)$ is low. This low $\text{O}_2(^1\Delta_g)$ yield has, of course, a bearing on the reactions of O_3 with, *e.g.*, H_2S , where it has been noted that sulfate is formed as the only detectable product. Interestingly, this reaction needs only ~ 2.3 mol ozone per mol H_2S .⁶⁸ This stoichiometry requires that an efficient chain reaction must occur.

4 DETECTION OF HYDROXYL AND SUPEROXIDE RADICALS AS WELL AS HYDROPEROXIDES

4.1 Introduction

In section 1.2, different types of ozone reactions in aqueous solution are presented, two of which lead to the formation of free radicals, i.e. $O_3^{\bullet-}$ [by electron transfer, reaction (4.1)] and $O_2^{\bullet-}$ [by an addition / elimination process, reaction (4.2)]. Both processes lead to the formation of $\bullet OH$ [cf. reactions (1.5)–(1.6), see Chapter 1].



The situation can become very complex at low substrate concentrations, since $\bullet OH$ reacts rapidly with ozone ($k = 1 \times 10^8 \text{ dm}^3 \text{ mol}^{-1} \text{ s}^{-1}$)¹⁰⁹ and thus can initiate a chain reaction with $HO_2^{\bullet}/O_2^{\bullet-}$ as intermediates.¹¹⁰ This chain reaction may lead to an unwanted self-destruction of ozone, similar to the OH^- -induced decomposition of ozone.

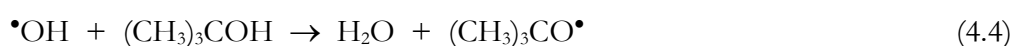
For a better understanding of ozone reactions in water, $\bullet OH$ and $O_2^{\bullet-}$ yields have to be known. More than 50 years of radiation chemistry has provided a great deal of knowledge about reactivity and detection of free radicals.^{11,11,80,110,111,111} In the γ -radiolysis of water $\bullet OH$ and other free radicals are formed. The radiation-chemical yields (G values) of the primary radicals are $G(\bullet OH) \approx G(e_{aq}^-) = 2.8 \times 10^{-7} \text{ mol J}^{-1}$, $G(H^{\bullet}) = 0.6 \times 10^{-7} \text{ mol J}^{-1}$, and $G(H_2O_2) \approx 0.7 \times 10^{-7} \text{ mol J}^{-1}$. Of the large number of known reactions of $\bullet OH$ with various compounds, a few are used in radiation chemistry for the detection of $\bullet OH$, e.g. the reaction with $FeSO_4$ (Fricke-dosimetry).⁷³ The Fricke-dosimetry is used in radiation chemistry for the determination of the dose rate of the gamma source.⁷³ Although $O_2^{\bullet-}$ is not a primary product in the γ -radiolysis of water, it is often formed in $\bullet OH$ -induced peroxy radical reactions and as a result its reactivity has also been extensively studied.¹¹²⁻¹¹⁵ Tetranitromethane (TNM) is used for the detection of $O_2^{\bullet-}$ (section 4.1.3).

For the application of the above methods to ozone reactions, compounds which do not readily react with ozone (ozone refractory compounds) must be used. Unfortunately, $FeSO_4$ reacts very fast with ozone, and is thus not suitable for the detection of $\bullet OH$ in the

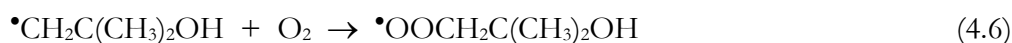
ozone reactions. We have identified two ozone refractory compounds that may be used for the detection of $\bullet\text{OH}$ in the ozone reactions, 2-methyl-2-propanol and dimethylsulfoxide. 2-Methyl-2-propanol reacts very fast with $\bullet\text{OH}$ ($k = 6 \times 10^8 \text{ dm}^3 \text{ mol}^{-1} \text{ s}^{-1}$)⁸⁰ and only very slowly with ozone ($k = 1 \times 10^{-3} \text{ dm}^3 \text{ mol}^{-1} \text{ s}^{-1}$), while DMSO reacts relatively faster with $\bullet\text{OH}$ ($k = 6.5 \times 10^9 \text{ dm}^3 \text{ mol}^{-1} \text{ s}^{-1}$) and with ozone at a rate constant of $8.2 \text{ dm}^3 \text{ mol}^{-1} \text{ s}^{-1}$. The mechanism of reaction of $\bullet\text{OH}$ with 2-methyl-2-propanol and with DMSO are presented in sections 4.1.1 and 4.1.2, respectively. Similarly, an ozone refractory compound should also be used for the $\text{O}_2^{\bullet-}$ detection. However, little is known about the reaction of TNM with ozone. In order to establish whether TNM is suitable for the detection of $\text{O}_2^{\bullet-}$ in ozone reaction, the rate constant of the reaction of ozone with $\text{C}(\text{NO}_2)_4$ was investigated and also with the ensuing product, the nitroform anion. Results of this investigation are given in section 4.3.1.

4.1.1 The reaction of 2-methyl-2-propanol with the hydroxyl radical

Hydroxyl radicals react with 2-methyl-2-propanol by abstracting an H-atom mainly from carbon (95%) [reaction (4.3)] and to a much lesser (~5%) extent from oxygen [reaction (4.4)].¹¹⁶ The tertiary butoxyl radical rapidly decomposes by β -fragmentation into acetone and a methyl radical (reaction 4.5, $k = 1.4 \times 10^6 \text{ s}^{-1}$).¹¹⁷

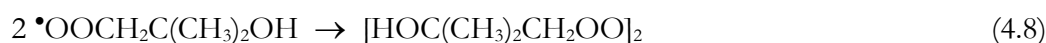


In the presence of dioxygen, the alkyl radicals add dioxygen yielding the corresponding peroxy radicals [reactions (4.6) and (4.7)]. As with other simple alkyl radicals,^{118,119} the rate of these reactions must be close to diffusion controlled ($k \approx 2 \times 10^9 \text{ dm}^3 \text{ mol}^{-1} \text{ s}^{-1}$).



The chemistry of methylperoxy radical has been investigated in some detail¹¹⁸, but since it plays only a minor role here, it will be no longer discussed.

The alkyl peroxy radicals decay bimolecularly, whereby a tetroxide is formed as a short-lived intermediate [reaction (4.8)] (for a review on peroxy radical reaction in aqueous solution see ref. ¹¹⁸). In the case of the 2-methyl-2-propanol-derived peroxy radicals, three main pathways of the decay of the tetroxide have been recognised. Reaction (4.9) leads to dioxygen, 2-methyl-2-hydroxypropanol and 2-methyl-2-hydroxypropanal, while reaction (4.10) gives rise to hydrogen peroxide and two mol 2-methyl-2-hydroxypropanal. These reactions are concerted processes and do not proceed *via* free-radical intermediates. The third reaction pathway leads to the formation of two mol formaldehyde, one mol dioxygen and two mol 2-hydroxyprop-2-yl radicals [reaction (4.11)], possibly *via* the oxyl radical $\text{HOC}(\text{CH}_3)_2\text{CH}_2\text{O}^\bullet$. The 2-hydroxyprop-2-yl radical adds readily dioxygen [reaction (4.12)], and this reaction is followed by a fast elimination of HO_2^\bullet .¹²⁰



The yields of the main products, formaldehyde, acetone, 2-methyl-2-hydroxypropanal and 2-methyl-2-hydroxypropanol have been determined in the radiolytic study.⁸¹

However, the formation of considerable amounts of $\text{HO}_2^\bullet/\text{O}_2^{\bullet-}$ in this system which also interact with the 2-methyl-2-propanol-derived peroxy radicals (*e.g.* the formation of an organic (hydro)peroxide has also been detected) prevents a quantitative comparison with the present system, where any $\text{O}_2^{\bullet-}$ formed in the course of the 2-methyl-2-propanol-derived peroxy radicals are immediately converted into further $\bullet\text{OH}$ by ozone [see reaction (1.8)]. In the radiolytic system, the formaldehyde yield was found to be ~25% of $\bullet\text{OH}$, and the ratio of the 2-hydroxy-2-methylpropanal and formaldehyde yields was ~1.5.⁸¹ Since there are other $\bullet\text{OH}$ reactions whose products are easier to determine, 2-methyl-2-propanol has not been often used for the detection of $\bullet\text{OH}$ in radiation chemistry studies.

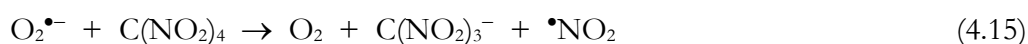
4.1.2 The reaction of DMSO with the hydroxyl radical

In the reaction of $\bullet\text{OH}$ with dimethylsulfoxide (DMSO), methanesulfinic acid is formed in 92% yield [reaction (4.14)].⁸²



4.1.3 The reaction of TNM with the superoxide radical

TNM reacts with $\text{O}_2^{\bullet-}$ yielding nitroform anion [reaction (4.15)]⁸⁵, a substance with a strong absorption 350 nm ($\epsilon = 15000 \text{ dm}^3 \text{ mol}^{-1} \text{ cm}^{-1}$).⁸⁵



Nitroform anion is relatively easy to determine, for this reason it has been used as the standard method for the detection of in radiation chemistry.^{113,114}

4.2 Detection of $\bullet\text{OH}$ in the ozone reactions

4.2.1 The 2-methyl-2-propanol system

The addition of a large excess of 2-methyl-2-propanol allows us to scavenge all $\bullet\text{OH}$ and to follow the reaction by measuring one of the ensuing products, formaldehyde, as described in section 2.5.1.

We have now determined the formaldehyde yield in the ozone reactions with various compounds in the presence of 2-methyl-2-propanol system. The data are presented in Table 4. The reaction of ozone with hydrogen peroxide [reaction (4.16)] in the presence of 2-methyl-2-propanol was used as a good estimate for the formation of formaldehyde yield and hence $\bullet\text{OH}$ radicals. Here, the formaldehyde and 2-hydroxy-2-methylpropanal yields in the ozone / hydrogen peroxide / 2-methyl-2-propanol system was determined (variation of $[\text{H}_2\text{O}_2] = 5 \times 10^{-4} \text{ mol dm}^{-3}$ and $1 \times 10^{-3} \text{ mol dm}^{-3}$; $[2\text{-methyl-2-propanol}] = 1 \times 10^{-2} \text{ mol dm}^{-3}$ and $2 \times 10^{-2} \text{ mol dm}^{-3}$, respectively).



According to our experience, yield data in ozone reactions are fraught with a somewhat higher intrinsic error (poorer dose yield plots, poorer day-to-day reproducibility) than

radiolytic yield data. Because of the importance of these data for establishing an $\bullet\text{OH}$ probe in ozone reactions, these yields were measured many times and $(30\pm 4)\%$ for the formaldehyde yield (*cf.* Figure 16) and a value of 1.3–1.4% for the 2-hydroxy-2-methylpropanal to formaldehyde ratio were obtained.

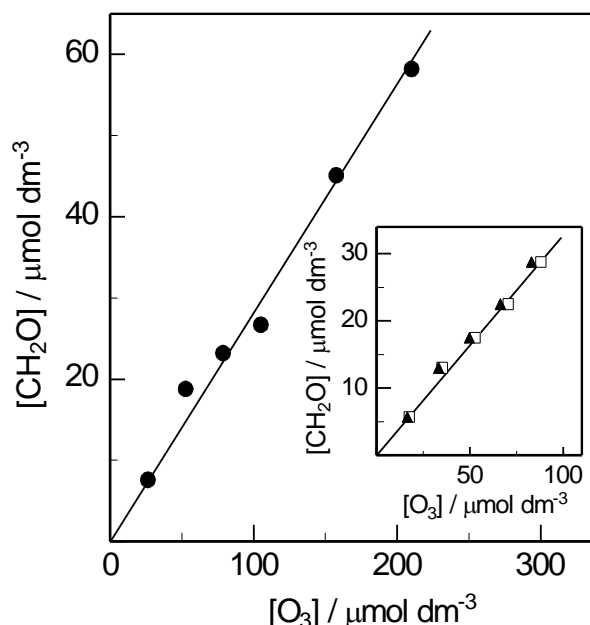


Figure 16 Formation of formaldehyde in the reaction of ozone with H_2O_2 ($5 \times 10^{-4} \text{ mol dm}^{-3}$) in the presence of 2-methyl-2-propanol ($1 \times 10^{-2} \text{ mol dm}^{-3}$). Formaldehyde yield determined by the 2,4-dinitrophenylhydrazone method. Inset: Formaldehyde yields determined by the Hantzsch method; determination of the ozone concentration before (\circ) and after (σ) preparing the samples.

Table 4 Formaldehyde yields in ozone reactions in % of ozone consumed at different pH in the presence of 2-methyl-2-propanol. The substrate and 2-methyl-2-propanol concentrations in these experiments were typically $1 \times 10^{-3} \text{ mol dm}^{-3}$ and 0.1 mol dm^{-3} respectively.

Substrate	pH	Formaldehyde Yield / %	$\bullet\text{OH}$ Yield / % *
<i>N,N</i> -Diethylaniline	7	13	27 ± 4.5
<i>o</i> -Phenylenediamine	7	14	29 ± 4.8
Diethylphenylenediamine	7	27	56 ± 9
<i>N,N,N',N'</i> -Tetramethylphenylenediamine	7	34	70 ± 11
Phenol	3	11	22 ± 3.8
Phenol	7	13	27 ± 4.5

Table 4 continued

Phenol	10	11	22±3.8
1,2-Dihydroxybenzene (Catechol)	7	11	22±3.8
1,4-Dihydroxybenzene (Hydroquinone)	7	20	42±7
2,6-Dimethylphenol	7	13	27±4.5
Pentachlorophenol	10	13	27±4.5
Pentabromophenol	10	1	2±0.3
2,4,6-Triiodophenol	10	0	0
1,2-Dimethoxybenzene	7	6.4	13±2.2
1,4-Dimethoxybenzene	7	10	20±3.5
1,3,5-Trimethoxybenzene	7	7.4	15.4±2.5
Bromide	7	0	0
Iodide	7	0	0

*Based on the correction factor of 0.48 ± 0.08 as described in section 4.2.2

4.2.2 Factors to be taken into account in the determination of $\bullet\text{OH}$ in ozone reactions with the 2-methyl-2-propanol / formaldehyde assay

It has been shown above, that in the reaction of $\bullet\text{OH}$ with 2-methyl-2-propanol, the formation of formaldehyde is connected with the concomitant release of $\text{O}_2^{\bullet-}$. Since the latter reacts rapidly with ozone giving rise to further $\bullet\text{OH}$, this additional source of formaldehyde has to be taken into account when the primary $\bullet\text{OH}$ yield is calculated from such data. In the above study, $\bullet\text{OH}$ was generated by the reaction of ozone with an excess of H_2O_2 , *i.e.* it did not matter if any $\text{O}_2^{\bullet-}$ gave rise to $\bullet\text{OH}$ *via* its reaction with ozone or whether $\bullet\text{OH}$ formation was entirely due to the reaction of ozone with H_2O_2 . However, in any other system, the formaldehyde yield will be higher than the above value of $(30 \pm 4)\%$ per one mol primary $\bullet\text{OH}$ due to the short chain reaction. The relationship between the yield of the chain carrier forming reaction (x) and the total yield of chain reaction product (y), $y = x/(1-x)$, was established solving the initial value problem of the set of ordinary differential equations modelling the reaction mechanism and taking the lines to infinite time. Applied to our system, a correction factor of 0.48 ± 0.08 is obtained by which the

measured formaldehyde yield has to be divided to arrive at the precursor •OH yield, i.e. as a rule of thumb one can take twice the formaldehyde yield. Usually, the •OH yield is low (<20%), and ozone depletion due to the secondary formation of •OH in this assay can be neglected.

4.2.3 The dimethylsulfoxide system

Detection of •OH yield using DMSO was carried out as described in section 2.5.1. Here, methanesulfinic acid and methanesulfonic acid were detected by ion chromatography. The yields of methanesulfinic acid and methanesulfonic acid in the reactions of ozone with various compounds in the presence of DMSO are given in Table 5. These data show that the determination of methanesulfonic acid is a prerequisite for the exact determination of •OH yields in ozone reactions by the DMSO method. In fact, major parts of methanesulfinic acid formed may be further oxidised, possibly induced by peroxy radicals. The data obtained from the DMSO system correlate very well with those from 2-methyl-2-propanol (Tables 4 and 5). Due to the relatively high reactivity of DMSO toward ozone, the use of DMSO for the detection of •OH is only suitable in system where the rate constant of the reaction ozone with the substrate is high. Under such conditions, the DMSO and 2-methyl-2-propanol methods can be used to support each other.

Table 5 Methanesulfinic and methanesulfonic acid yields in ozone reactions in % of ozone consumed at different pH in the presence of DMSO. The substrate and DMSO concentrations in these experiments were typically $1 \times 10^{-3} \text{ mol dm}^{-3}$ and $5 \times 10^{-2} \text{ mol dm}^{-3}$ respectively.

Substrate	pH	Methanesulfi nic acid Yield / %	Methanesulfo nic acid Yield / %	Sum / %	•OH Yield / % *
Phenol	10	16	4	20	27±4.5
1,2-Dihydroxybenzene	7	22	0	22	22±3.5
1,4-Dihydroxybenzene	7	27	6	33	42±7

* •OH yields obtained from the 2-methyl-2-propanol system.

4.2.4 Conditions for the formation of •OH in ozone reactions.

It has been mentioned above that •OH may be formed in an electron-transfer process [reaction (4.1)]. This reaction has always to compete with other reactions that are available to ozone. Here, we are concerned with the question to what extent electron transfer occurs in aqueous solution and which reactions compete with this process. In Table 6 for a number of substrates, the •OH yields calculated from formaldehyde yields in the presence of an excess 2-methyl-2-propanol, together with the substrate reduction potentials at pH 7 are given. The low reduction potential of ozone $E^7(\text{O}_3^{\bullet-}/\text{O}_3) = 1.01 \text{ V}^{15}$ has consequences as to the mechanism of the formation of •OH in ozone reactions, *i.e.* electron transfer *vs.* more complex mechanisms, *e.g.*, *via* $\text{O}_2^{\bullet-}$, as •OH formation is also observed with many compounds whose reduction potentials are considerably higher than 1.01 V. This low reduction potential does certainly not allow the conclusion¹²¹ that the Criegee mechanism for the reactions of ozone with olefins has to be revised and proceeds by an electron transfer in the first step, although the rate constants of the ozone reaction and the gas phase ionisation potentials of selected (electron rich) olefins correlate.¹²¹ This correlation only reflects the electrophilic nature of ozone. Even •OH which has a higher reduction potential than ozone [$E^7(\text{OH}^-/\bullet\text{OH})=1.9 \text{ V}$],¹⁵ •OH reacts mainly by addition reaction.^{53,54,122,123} For example in the reaction of ozone •OH with substrate having lower reduction potential, 1,4-dimethoxybenzene (1.3V),¹²⁴ *p*-anisidine (1.03)¹⁵ and *p*-phenylenediamine (0.73),¹⁵ the electron transfer component is only 6, 30 and 85% respectively.¹²⁵ This implies that electron transfer reactions compete with other reactions *e.g.* •OH addition to the ring.

The reduction potential for the substrate given in Table 6 are for pH 7. In some cases the measured value could not be found in the literature hence they have to be calculated from equations (4.17) and (4.18) for monoprotic and diprotic substances, respectively:

$$E^{\text{pH}} = E^o + \frac{RT}{F} \ln(10^{-\text{p}K} + 10^{-\text{pH}}) \quad (4.17)$$

$$E^{\text{pH}} = E^o + \frac{RT}{F} \ln(10^{-(\text{p}K_1+\text{p}K_2)} + 10^{-(\text{p}K_1+\text{pH})} + 10^{-2\text{pH}}) \quad (4.18)$$

Where R is the general gas constant, T is the absolute temperature, F is the Faraday constant and E^o is the standard potential.

Error! Use the Home tab to apply Überschrift 1 to the text that you want to appear here.

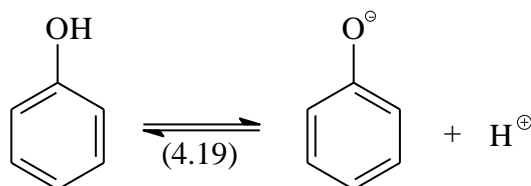
Error! Use the Home tab to apply Überschrift 1 to the text that you want to appear here.

Table 6 Yields of $\bullet\text{OH}$ in the reactions of ozone with a number of ozone-reactive substrates and the reduction potential of the substrates at pH 7.

Substrate	pK_a	E^7 / mV	$\bullet\text{OH}$ yield / %
N,N,N',N' - Tetramethylphenylenediamine	2.5 6.05	240 ref. ¹⁵	70±11
<i>o</i> -Phenylenediamine	0.6	342 (pH 13.5) ref. ¹⁵	29±4.8
	4.7	342*	
Hydroquinone	9.91 11.56	451 ref. ¹⁵	42±7
Catechol	9.25 12.37	530 ref. ¹⁵	22±3.8
N,N -Diethylaniline	5.6	860 (pH 9.6) ref. ¹⁵ 861*	27±4.5
Phenol	10	860 ref. ¹⁵	27±4.5
1,4-Dimethoxybenzene	-	1300 ref. ¹²⁴	20±3.5
Bromide	-	2000 ref. ¹⁵	0
Adenine	-	1420 ref. ¹²⁶	42±7
1,2-Dimethoxybenzene	-	1440 ref. ¹²⁴	13±2.2
Anisole	-	1620 ref. ¹²⁴	8.5±1.4
Iodide	-	1400 ref. ¹⁵	0

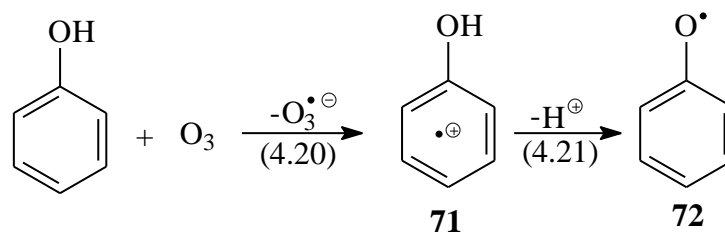
*Calculated for pH 7

For the reaction of phenol with ozone at pH 7 or higher, one has to take the phenolate into consideration. At high pH, phenol dissociates [equilibrium (4.19), $\text{pK}_a = 10$].



The $\bullet\text{OH}$ yields in the reaction of ozone with phenol are pH independent even at pH 3, where phenol dominates over phenolate, $\bullet\text{OH}$ radicals are formed. At low pH, phenol reacts with ozone forming a radical cation **71** [reaction (4.20)]. The phenol radical cation deprotonates rapidly into a phenoxy radical **72** [reaction (4.21)].⁴⁶ While in the case of

phenolates, phenoxyl radical is directly formed. The same reaction sequence may be written for the other phenols.



4.3 Detection of superoxide in ozone reactions

4.3.1 Reaction of tetranitromethane and nitroform anion with ozone

In order to use this method as a tool for detecting $O_2^{\bullet-}$ formation in ozone reaction, it is important to investigate the reactivity of TNM and nitroform (the ensuing product of TNM and $O_2^{\bullet-}$) toward ozone. TNM reacts slowly with ozone. The reaction has been followed spectrophotometrically at 260 nm as well as by changes in conductance as a function of time. From these data, rate constants of $k = 10.2 \text{ dm}^3 \text{ mol}^{-1} \text{ s}^{-1}$ (conductometry) and $9.9 \text{ dm}^3 \text{ mol}^{-1} \text{ s}^{-1}$ (spectrophotometry) are calculated.¹²⁷

Using the stopped-flow technique, the decay of the $C(NO_2)_3^-$ at 350 nm was followed in the presence of a large excess of ozone, where a rate constant of $k = 1.4 \times 10^4 \text{ dm}^3 \text{ mol}^{-1} \text{ s}^{-1}$ was obtained. The $C(NO_2)_3^-$ used in that study was prepared by the hydrolysis of TNM. Nitrite ion which is a major product and reacts very fast with ozone had to be destroyed by ozonation prior to a determination of the rate constant for the reaction of ozone with the $C(NO_2)_3^-$. The remaining nitrite concentration was ~3% of that of the $C(NO_2)_3^-$.¹²⁷ The high rate constant of ozone reaction with the $C(NO_2)_3^-$ has to be taken into consideration when using TNM for the detection of $O_2^{\bullet-}$ in ozone reactions.

4.3.2 The tetranitromethane/nitroform anion system

Nitroform anion yields in reactions ozone with various compounds have been measured and are presented in Table 7. The combined results of $\bullet OH$ and $O_2^{\bullet-}$ measurements can be very useful to distinguish between electron transfer reactions and addition/elimination

Error! Use the Home tab to apply Überschrift 1 to the text that you want to appear here.

Error! Use the Home tab to apply Überschrift 1 to the text that you want to appear here.

reactions. The addition/elimination reactions between ozone and a phenolic compounds [reaction (4.22)-(4.23)] in which HO_2^\bullet is released could be one of the $\text{O}_2^{\bullet-}$ sources.

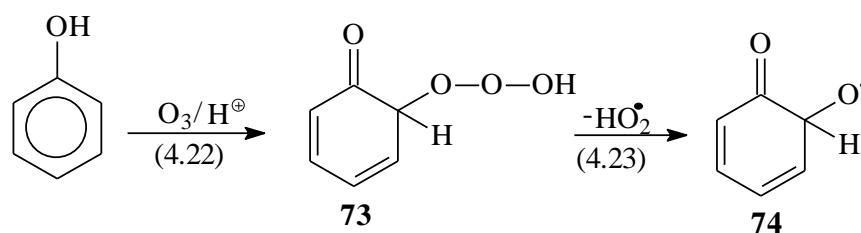
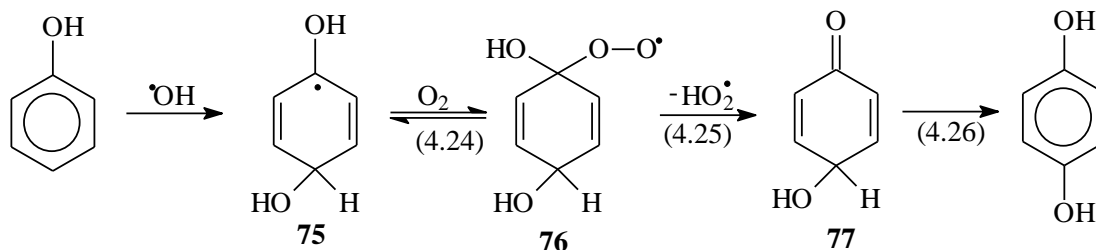


Table 7 Nitroform anion yields in ozone reactions in % of ozone consumed at different pH in the presence of TNM. The substrate and TNM concentrations in these experiments were typically both $1 \times 10^{-3} \text{ mol dm}^{-3}$.

Substrate	pH	$\text{C}(\text{NO}_2)_3^-$ Yield (%)
Phenol	3	3
Phenol	4	19.5
1,2-Dimethoxybenzene	7	4
1,4-Dimethoxybenzene	7	9
1,3,5-Trimethoxybenzene	7	10

In the reaction of ozone with phenol, the $\text{O}_2^{\bullet-}$ yields are higher at pH 4 (19.5%) than at pH 3 (3%) (*cf.* Figure 17). In addition the $\text{O}_2^{\bullet-}$ yield at pH 4 is similar to that of $^\bullet\text{OH}$. This suggest that, $\text{O}_2^{\bullet-}$ is not formed as a result of reaction (4.23), but it is due to the $^\bullet\text{OH}$ attack on phenol followed by dioxygen addition [reaction (4.24)-(4.26)] (see Chapter 5 for more details). This is an important result as it rules out the possibility of reaction (4.22) as has been suggested in earlier studies.¹²⁸⁻¹³⁰ A detailed mechanism of the $^\bullet\text{OH}$ reaction with phenol is given in section 5.2.



In the reaction of ozone with methoxybenzenes, it is not conclusive as to whether the formation of $\text{O}_2^{\bullet-}$ occurs as result of direct ozone reaction, *e.g.*, the reaction of 1,4-dimethoxybenzene with ozone [reaction (4.27)-(4.29)] or by electron transfer reaction. Although the yields of $\text{O}_2^{\bullet-}$ in these systems are low (from 6% in 1,2-dimethoxybenzene to

Error! Use the Home tab to apply Überschrift 1 to the text that you want to appear here.
 Error! Use the Home tab to apply Überschrift 1 to the text that you want to appear here.

10% in 1,3,5-trimethoxybenzene), (*cf.* Table 7), they are of importance for understanding of the reaction mechanism. Details on the ozonolysis of methoxybenzenes are discussed in Chapter 8.

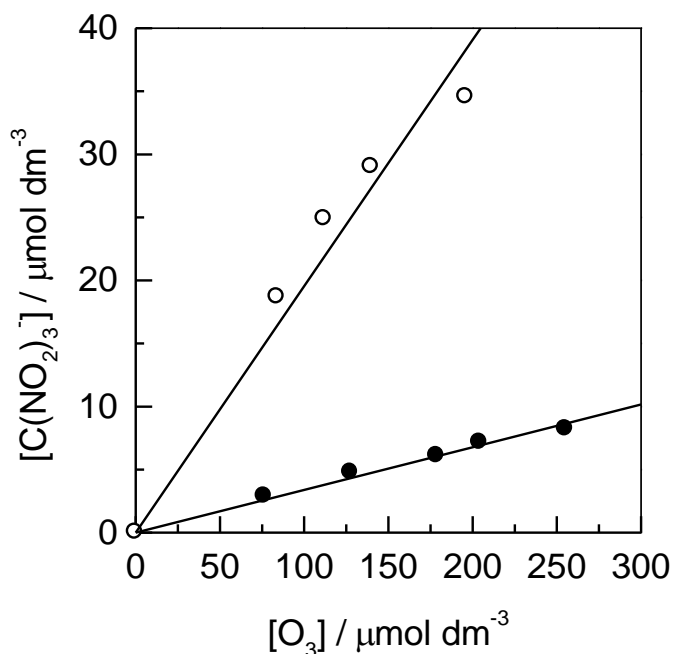
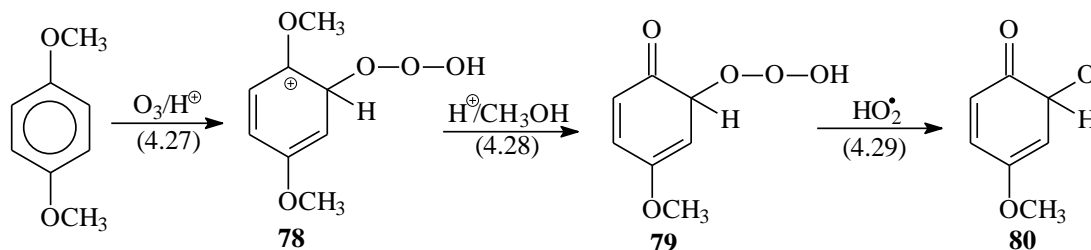


Figure 17 Ozonolysis of phenol in the presence of TNM, yields of nitroform anion at pH 3 (λ) and pH 4 (μ).

4.3.3 Difficulties in the use of tetranitromethane for the detection of superoxide in ozone reactions

The first question that should be answered before applying TNM for the detection of $\text{O}_2^{\bullet-}$ is as to whether TNM reacts with the substrate or with the ensuing products (other than $\text{O}_2^{\bullet-}$) in the ozone reactions. Being an oxidising agent, TNM does not only react with reducing radicals such as $\text{O}_2^{\bullet-}$, but may also react with some reducing compounds. A case

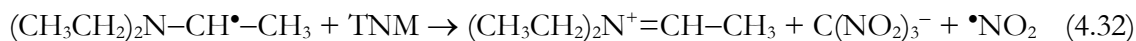
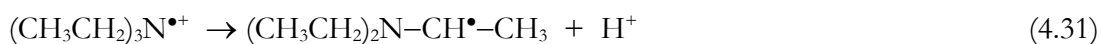
in point is the reaction of TNM with hydroquinone. At natural pH, the reaction of TNM with hydroquinone is quite fast, but relatively slow at pH 4 or lower. Hydroquinone is one of the products in the reaction of ozone with phenol. Therefore, $O_2^{\bullet-}$ measurements using TNM assay were only possible at pH 4 or below.

In $\bullet OH$ -induced peroxy radical reactions, TNM is a well established tool for the detection of $O_2^{\bullet-}$. The reason for this is the practically always fast ($k > 10^8 \text{ dm}^3 \text{ mol}^{-1} \text{ s}^{-1}$) reaction of $\bullet OH$ with the substrates, *i.e.* the latter protect, at sufficiently high substrate concentration, $C(NO_2)_3^-$ from being attacked by $\bullet OH$. On the other hand, the ozone rate constants span many orders of magnitude. Thus in systems where the ozone rate constant with the substrate is much lower than that with $C(NO_2)_3^-$, the TNM assay may underestimate the $O_2^{\bullet-}$ yield because of a consumption of $C(NO_2)_3^-$ by ozone. Raising the substrate concentration to account for this may not be always possible due to solubility limitations.

There is a third problem not encountered in the $\bullet OH$ -induced peroxy radical chemistry. In the later, there is practically never a species present that could compete with TNM for $O_2^{\bullet-}$, *i.e.* the TNM concentration can be kept low. In the ozone case, however, ozone reacts fast with $O_2^{\bullet-}$ ($k = 1.6 \times 10^9 \text{ dm}^3 \text{ mol}^{-1} \text{ s}^{-1}$), *i.e.* about equally fast as TNM ($k = 2 \times 10^9 \text{ dm}^3 \text{ mol}^{-1} \text{ s}^{-1}$). In order to prevent the reaction of ozone with $O_2^{\bullet-}$, TNM should be present at a ~ 10 -fold concentration with respect to ozone. At an ozone concentration of $10^{-4} \text{ mol dm}^{-3}$, typical for this kind of study, the TNM concentration must be raised to $10^{-3} \text{ mol dm}^{-3}$. This has some implications as to subsequent chemistries with reducing radicals. With such species, dioxygen and TNM react at about the same rate ($2 \times 10^9 \text{ dm}^3 \text{ mol}^{-1} \text{ s}^{-1}$).

In their reaction with dioxygen, carbon-centred radicals give rise to peroxy radicals. Only certain peroxy radicals can release $O_2^{\bullet-}$ in a unimolecular reaction (*e.g.* α -hydroxyalkylperoxy radicals), but most peroxy radicals give rise to some $O_2^{\bullet-}$ upon their bimolecular decay (*via* α -hydroxyalkylperoxy radicals, for a detailed review on peroxy radical reaction in aqueous solution see ref.¹¹⁸). On the other hand, TNM may monitor reducing radicals quantitatively in the primary ozone reaction, *e.g.* when ozone reacts by electron transfer [*cf.* the mechanism proposed for the reaction ozone with amines,¹⁴ reactions (4.30)-(4.32)].





As a consequence of this, in ozone reactions TNM does not monitor only reactions that release $\text{O}_2^{\bullet-}$ directly, but also other reducing radicals that are produced in the course of ozone reactions.

4.4 Detection of hydroperoxides in ozone reactions

4.4.1 Hydrogen peroxide and organic hydroperoxides

In ozone reactions, hydroperoxides are common products. They are sometimes only very short-lived, too short-lived to be detectable by a peroxide assay, and their formation can only be inferred from the final products. However, there is a wide span of hydroperoxides that live seconds, minutes or “for ever”. Hydrogen peroxide is such a long-lived hydroperoxide, but it may react with an ozonolysis product, and then it can fade away even on the time scale of typical analytical procedures.

For any mechanistic study, a material balance is desirable. Hence for the study of ozone reactions, reliable assays for hydroperoxides which allow their quantitative determination are required. In the following, some established assays will be discussed and some new ones presented. The use of Fe(II) and iodide-based assays were investigated in this work.

Fe(II)-based assays. Aqua- Fe^{2+} is known to reduce H_2O_2 and organic hydroperoxides. For H_2O_2 , the rate constant is $\sim 60 \text{ dm}^3 \text{ mol}^{-1} \text{ s}^{-1}$ at $25 \text{ }^\circ\text{C}$.¹³¹ The rate of reaction is strongly temperature dependent,¹³¹ and the value of $48 \text{ dm}^3 \text{ mol}^{-1} \text{ s}^{-1}$ determined at $18 \text{ }^\circ\text{C}$ (λ in Figure 18) in this work, agrees very well with these data. The rate constant of the reaction of hydroxymethylhydroperoxide (produced in the reaction of 1,1-dichloroethene with ozone, *cf.* ref.²⁴), with Fe^{2+} is not much slower ($k = 39 \text{ dm}^3 \text{ mol}^{-1} \text{ s}^{-1}$; μ in Figure 18). Noticeably slower is the reaction with tertiary butylhydroperoxide ($k = 13 \text{ dm}^3 \text{ mol}^{-1} \text{ s}^{-1}$; σ in Figure 18), but these differences are too small for a characterisation of a given hydroperoxide based on its kinetics with aqua- Fe^{2+} .

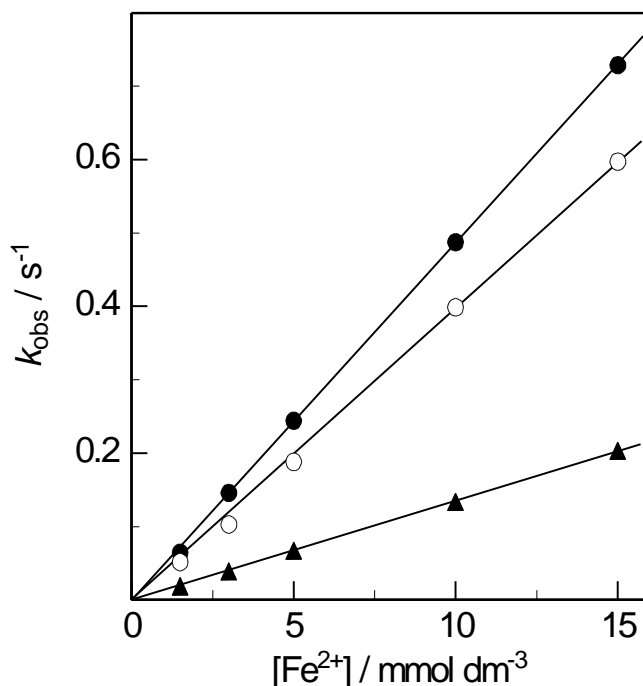


Figure 18 Rate of reaction of Fe²⁺ in 0.1 mol dm⁻³ H₂SO₄ with H₂O₂ (λ) hydroxymethylhydroperoxide (μ) and tertiary butylhydroperoxide (σ) at 18 °C as a function of the Fe²⁺ concentration. The kinetics of the reaction was followed by stopped-flow.

This ready reaction of Fe²⁺ with hydroperoxides has been often used as an assay for their quantification, but the question has to be asked, whether such data are reliable. In principle, the stoichiometry of the reaction of hydroperoxides with Fe²⁺ is simple, *i.e.* one mol hydroperoxide may yield two mol Fe³⁺ [reactions (4.33) and (4.34)]; *e.g.* $k(\bullet\text{OH} + \text{Fe}^{2+}) \approx 3 \times 10^8 \text{ dm}^3 \text{ mol}^{-1} \text{ s}^{-1}$].⁸⁰ In organic hydroperoxides two pathways are conceivable, reaction (4.34) and the formation of $\bullet\text{OH}$ plus an alkoxide ion, but only the former route is taken in a one-electron reduction process.¹³² The reason for this is the much higher solvation energy of OH⁻ as compared to RO⁻.



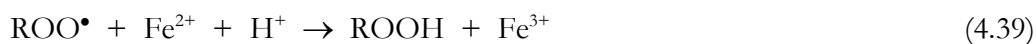
A system which seems to follow this sequence of reactions with practically no side reaction is the reaction of formic peracid with Fe(CN)₆⁴⁻. At pH ~3.7 the rate constant of this reaction is 4.3 dm³ mol⁻¹ s⁻¹, and ~1.9 mol Fe(CN)₆³⁻ and ~0.9 mol formic acid are formed. These yields were independent of the Fe(CN)₆⁴⁻ concentration ((0.4 – 4) × 10⁻³ mol dm⁻³) and were not affected by an addition of 2-methyl-2-propanol. This indicates that no

$\bullet\text{OH}$ are formed in this electron transfer reaction (confirming the earlier¹³² conclusion) and that the $\text{HC(O)O}\bullet$ radical undergoes an otherwise very fast 1,2-H-shift only slowly if at all. The reason for this could be a resonance stabilisation of the alkoxy radical by the carbonyl group.

In reality, however, the $\text{RO}\bullet$ radicals are usually very short-lived and may react with the substrate RH [reaction (4.35)], decompose by β -fragmentation [*e.g.* reaction (4.36)], $k = 1.4 \times 10^6 \text{ s}^{-1}$ ¹¹⁷ or undergo an 1,2-H-shift¹³³ when α -hydrogens are available [*e.g.* reaction (4.37)]. In water, the 1,2-shift reaction is also very fast, typically $\sim 10^6 \text{ s}^{-1}$.



In the presence of dioxygen, the alkyl radicals are rapidly converted into the corresponding peroxy radicals [reaction (4.38)] which are subsequently reduced by Fe^{2+} into hydroperoxides [reaction (4.39)].



Thus, a short chain reaction is induced. To exemplify this point, the formation of Fe^{3+} in the reaction of H_2O_2 with Fe^{2+} in the presence of 2-propanol is shown in Figure 19. Here, quantitative oxidation of Fe^{2+} by $\bullet\text{OH}$ is only achieved at high $[\text{Fe}^{2+}]/[2\text{-propanol}]$ ratios ($k(\bullet\text{OH} + 2\text{-propanol}) = 1.9 \times 10^9 \text{ dm}^3 \text{ mol}^{-1} \text{ s}^{-1}$) where the Fe^{3+} yield approaches the value $2 \text{ Fe}^{3+}/\text{H}_2\text{O}_2$.

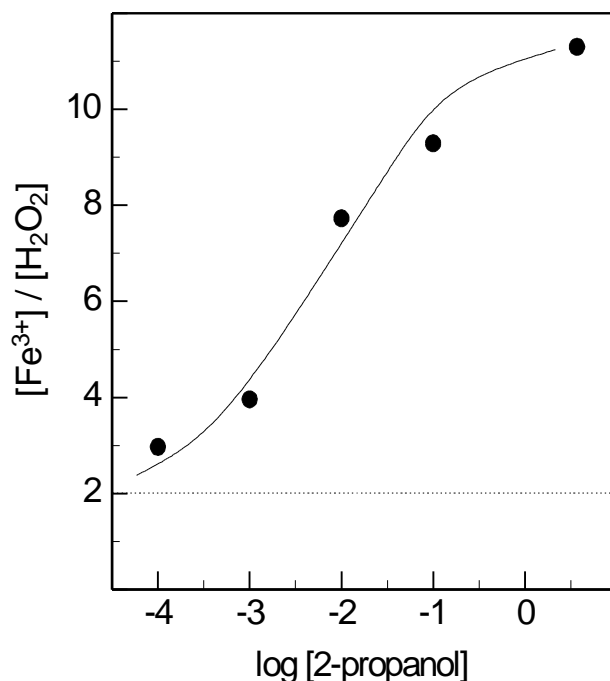


Figure 19 Reaction of H₂O₂ (varied between 2×10^{-4} and 2×10^{-3} mol dm⁻³) with Fe²⁺ (6×10^{-3} mol dm⁻³) in the presence of 2-propanol at pH 1.5. Formation of Fe³⁺ as a function of the 2-propanol concentration.

When Fe²⁺ reacts with organic hydroperoxides, it is no longer guaranteed that even at low substrate concentrations two mol Fe³⁺ are formed per hydroperoxide reacted. The reason for this is the occurrence of the fast unimolecular processes. An example is tertiary butylhydroperoxide. Here, four mol Fe³⁺ are formed per mol hydroperoxide in the presence of dioxygen, but only 0.8 mol Fe³⁺ in its absence (Figure 20).

This low yield which is even below unity deserves a comment. The rapid fragmentation of the tertiary butoxyl radical [reaction (4.36)] prevents a further oxidation of Fe²⁺ according to reaction (4.34). In reaction (4.36), methyl radicals are formed. They are capable of abstracting an H-atom from tertiary butylhydroperoxide (*cf.* $k(\bullet\text{CH}_3 + \text{H}_2\text{O}_2) = 2.7 \times 10^4 \text{ dm}^3 \text{ mol}^{-1} \text{ s}^{-1}$).¹³⁴ This reaction consumes tertiary butylhydroperoxide which thus is no longer capable of reacting with Fe²⁺. The fast termination reactions of the methyl and tertiary butylperoxyl radicals will eliminate the latter before it can be reduced by Fe²⁺ to a major extent.

It is thus concluded that Fe²⁺-based hydroperoxide assays, although most useful for their detection, are often not well-suited for their quantification.

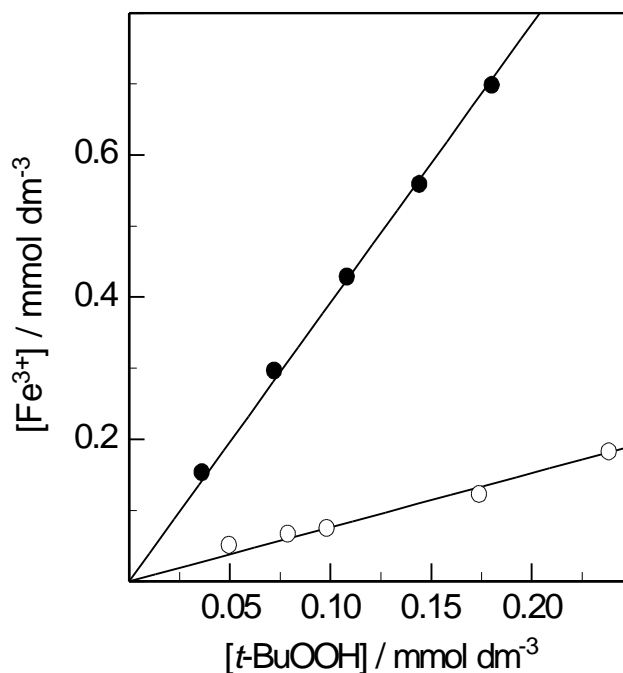


Figure 20 Formation of Fe^{3+} in the reaction of tertiary butylhydroperoxide with Fe^{2+} ($3 \times 10^{-3} \text{ mol dm}^{-3}$) at pH 1.5 as a function of the tertiary butylhydroperoxide concentration in the presence of air (λ) and in deoxygenated solution (μ).

Iodide assay. Iodide is known to react very slowly with hydrogen peroxide and many other hydroperoxides, but this reaction can be considerably speeded up by molybdate catalysis,⁷⁶ for example with H_2O_2 by three orders of magnitude.

An advantage of this assay is that the kinetics of the reaction varies considerably from hydroperoxide to hydroperoxide.²⁴ This can be used to characterise a given hydroperoxide, and if the rate constants of two hydroperoxides with this reagent differ significantly (\geq a factor of ~ 10), this assay can be used to quantify the yields of these hydroperoxides by a kinetic analysis. The yields of hydrogen peroxide in the reaction of ozone with various compounds are given in Table 8.

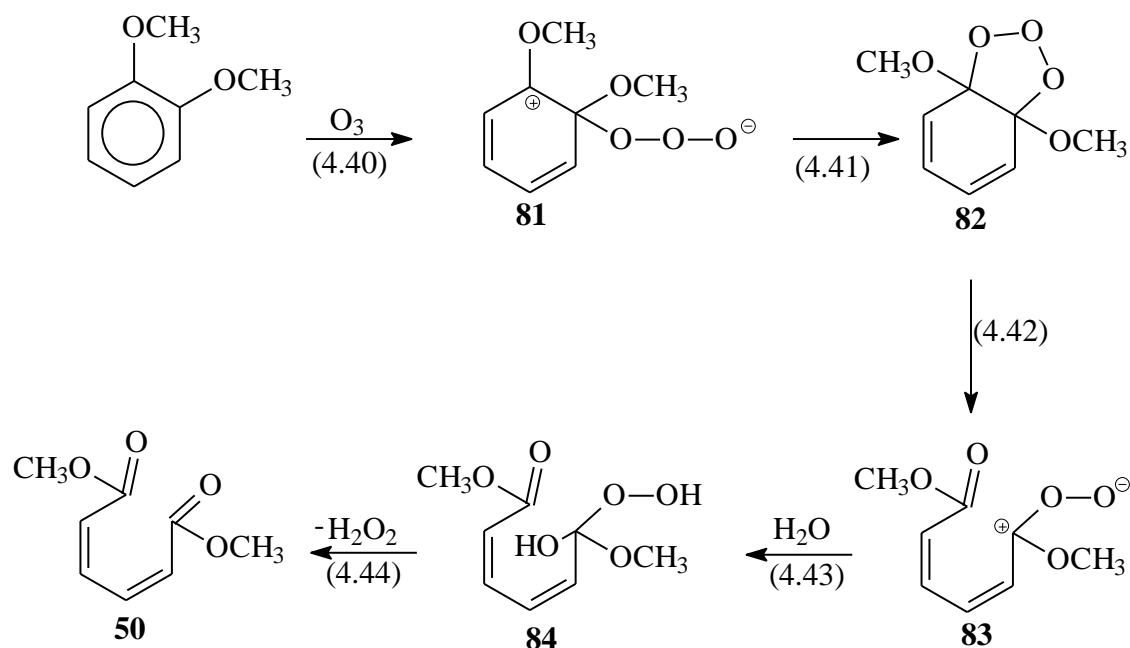
In the reaction of ozone with phenolic compounds, hydrogen peroxide is likely to be formed via a Criegee-type reaction pathway (*cf.* Scheme 7, for the reaction of ozone with 1,2-dimethoxybenzene). In the reaction of ozone with 1,2-methoxybenzene, the yield of hydrogen peroxide correlates with that of dimethyl(2Z,4Z)-hexa-2,4-dienoate **50**.

Error! Use the Home tab to apply Überschrift 1 to the text that you want to appear here.

Error! Use the Home tab to apply Überschrift 1 to the text that you want to appear here.

Table 8 Hydrogen peroxide yields in ozone reactions in % of ozone consumed at natural pH. The substrate concentrations in these experiments were typically $1 \times 10^{-3} \text{ mol dm}^{-3}$.

Substrate	H ₂ O ₂ Yield/(%)
Phenol	4.8
1,2-Dihydroxybenzene (Catechol)	5.1
1,4-Dihydroxybenzene (Hydroquinone)	5.6
1,3,5-Trihydroxybenzene (Phloroglucinol)	27
Anisole	23
1,2-Dimethoxybenzene	27
1,4-Dimethoxybenzene	56
1,3,5-Trimethoxybenzene	6.5



Scheme 7 The Criegee component in the reaction of ozone with 1,2-dimethoxybenzene

4.4.2 Detection of reactive hydroperoxides

Reactive hydroperoxides such as formic peracid and hydroperoxides of similar reactivity are capable of oxidising sulfides and disulfides by O-transfer [reaction (4.45)].



The reaction with formic peracid can be readily followed by conductance measurements, because formate ions and protons are liberated in this reaction ($\text{p}K_{\text{a}}(\text{formic peracid}) = 7.1$, $\text{p}K_{\text{a}}(\text{formic acid}) = 3.8$). The rate constant with the sulfide is considerably higher than that of the disulfide (Figure 21).

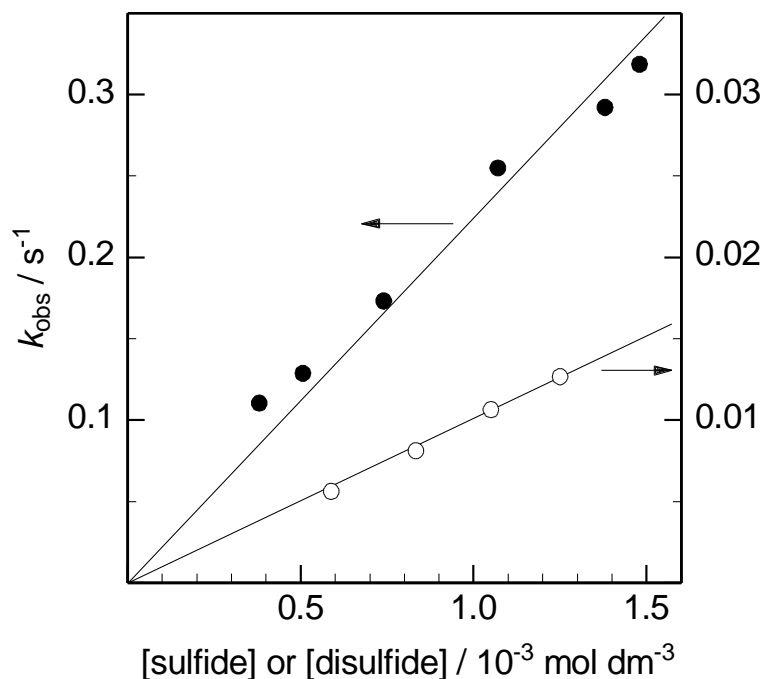


Figure 21 Rate of reaction of formic peracid with $(\text{HOCH}_2\text{CH}_2)_2\text{S}$ (λ) ($k = 220 \text{ dm}^3 \text{ mol}^{-1} \text{ s}^{-1}$) and $\text{HOCH}_2\text{CH}_2\text{SSCH}_2\text{CH}_2\text{OH}$ (μ) ($k = 10 \text{ dm}^3 \text{ mol}^{-1} \text{ s}^{-1}$) as a function of the sulfide/disulfide concentration. The kinetics were followed by the build-up of conductance due to the formation of formic acid.

Although they can be separated readily from their parent sulfides by HPLC, simple aliphatic sulfoxides do not have sufficiently strong absorptions at $\lambda > 200 \text{ nm}$ to use them for the quantitative determination of reactive hydroperoxides, but the water soluble sulfide methionine also gives this reaction. Thus, methionine can be used with advantage to quantify reactive hydroperoxides.

5 REACTIONS OF OZONE AND HYDROXYL RADICAL WITH PHENOL

5.1 Reactions of phenol with ozone

Phenol is very reactive toward ozone [$k(\text{phenol} + \text{O}_3) = 1.3 \times 10^3 \text{ dm}^3 \text{ mol}^{-1} \text{ s}^{-1}$; $k(\text{phenolate} + \text{O}_3) = 1.4 \times 10^9 \text{ dm}^3 \text{ mol}^{-1} \text{ s}^{-1}$]⁶⁹ and thus is readily degraded.^{41,42,48,49,55,56} As a consequence of the large differences in rates of phenol and phenolate, in neutral and slightly acidic solutions ozone reacts practically only with the phenolate in equilibrium (*cf.* Figure 22). In order to study the reaction of phenol, the pH has to be lowered below 4. It is expected that the reaction of ozone with phenol is much more complex than has been thought before. In this Chapter, it will be tried to disentangle some of these complexities.

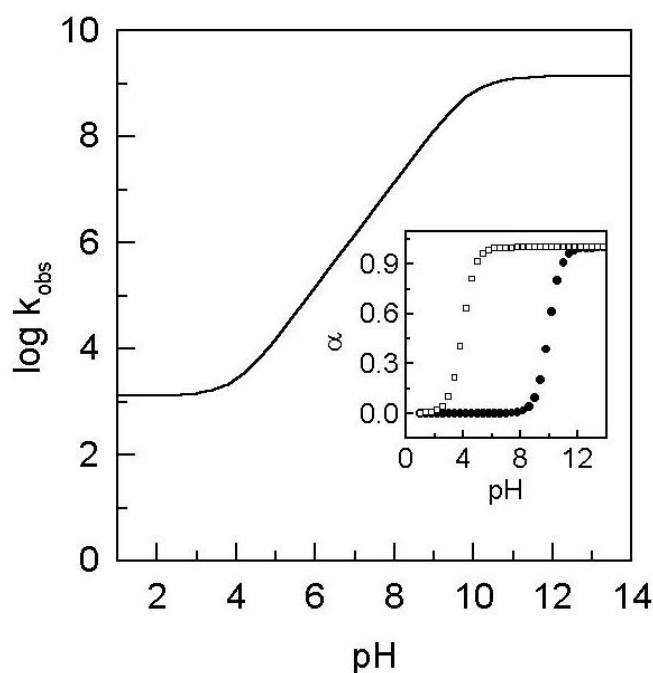


Figure 22 Variation of $\log k(\text{O}_3 + \text{phenol})$ with pH. Inset: The pK curve of phenol, fraction of phenolate in aqueous solution (λ) and the “reactivity pK” curve, the fraction of phenolate reacting with ozone(o).

5.1.1 Products yield

In the ozonolysis of phenol at pH ~ 7 , the major products detectable by HPLC are hydroquinone, catechol, 1,4-benzoquinone and *cis, cis*-muconic acid [(2*Z*,4*Z*)-hexa-2,4-dienedioic acid] (Table 9, on page 67). At low phenol conversions, the yields of products increase linearly with increasing ozone concentration (Figure 23).

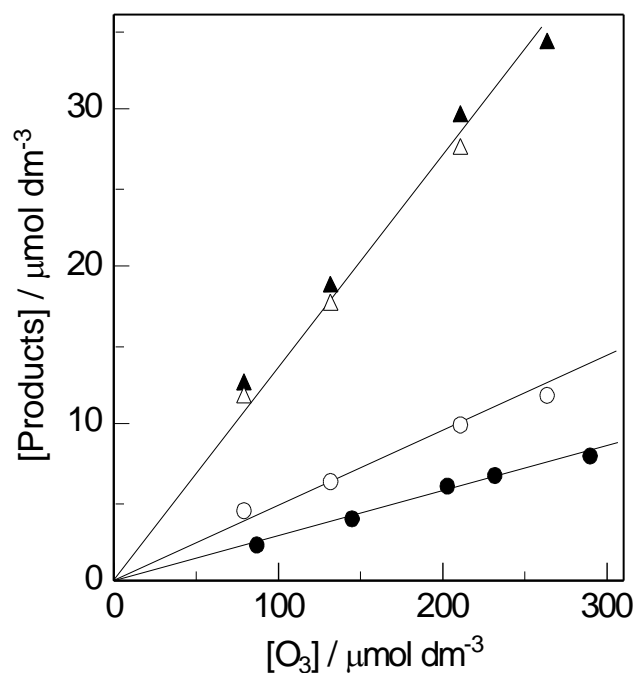
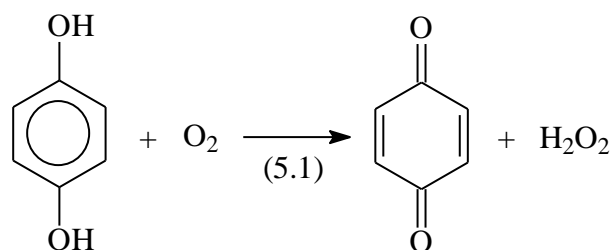


Figure 23 Ozonolysis of phenol (3×10^{-3} mol dm⁻³) in aqueous solution at pH 7. Yields of hydroquinone (σ), catechol (Δ), 1,4-benzoquinone (λ) and *cis,cis*-muconic acid (μ) as a function of the ozone concentration.

4, 4'-Dihydroxybiphenyl and 2,4'-dihydroxybiphenyl are formed only in low yields. At low pH *i.e.* pH 3, the yields of catechol and hydroquinone are considerably reduced from ~ 15 to ~ 2 % each. The *cis,cis*-muconic acid yield remains practically unaffected while the benzoquinone yield is increased from 4.6 to 10 %. The mechanistic analysis of these observations are presented in section 5.1.3.

The product yields at pH 10 must be treated with caution, because most of the products are unstable at high pH. After ozonation was carried out, the pH was lowered immediately by adding an appropriate concentration of sulfuric acid. This was necessary to avoid auto-oxidation of the products at high pH. As shown in Table 9, the yield of benzoquinone at

pH 10 is significantly higher than at lower pH, because of the autoxidation reaction as a results of hydroquinone deprotonation [reaction (5.1), $pK_1 = 9.91$ and $pK_2 = 11.56$].⁷⁰



Experiments to determine the stoichiometry of the reaction of phenol with ozone were carried out using 2.5×10^{-4} mol dm⁻³ of phenol and 5×10^{-5} to 2×10^{-4} mol dm⁻³ of ozone. Under these conditions, only 0.48 mol phenol are destroyed per mol ozone consumed at pH 7 (Figure 24). Here, a pH dependence of the phenol consumption is also observed, whereby 0.39 mol and 0.6 mol phenol are destroyed per mol ozone consumed at pH 3 and 10, respectively. This deviation from stoichiometry raises questions as to whether highly reactive species are produced in the reaction, which compete with phenol for ozone. It will be shown in section 5.1.2, that, although some products formed in the ozone reaction with phenol (catechol and hydroquinone) are more reactive than phenol, their effective rates of reaction (k_{obs}) are likely to be low, given their low concentration.

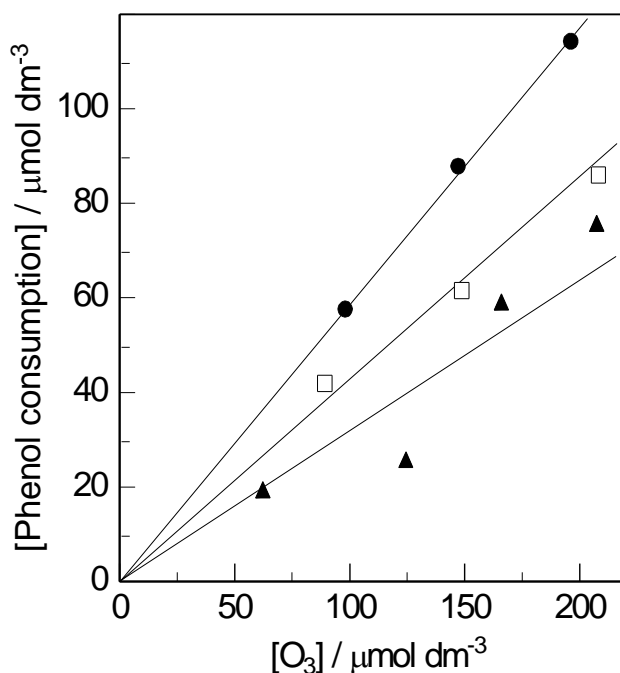


Figure 24 Ozonolysis of phenol (2.5×10^{-4} mol dm⁻³) in aqueous solution. Consumption of phenol as a function of the ozone concentration at pH 3 (σ), 7 (o) and 10 (λ).

An even more pronounced deviation from stoichiometry (0.33) has been reported before.⁵⁹ This study⁵⁹ reports similar catechol (12.4%) and hydroquinone (8.6%), but higher *cis,cis*-muconic acid (12.3%) yields. The formation of 1,4-benzoquinone was not detected. The combined yields of the above products (~37%) noticeably deviates from that of phenol consumption (48%) (*cf.* Table 9).

Table 9 Ozonolysis of phenol (3×10^{-3} mol dm⁻³). Products and their yields in % of ozone consumed. When two values are given, a second run at four different ozone concentrations was carried out. 2-Methyl-2-propanol (*t*-BuOH), DMSO and TNM concentrations in these experiments were typically 0.1 mol dm⁻³, 5×10^{-2} mol dm⁻³ and 1×10^{-3} mol dm⁻³, respectively.

Product (Scavenger)	≤ pH 3	pH 6–7	pH 10
Hydroquinone	~1.6 / 1.1 ^a	13.3 / 16	0.8
Hydroquinone (<i>t</i> -BuOH)		< 1	
Catechol	4.6 / 1.8 ^a	13.6	20
Catechol (<i>t</i> -BuOH)		2	
1,4-Benzoquinone	9.6 / 10.4 / 6.1 ^a	4.6 / 4.6	32
1,4-Benzoquinone (<i>t</i> -BuOH)		13	
<i>cis,cis</i> -Muconic acid	4.8 / 4 / 3 ^a	2.8	1
<i>cis,cis</i> -Muconic acid (<i>t</i> -BuOH)		2.0	
4,4'-Dihydroxybiphenyl			~1
2,4'-Dihydroxybiphenyl			~1
Singlet dioxygen	~0	5.6	8
2-Methyl-2-hydroxypropanal (<i>t</i> -BuOH)		15.4	-
Formaldehyde (<i>t</i> -BuOH)	10 / 11	14 / 13	11
Methanesulfinic acid (DMSO)			16
Methanesulfonic acid (DMSO)			4
Nitroform anion (TNM)	3		
Hydrogen peroxide	8.5	4.8	2
Hydrogen peroxide (<i>t</i> -BuOH)		16	
Hydrogen peroxide (DMSO)		13	
Organic hydroperoxide		0	
Organic hydroperoxide (<i>t</i> -BuOH)		2.6	
Phenol consumption	33 ^a	48 ^a	59 ^a
Phenol consumption (<i>t</i> -BuOH)		42 ^a	

^aat phenol concentration of $2.5 \times 10^{-4} \text{ mol dm}^{-3}$

5.1.2 Reactivity of ozone/phenol products with ozone

In order to correlate the consumption of phenol with the yield of the ozonation products, we decided to investigate the rate constants of ozone reaction with benzoquinone, catechol, hydroquinone, which are the major products as indicated above. The only suitable method at our disposal is competition kinetics (*cf.* section 2.6.2). In these experiments, 3-buten-1-ol was used a competitor. In the reaction of 3-buten-1-ol with ozone, formaldehyde is formed [reaction (2.12), $k = 7.9 \times 10^4 \text{ dm}^3 \text{ mol}^{-1} \text{ s}^{-1}$].^{71,84} The competition kinetics was used instead of the stopped flow technique because UV absorption of ozone and that of the substrates coincide.

Problems were experienced in the determination of formaldehyde yields in the ozone/benzoquinone/3-buten-1-ol system. Since formaldehyde was measured by derivatisation with 2,4-dinitrophenylhydrazine (*cf.* section 2.4.2), 1,4-benzoquinone competes against formaldehyde for 2,4-dinitrophenylhydrazine. As a consequence an excess of the 2,4-dinitrophenylhydrazine had to be used. From the slope obtained from the competition plot (Figure 25), which is $k_1/k_2 = 0.03$ (where $k_2 = 7.9 \times 10^4 \text{ dm}^3 \text{ mol}^{-1} \text{ s}^{-1}$, the rate constant of the reaction of ozone with 3-buten-1-ol), the rate constant for the reaction of 1,4-benzoquinone with ozone $k_1 = 2.5 \times 10^3 \text{ dm}^3 \text{ mol}^{-1} \text{ s}^{-1}$ was obtained.

For the reaction of ozone with catechol the competition plot (*cf.* Figure 26) gives a slope of 6.5 from which a rate constant ($k = 5.2 \times 10^5 \text{ dm}^3 \text{ mol}^{-1} \text{ s}^{-1}$) at pH 7 was obtained. Similarly, $k = 2.3 \times 10^6 \text{ dm}^3 \text{ mol}^{-1} \text{ s}^{-1}$ and $1.8 \times 10^6 \text{ dm}^3 \text{ mol}^{-1} \text{ s}^{-1}$ at pH 7 and pH 3 respectively, were obtained from the slope of the competition kinetic plots (29.1 at pH 7 and 23.8 at pH 3) for the reaction of ozone with hydroquinone (*cf.* Figure 27). These rate constants are in good agreement with those determined by Gurol et al.³⁴(*cf.* Appendix A).

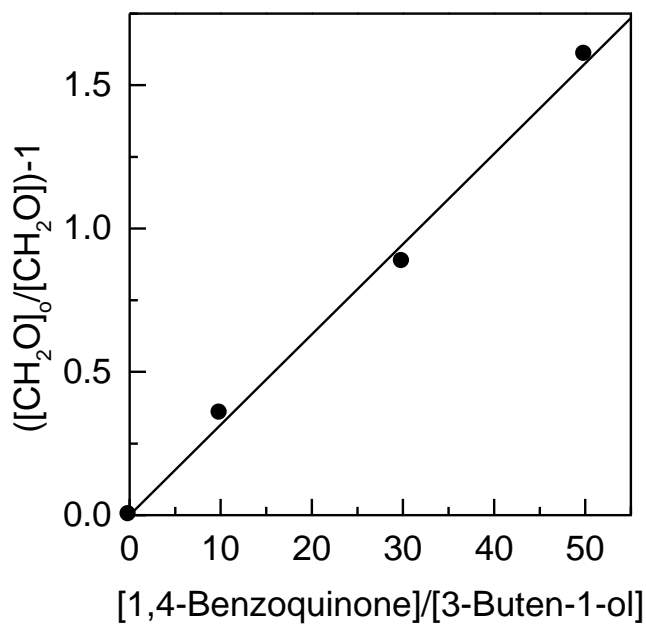


Figure 25 Plot of the competition of 3-buten-1-ol with 1,4-benzoquinone at pH 7 for the reaction of ozone. Formaldehyde yields result from the reaction of ozone with 3-buten-1-ol.

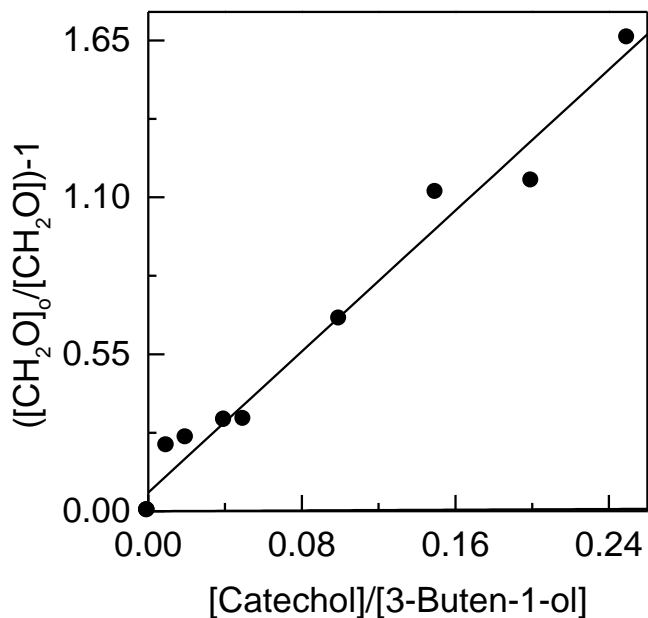


Figure 26 Plot of the competition of 3-buten-1-ol with catechol at pH 7 for the reactions of ozone. Formaldehyde yields result from the reaction of ozone with 3-buten-1-ol.

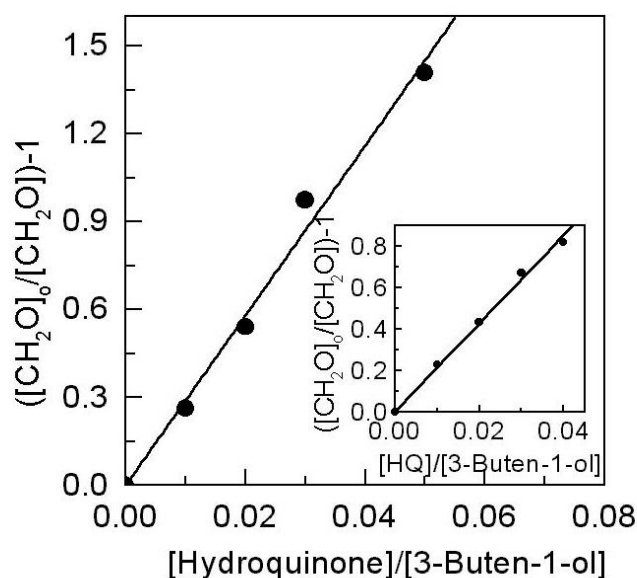


Figure 27 Plot of the competition of 3-buten-1-ol with hydroquinone at pH 7 for the reactions of ozone. Inset: Plot of the competition of 3-buten-1-ol with hydroquinone at pH 3 for the reactions of ozone. Formaldehyde yields result from the reaction of ozone with 3-buten-1-ol.

5.1.3 Mechanistic considerations

It is generally accepted that electrophilic agents react with aromatic compounds by attacking at the position of highest electron density. Recently, a new mechanism for the electrophilic aromatic substitution reaction has been proposed.¹³⁵⁻¹³⁷ It has been shown that in the reaction of aromatics with I_2 , Br_2 or HCl , π -complexes are formed.¹³⁵ *Ab initio* calculations have revealed that the nitrosation of benzene and toluene with NO^+ proceeds through initial formation of intermediate electron donor-acceptor π -complex.¹³⁶ A similar conclusion was also drawn from the molecular modelling studies of the sulfonation of toluene with SO_3 .¹³⁷ No such studies have been carried out for the reaction of ozone with aromatic compounds yet. However, ozone being an electrophile,⁵ its initial interaction should be similar to that of the electrophiles mentioned above. Thus, it is proposed here that the reaction of ozone with phenol occurs *via* the formation of a π -complex. [equilibrium (5.2), Scheme 8 on page 73]. Ozone binds to phenol through its highly delocalised electron cloud to form a π -complex in a reaction which is most likely reversible.

In order to understand the mechanism of the reaction of ozone with phenol, it is important to distinguish the two cases, namely, the reaction of ozone with non-dissociated phenol which will be simply denoted as phenol and that of ozone with dissociated phenol denoted as phenolate.

Although ozone is likely to form π -complexes with the phenolate as with phenol, their subsequent decay are different from each other. The π -complex may decompose following various pathways as shown in Scheme 8 for phenol and Scheme 9 for phenolate. In water, which has a high dielectric constant, one of the decomposition pathways may lead to the formation of phenol radical cation **71** and ozonide ($O_3^{\bullet-}$) [reaction (5.3)]. This process is also referred to as electron transfer. For phenol, this pathway makes up only 20%, and is independent of pH (see the formaldehyde, and the methanesulfinic and methanesulfonic acid yields in Table 9). The reduction potential of phenol ($E(\text{PhO}^{\bullet}/\text{PhOH}) = 0.86 \text{ V}$) at pH 7 can be used to calculate the reduction potential of phenol at any given pH using equation (4.17). As shown in Figure 28, the reduction potential strongly depends on pH. At $\text{pH} \leq 3$, the electron potential approaches 1 V, very close to that of ozone. At the pH below 3, the electron transfer process should be endothermic. The obtained data, show a pH independence of $\bullet\text{OH}$ yield at pH 3, 7 and 10. The reduction potential of ozone as a function of pH (Figure 28) was calculated by assuming a $\text{p}K_a$ value of HO_3^{\bullet} as 3.5 and $E(\text{O}_3^{\bullet-}/\text{O}_3) = 1.01 \text{ V}$. The $\text{p}K_a$ value of HO_3^{\bullet} is extrapolated from that of HO_2^{\bullet} which is 4.8, and from the fact that the increase in the number of oxygen decreases the $\text{p}K_a$ value as for $\text{H}_2\text{O}_2 > \text{H}_2\text{O}_3$.¹³⁸

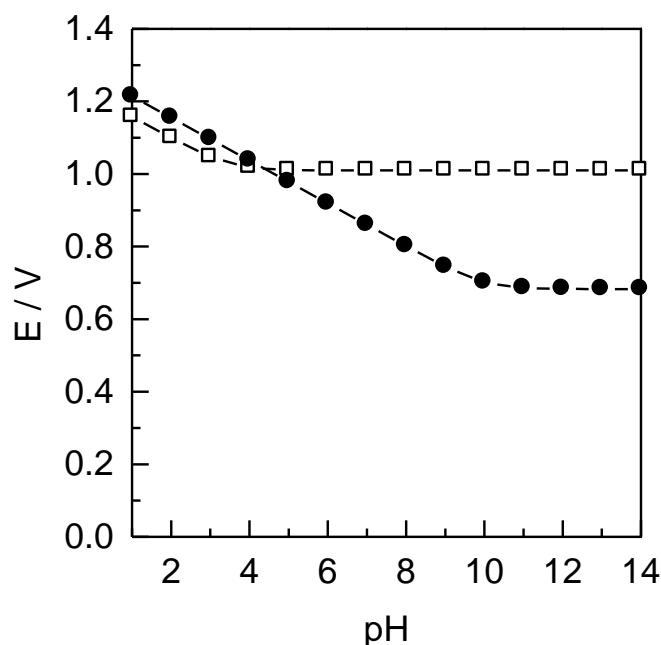
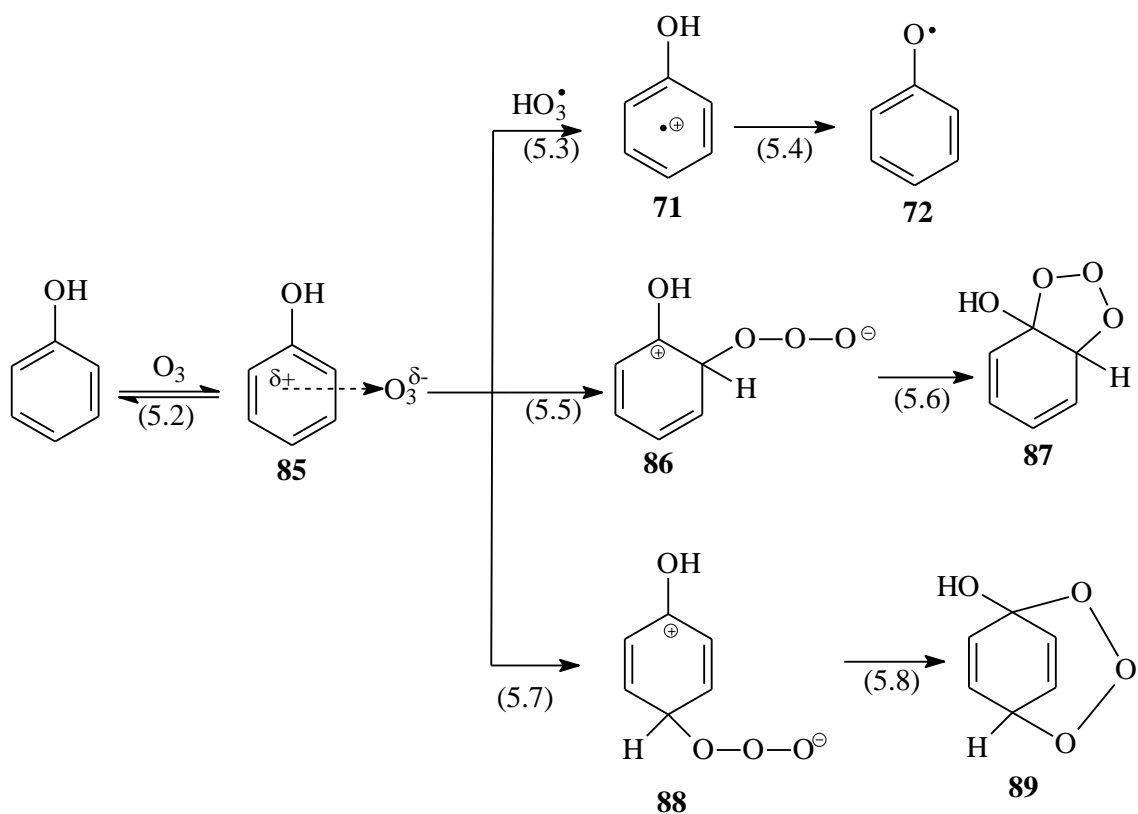


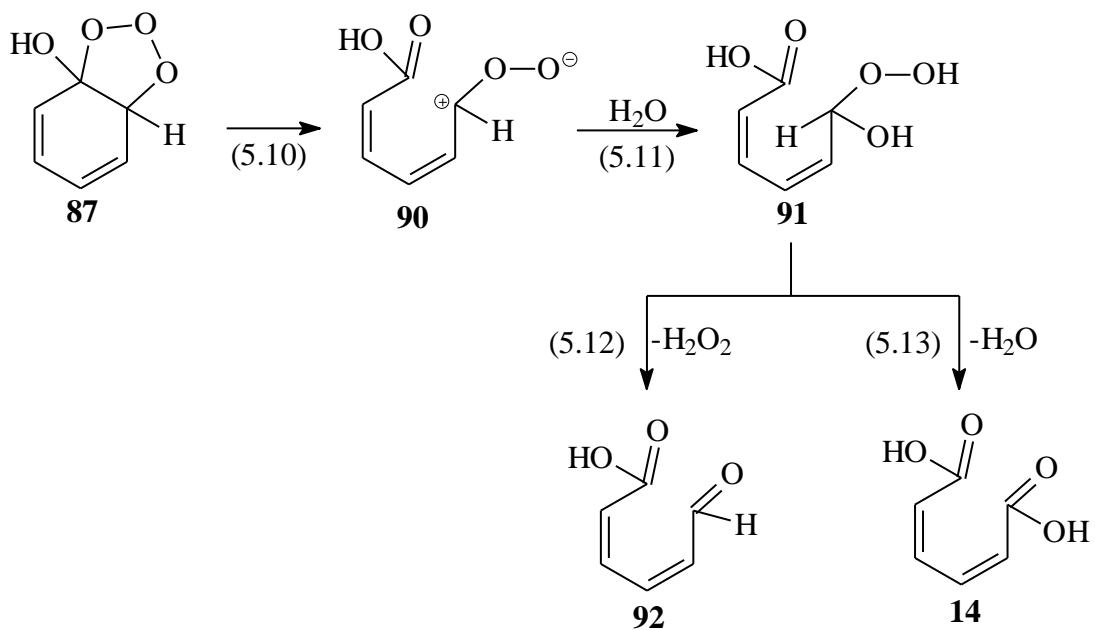
Figure 28 Calculated reduction potentials of phenol (λ) and ozone (o) as a function of pH.

The radical formation process in the decomposition of the π -complex competes with other pathways which lead to the formation of σ -complexes **86** and **88** [reactions (5.5) and (5.8)] in case of phenol (Scheme 8). Similarly the σ -complexes **94** and **96** are formed in case of phenolate (Scheme 9). The high electron density at the *ortho* and *para* position of phenol, causes ozone to bind at these respective positions.

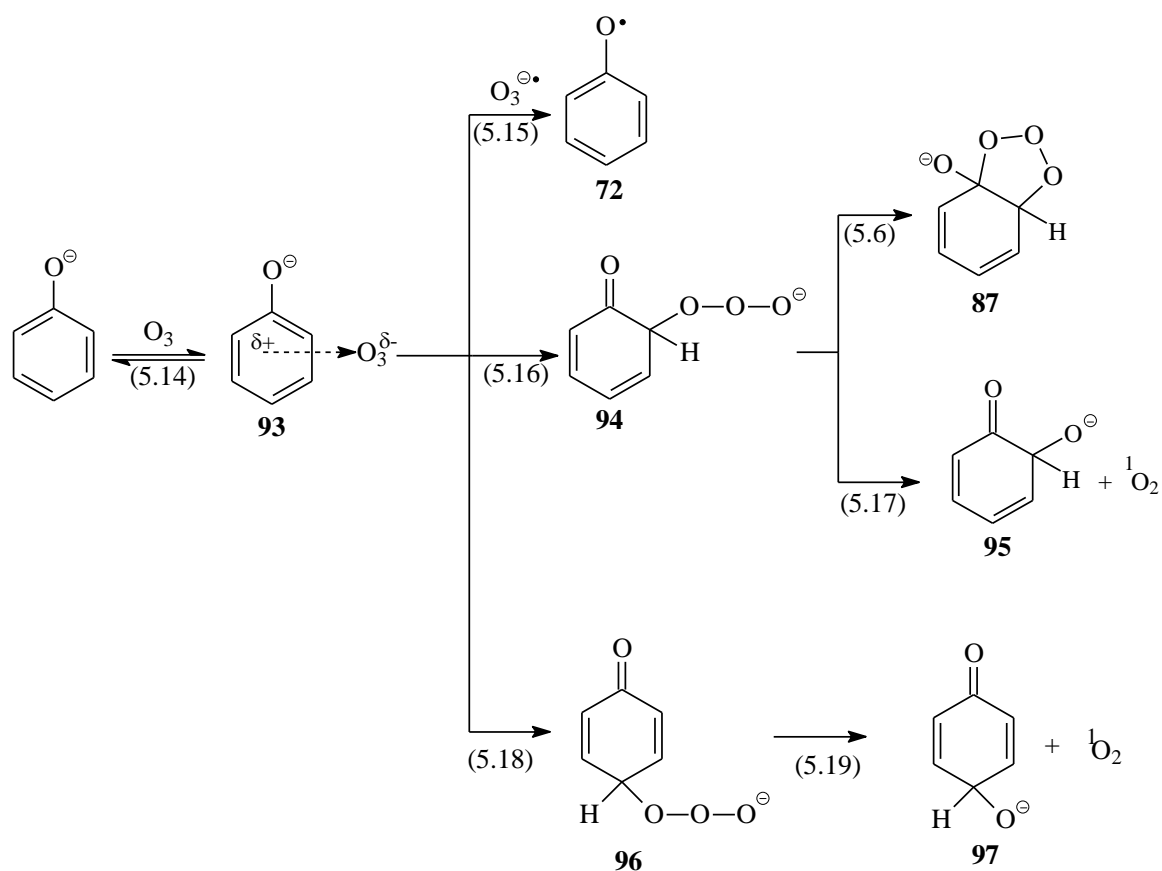
The zwitterion **86**, undergoes a 1,3-dipolar cycloaddition similar to the simple olefins to yield a 1,2,3-trioxolane **87**. The trioxolane **87**, undergoes a heterolytic bond cleavage in a similar way as the Criegee primary ozonide yielding **90**, which in turn hydrolyses to yield the hydroxyhydroperoxides **91**. Hydroxyalkylhydroperoxides decompose typically into hydrogen peroxide and a carbonyl compound [reaction (5.12)].²⁴ However, the effect of conjugation has not yet been investigated which may cause **91** to decompose by water elimination [reaction (5.13)]. The hydrogen peroxide yield was determined to be 4.8% at natural pH, but a corresponding product (2*Z*,4*Z*)-6-oxo-hexa-2,4-dienoic acid **92** was not detected. It is herewith shown that, under the experimental conditions used, *cis,cis*-muconic acid is not a secondary product due to the ozonolysis of catechol, thus making reaction (5.13) to be the only route leading to the formation of *cis,cis*-muconic acid.



Scheme 8 Mechanism of the ozonolysis of phenol at $\text{pH} \leq 3$.



In the non-radical decomposition of the ozone-phenolate π -complex an unstable zwitterion is formed, whereby the deprotonated O-atom form a double bond rapidly with the positively charged carbon atom, giving rise to **94** and **96**. The two *ortho*- and *para*-intermediates **94** and **96**, decompose by releasing $\text{O}_2(^1\Delta_g)$ [reactions (5.17) and (5.19)]. The intermediate formed as a result of $\text{O}_2(^1\Delta_g)$ elimination **95** may undergo a hydrogen shift to yield catechol [reactions (5.20) and (5.21)], while hydroquinone is formed from **97**. However, not all hydroquinone and catechol determined in the ozonolysis of phenol are formed *via* the reaction pathway mentioned above.

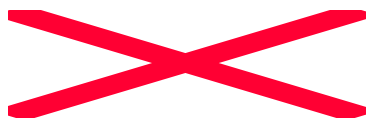


Scheme 9 Mechanism of the ozonolysis of deprotonated phenol (phenolate) at $\text{pH} \geq 3$.

The $\bullet\text{OH}$ radical induced oxidation of phenol also gives rise to the formation of catechol and hydroquinone (*cf.* section 5.2). The data in Table 9 reveal that the formation of catechol and hydroquinone at $\text{pH} 7$ is suppressed to a large extent when the reaction is carried out in the presence of 2-methyl-2-propanol, an $\bullet\text{OH}$ radical scavenger. This strongly points to the importance of $\bullet\text{OH}$ in this system.

Error! Use the Home tab to apply Überschrift 1 to the text that you want to appear here.

Error! Use the Home tab to apply Überschrift 1 to the text that you want to appear here.

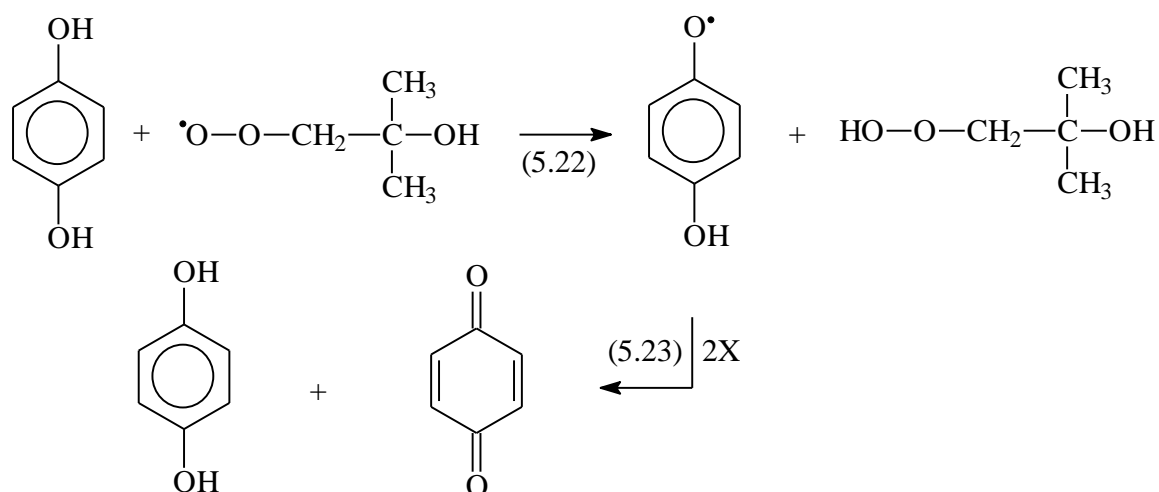


The mechanisms given in Scheme 8 and 9 explain to a large extent the data obtained in the ozonolysis of phenol at pH 3, 7 and 10. The decrease in the *cis,cis*-muconic acid yield from 4.8% at pH 3 to 1% of the ozone consumed at pH 10, confirms the proposal that muconic acid is formed as result of ozone reaction with the non-dissociated phenol [reactions (5.6)-(5.6) and (5.10)-(5.13)]. However, in neutral solution, the 1,3-dipolar cycloaddition may occur [*cf.* reaction (5.6) in Scheme 8)], which would give rise to *cis,cis*-muconic acid. The yield [$O_2(^1\Delta_g)$] was determined to be 0% at pH 3, 5.6% at pH 7 and 8% at pH 10, this indeed reveals that the dissociated phenol (phenolate) is responsible for the formation of $O_2(^1\Delta_g)$ in accordance with reactions (5.17) and (5.19).

The reactivity and decay of the phenoxy radical has been subject of intensive investigation.^{46,139} Unlike carbon-centred radicals, phenoxy radicals do not react with oxygen. Their decay is dominated by the bimolecular reaction, which leads to the formation of dimers, e.g., 4,4'-dihydroxybiphenyl and 2,4'-dihydroxybiphenyl. The phenoxy radical yield is expected to be ~20%, equivalent to that of $\bullet OH$, but the yield of 4,4'-dihydroxybiphenyl obtained is only 1%, with that of 2,4'-dihydroxybiphenyl being in the same range. This raises a question as to whether there are other processes in this system (which have not been observed in γ -radiolysis investigations) in which phenoxy radical is consumed. One of these processes could be the reaction of ozone with phenoxy radical. Being a diradical, ozone may react with phenoxy radical.

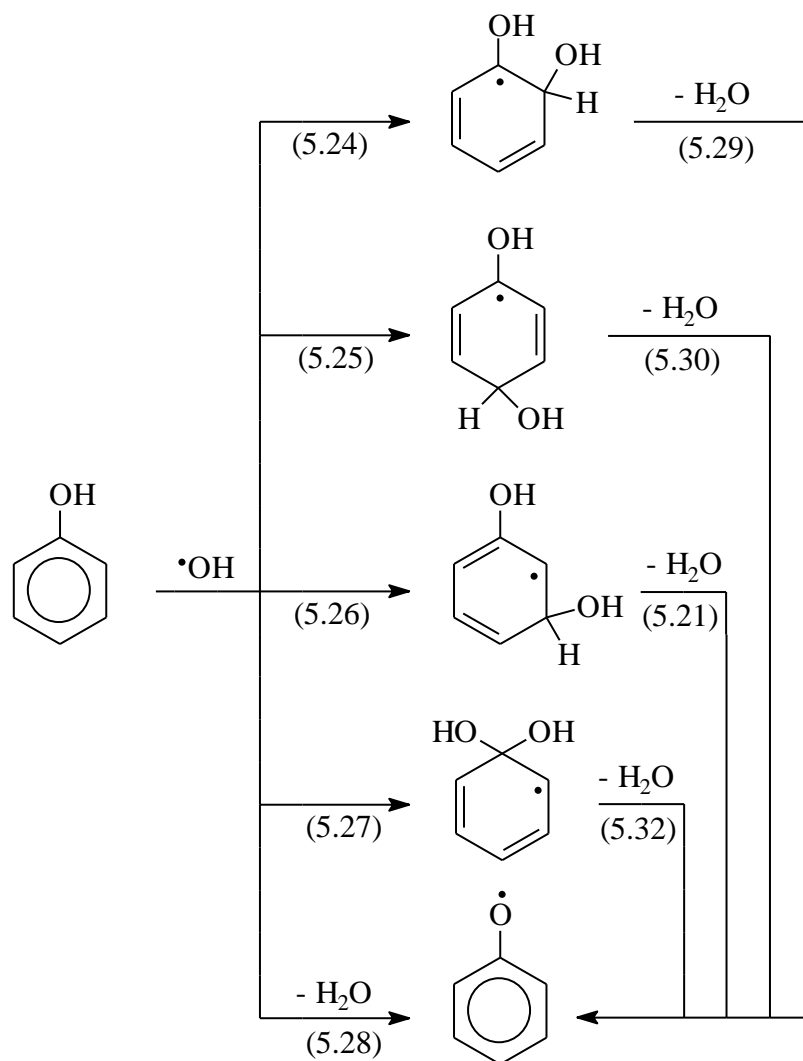
The chemistry of the phenol/ozone system is changed completely when the reaction is carried out in the presence of 2-methyl-2-propanol. Not only is the $\bullet OH$ induced reaction suppressed, but the yield of some products are also altered. The yield of 1,4-benzoquinone increases from 4.6% in the absence of 2-methyl-2-propanol to 13% in the presence of 2-methyl-2-propanol. This observation cannot be explained by the $\bullet OH$ scavenging effect of 2-methyl-2-propanol as a chain reaction suppressant. In the reaction of $\bullet OH$ with 2-methyl-2-propanol, an alkyl radical is formed [reaction (4.3) on page 45], which readily reacts with dioxygen to yield an alkylperoxy radical [reaction (4.6) on page 45] (*cf.* section 4.1.1 for more detail). There are some studies on the reaction of peroxy radical with

phenols.¹⁴⁰ The alkylperoxy radical can react with hydroquinone by H-atom abstraction, yielding a 4-hydroxyphenoxy radical [reaction (5.22)].¹⁴⁰ The 4-hydroxyphenoxy radical react bimolecularly by disproportionating into benzoquinone and hydroquinone [reaction (5.23)]. This might be a reasonable explanation for a higher 1,4-benzoquinone yield observed in the presence of 2-methyl-2-propanol.



5.2 Reactions of phenol with $\bullet\text{OH}$

Although the formation of phenoxy radicals is thermodynamically favoured,¹⁴¹ the reaction of $\bullet\text{OH}$ radicals with phenol mainly leads to the formation of the four isomeric dihydroxycyclohexadienyl radicals (OH-adducts). As shown in Scheme 10, the $\bullet\text{OH}$ radical preferentially adds to the *ortho*- [reaction (5.24), 48%] and *para*- positions [reaction (5.25), 36%].¹²³ Addition to the *meta*-position [reaction (5.26)] amounts to only 8%.¹²³ Addition to the *ipso*-position [reaction (5.27)] is expected to be quite negligible, and the resulting *ipso*-OH-adduct possibly dehydrates promptly to give the phenoxy radical [reaction (5.32)]. The fraction of *ipso*-OH-adduct is therefore not distinguishable from direct H-abstraction by $\bullet\text{OH}$ [reaction (5.28)]. Based on the material balance of OH radicals, their total yield [reactions (5.27) and (5.28)] is attributed to the 8% of OH radicals otherwise not accounted for.¹²³



Scheme 10 Mechanism of the reaction of phenol with $\bullet\text{OH}$.

The OH-adduct-radicals undergo spontaneous and H^+ - as well as OH^- -catalysed elimination of water to yield the more resonance-stabilised phenoxyl radical [reactions (5.29) – (5.32)].⁵⁴ The rate of this dehydration reaction differs among the different isomeric OH-adduct-radicals. By monitoring the kinetics of absorbance build-up of the phenoxyl radical at 400 nm, or the decay of the dihydroxycyclohexadienyl radicals at 330 nm under various pH conditions, it was reported that H^+ -catalysed dehydration reaction consisted of two separate processes, a fast and a slow component with approximately equal contributions.⁵⁴ More recently, based on the pH dependence of the yields of hydroquinone and catechol in the presence of an oxidant, it was possible to assign the faster process to the water elimination reaction of the *para*-OH-adduct radical and the slower process to that

of the *ortho*-OH-adduct radical.¹²³ The results of the reaction of $\bullet\text{OH}$ with phenol obtained by γ - and pulse radiolysis studies are presented in the sections below.

5.2.1 Conversion of the dihydroxycyclohexadienyl radicals into phenoxy radicals

The transient spectra observed in the pulse radiolysis of N_2O -saturated solution of phenol at pH 6.8 (Figure 29) are in good agreement with the reported observations.¹⁴² Immediately after a 0.4 μs pulse, the only prominent absorption comes from the phenol OH-adduct radicals at 330 nm and very little absorption of the phenoxy radical at 400 nm¹⁴³

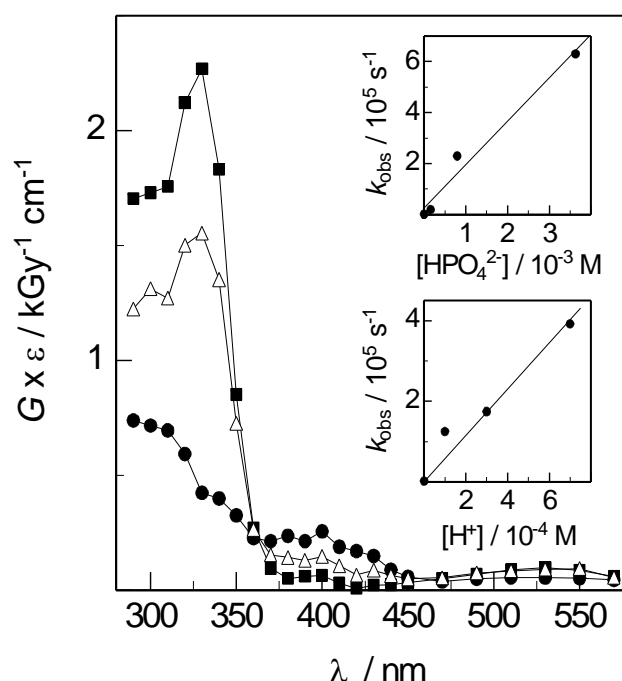


Figure 29 Pulse radiolysis of N_2O -saturated solution of phenol ($10^{-3} \text{ mol dm}^{-3}$) at pH 6.8. Transient absorption spectra observed 2 μs (v), 30 μs (Δ), and 200 μs (λ) after the pulse ($\sim 4 \text{ Gy}$ per pulse). Inset A: k_{obs} of absorbance build-up at 400 nm as function of the HPO_4^{2-} concentration. Inset B: k_{obs} as function of the proton concentration.

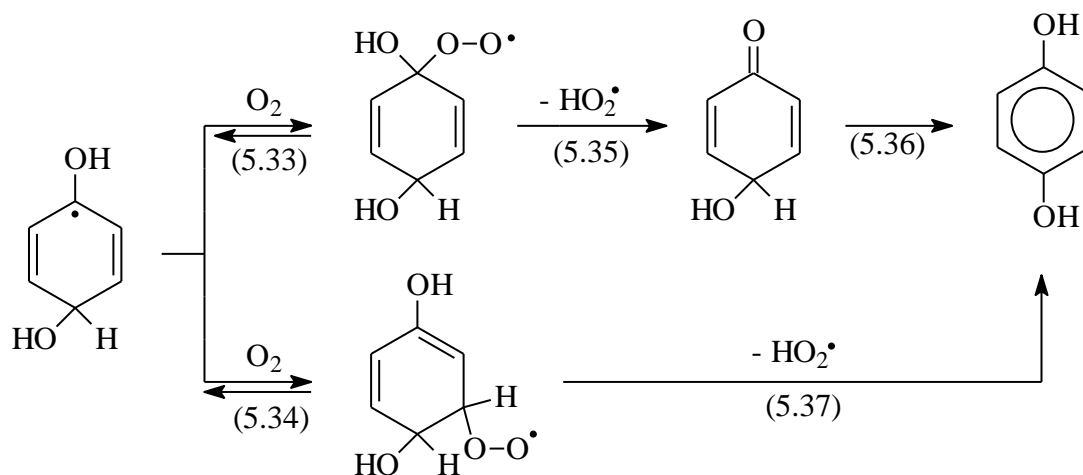
Monitored 200 μs after the pulse, the absorption at 400 nm increases at the expense of that at 330 nm. The rate of absorption build-up at 400 nm as well as the decay at 330 nm are dose rate dependent for doses between 1.5 and 10 Gy/pulse, since the bimolecular decay of the radicals also contributes to the kinetics. By extrapolating the reciprocal of the first half-lives of absorption decay at 330 nm to zero dose, the rate constant of phenoxy radical formation at neutral pH, $k = 1.8 \times 10^3 \text{ s}^{-1}$ was obtained. A similar value was

obtained for the build-up at 400 nm. A higher value ($\sim 5 \times 10^3 \text{ s}^{-1}$) has been reported¹⁴² for the uncatalysed dehydration of the dihydroxycyclohexadienyl radicals (a somewhat higher value would be obtained if the experimental data were not corrected for the bimolecular decay of radicals by extrapolation to zero dose). As will be shown below, the dehydration of the *para*-OH-adduct in acidic solution is faster than that of the *ortho*-OH-adduct. The above rate constant can thus be attributed to the uncatalysed dehydration of the *para*-OH-adduct. The corresponding value for the *ortho*-OH-adduct would be still lower and therefore not measurable under pulse radiolysis conditions. By monitoring the absorption decay at 370 nm at varying dose per pulse, the rate constant of bimolecular decay of the OH-adduct radicals was obtained to be $2k = 2.0 \times 10^8 \text{ dm}^3 \text{ mol}^{-1} \text{ s}^{-1}$. For a compilation of rate constants see the Appendix C.

At $\text{pH} < 5$, the formation of the phenoxyl radical was observed to consist of two parallel processes, a fast build-up followed by a slower build-up with approximately equal yields. The rates of these two processes increase with increasing proton concentrations. From the linear plot of the observed first-order rate constant of the first absorption build-up at 400 nm *versus* the proton concentration at pH 3.4 to 4.8 (inset B in Figure 29), the rate constant of the fast H^+ -catalysed phenoxyl radical formation was obtained, $k(\text{H}^+)_{\text{fast}} = 1.7 \times 10^9 \text{ dm}^3 \text{ mol}^{-1} \text{ s}^{-1}$. Similarly, $k(\text{H}^+)_{\text{slow}} = 1.1 \times 10^8 \text{ dm}^3 \text{ mol}^{-1} \text{ s}^{-1}$ was obtained from the second and slower absorption build-up (data not shown), these values are in good agreement with the reported values.^{54,142} The OH^- -catalysed dehydration reaction of the OH-adduct radicals of phenol has been reported to be faster than the H^+ -catalysed reaction ($k_{\text{obs}} > 1 \times 10^5 \text{ s}^{-1}$ at pH 8.6 and $1.05 \times 10^7 \text{ s}^{-1}$ at $\text{pH} \approx 11$).⁵⁴ Efficient catalysis of water elimination by phosphate buffer has also been observed.¹⁴² By monitoring the absorption build-up at 400 nm with increasing H_2PO_4^- concentration at pH 5.8 to 4.8, we found no catalytic effect of H_2PO_4^- . The catalytic effect of phosphate buffer is due solely to the presence of HPO_4^{2-} . The value for the rate constant of the HPO_4^{2-} -catalysed dehydration reaction has been determined in weakly basic solution of phenol (pH 8.1 – 8.7) with varying HPO_4^{2-} concentration (the contribution from OH^- has been corrected taking $k(\text{OH}^-) = 1 \times 10^{10} \text{ dm}^3 \text{ mol}^{-1} \text{ s}^{-1}$) to be $k(\text{HPO}_4^{2-}) = 5.8 \times 10^7 \text{ dm}^3 \text{ mol}^{-1} \text{ s}^{-1}$ (inset A in Figure 29).

5.2.2 Reaction of the dihydroxycyclohexadienyl radicals with dioxygen

In the presence of dioxygen, the *C*-centred dihydroxycyclohexadienyl radicals will rapidly add dioxygen to yield the corresponding peroxy radicals [e.g., reactions (5.33) and (5.34) for the *para*-OH-radical adduct]. The phenoxyl radical does not react with dioxygen (see ref.¹²²)



In the pulse radiolysis of N_2O/O_2 (4:1)-saturated solution of phenol at pH 6.8, the initial absorption of the OH-adduct radicals at 330 nm decreases rapidly as these radicals are converted to the corresponding peroxy radicals which absorb more weakly at this wavelength. Figure 30 shows the observed first-order rate constant of absorbance decay at varying dioxygen concentrations.

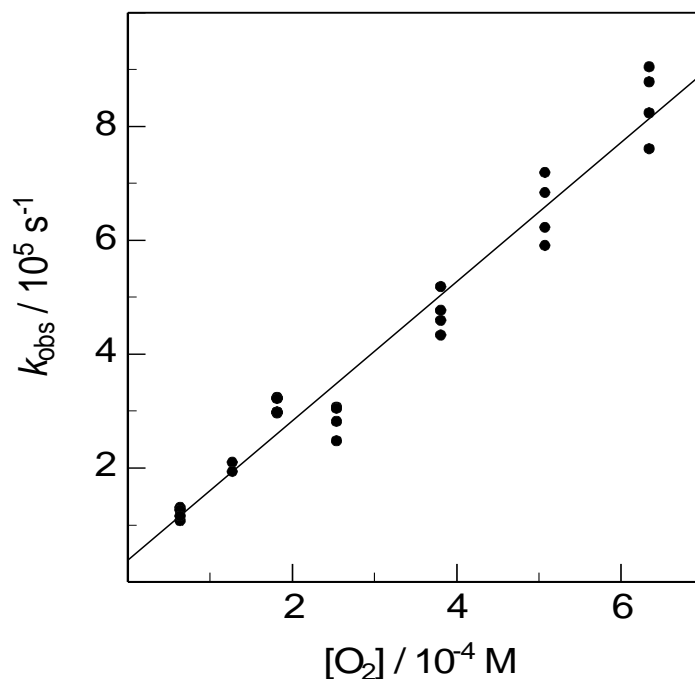


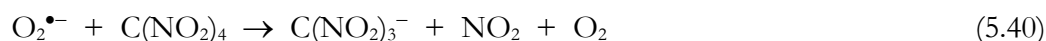
Figure 30 Dioxygen concentration dependence of the observed first-order rate constant of absorption decay at 330 nm in the pulse radiolysis of $\text{N}_2\text{O}/\text{O}_2$ (4:1)-saturated solution of phenol at pH 6.8 (~ 5 Gy/pulse).

From the slope, the rate constant of dioxygen addition to the dihydroxycyclohexadienyl radicals of $k = 1.2 \times 10^9 \text{ dm}^3 \text{ mol}^{-1} \text{ s}^{-1}$ is obtained. There is a small intercept ($3.8 \times 10^4 \text{ s}^{-1}$) which includes the contribution ($1.8 \times 10^3 \text{ s}^{-1}$) from the dehydration reactions (see above), the contribution from the bimolecular decay ($\sim 10^3 \text{ s}^{-1}$ at 6 Gy/pulse), as well as from the subsequent rapid HO_2^\bullet -elimination of the dihydroxycyclohexadienylperoxyl radicals [*cf.* reactions (5.35) or (5.37)], see below]. These leave little room for the reverse dioxygen addition reactions [*cf.* reactions (-5.33) or (-5.34)]. This is in contrast to the other hydroxycyclohexadienylperoxyl radicals where the reversibility of the dioxygen addition reaction is much more pronounced.^{144,145}

5.2.3 HO_2^\bullet -elimination reaction of dihydroxycyclohexadienylperoxyl radicals

In the pulse radiolysis of $\text{N}_2\text{O}/\text{O}_2$ -(4:1)-saturated solution of phenol containing tetranitromethane (TNM, $3 \times 10^{-4} \text{ mol dm}^{-3}$), the absorption of the nitroform anion ($\text{C}(\text{NO}_2)_3^-$) at 350 nm increase rapidly following an initial jump which is due to the reaction

of HO₂[•]/O₂^{•-} from primary hydrogens [reactions (5.38) and (5.39)] with TNM [reaction (5.40)].



The rate constant of the second step of C(NO₂)₃⁻ formation is 1.3 × 10⁵ s⁻¹. The yield of this absorption build-up corresponds to G(C(NO₂)₃⁻) = G(O₂^{•-}) = 4.6 × 10⁻⁷ mol J⁻¹ or 80% of •OH. The yield of O₂^{•-} corresponds approximately to the sum of the *ortho*- and *para*-OH-adduct radicals. Since reaction (5.40) is not the rate-determining step (k_{5.34} = 1.9 × 10⁹ dm³ mol⁻¹ s⁻¹),¹²² the rate constant determined above (1.3 × 10⁵ s⁻¹) is thus the overall rate of HO₂[•]-elimination of the peroxy radicals of these two isomeric dihydroxycyclohexadienyl radicals [*e.g.* reactions (5.35), (5.37) of the *para*-OH-adduct-radical].

5.2.4 Product studies

HO₂[•]-elimination reactions of the peroxy radicals of the *ortho*- and *para*-OH-adduct radicals yield catechol and hydroquinone, respectively [*cf.* reactions (5.35)-(5.37) for the formation of hydroquinone]. In the steady state γ-radiolysis of N₂O/O₂ (4:1)-saturated solution of phenol at pH 6.8, we found G(catechol) = 2.3 × 10⁻⁷ mol J⁻¹ and G(hydroquinone) = 1.8 × 10⁻⁷ mol J⁻¹. In acidic solution, the water elimination reactions (5.31) and (5.32) become faster with increasing H⁺ concentration and compete with dioxygen addition. Based on this competition between the proton-catalysed water elimination and dioxygen addition, one can write equation (5.41) for the formation of hydroquinone, which can be rearranged to give the equation (5.42). An analogous equation may be written for the formation of catechol.

$$G(\text{HQ}) = f \times G(p\text{-OH-A}) \times \frac{k_{5.33,5.34}[\text{O}_2][p\text{-OH-A}]}{k_{5.33,5.34}[\text{O}_2][p\text{-OH-A}] + k_{5.30}[\text{H}^+][p\text{-OH-A}]} \quad (5.41)$$

$$\frac{G(\text{HQ})_o}{G(\text{HQ})} - 1 = \frac{k_{5.30}[\text{H}^+]}{k_{5.33,5.34}[\text{O}_2]} \quad (5.42)$$

Here $G(\text{HQ})_0$ is the G value of hydroquinone formation in the absence (*i.e.* lowest H^+ concentration at neutral pH) and $G(\text{HQ})$ in the presence of H^+ . The term f denotes the fraction of the reactions of the *para*-OH-adduct radicals (abbreviated as *p*-OH-A) that leads to the formation of hydroquinone while $k_{5.33,5.34}$ is the rate constant for the reaction (5.33) or (5.34)

A plot of $G(\text{HQ})_0/G(\text{HQ}) - 1$ vs. the proton concentration (Figure 31) yields a straight line with the slope of $3.1 \times 10^3 \text{ dm}^3 \text{ mol}^{-1} \text{ s}^{-1}$. Taking $k_{5.31,5.32}(\text{O}_2 + \textit{p}\text{-OH-A}) = 1.2 \times 10^9 \text{ dm}^3 \text{ mol}^{-1} \text{ s}^{-1}$ (see above), $k_{5.30} = 1.0 \times 10^9 \text{ dm}^3 \text{ mol}^{-1} \text{ s}^{-1}$ is obtained. The analogous plot for the formation of catechol is also shown in Figure 31, and based on the same assumptions $k_{5.29} = 2.1 \times 10^8 \text{ dm}^3 \text{ mol}^{-1} \text{ s}^{-1}$ is obtained. The value of $k_{5.30} = 1.0 \times 10^9 \text{ dm}^3 \text{ mol}^{-1} \text{ s}^{-1}$ obtained in this way is somewhat lower than the value of $k(\text{H}^+)_{\text{fast}} = 1.7 \times 10^9 \text{ dm}^3 \text{ mol}^{-1} \text{ s}^{-1}$ obtained above by pulse radiolysis, but is in good agreement with the reported value for $k(\text{dehydration}) \sim 1 \times 10^9 \text{ dm}^3 \text{ mol}^{-1} \text{ s}^{-1}$ of the *para*-dihydroxycyclohexadienyl radicals.¹²³ On the other hand, the value of $k_{5.29} = 2.1 \times 10^8 \text{ dm}^3 \text{ mol}^{-1} \text{ s}^{-1}$ obtained here is higher than the value of $k(\text{H}^+)_{\text{slow}}$ obtained above by pulse radiolysis and the reported value (both $\sim 1 \times 10^8 \text{ dm}^3 \text{ mol}^{-1} \text{ s}^{-1}$)¹²³ for the dehydration of the *ortho*-dihydroxycyclohexadienyl radicals.

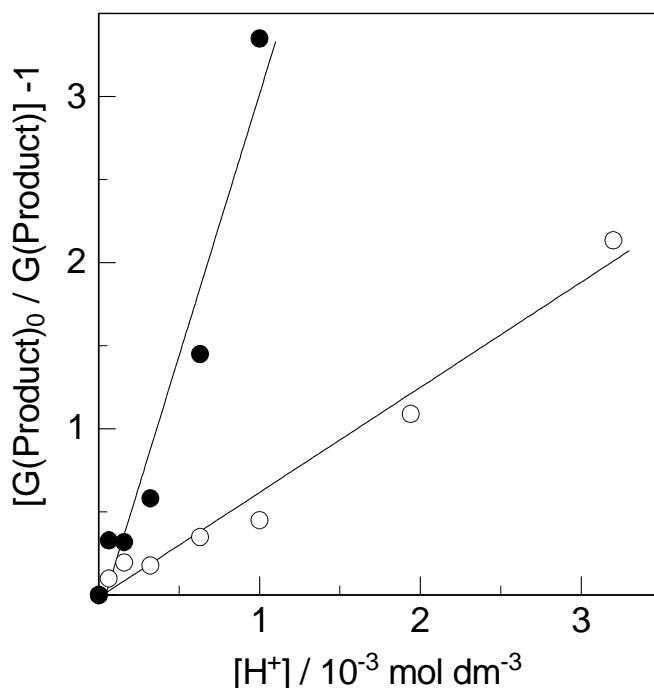


Figure 31 Proton concentration dependence of the term $G(\text{Product})_0/G(\text{Product}) - 1$ in the γ -radiolysis of $\text{N}_2\text{O}/\text{O}_2$ (4:1)-saturated solution of phenol, (λ) Product = hydroquinone, (μ), Product = catechol.

Error! Use the Home tab to apply Überschrift 1 to the text that you want to appear here.
Error! Use the Home tab to apply Überschrift 1 to the text that you want to appear here.

It is noted that the yields using dioxygen as an oxidant are lower (catechol 40% of $\bullet\text{OH}$, hydroquinone 31% of $\bullet\text{OH}$) than when *p*-benzoquinone was used to oxidise the dihydroxycyclohexadienyl radicals (catechol 48% of $\bullet\text{OH}$, hydroquinone 36% of $\bullet\text{OH}$).¹²³ This relative difference of 12% is significant (*i.e.* not within experimental error), and it is concluded, that in the case of dioxygen other reactions besides $\text{HO}_2\bullet$ -elimination reactions may proceed, albeit to a much lower extent than observed with other aromatic compounds, *e.g.* benzene.¹²² In the benzene study,¹²² material balance has been obtained, and from the products that are formed under these conditions it has been concluded that peroxy radicals of the kind formed in reactions (5.33) or (5.34) can also undergo intramolecular endoperoxide formation and subsequent fragmentation. In the present system, the $\text{HO}_2\bullet$ -elimination being that fast, this process will contribute less to the overall decay processes.

6 REACTIONS OF OZONE WITH DIHYDROXY BENZENES

Although extensive studies have been carried out on the reaction of ozone with phenol^{34,41,42,48-51,53,56,57,59}, very little has been done on its hydroxyl-derivatives. As shown in Chapter 5, the major products of the ozonolysis of phenol are catechol and hydroquinone. In this Chapter, the mechanism of the reactions of ozone with catechol and hydroquinone is discussed. The investigation of the ozone reactions with catechol and hydroquinone, does not only contribute to the understanding of ozone reactions with aromatic compounds but will also be useful in identifying reaction steps which lead to the full mineralisation of phenol by ozone.

6.1 Reactions of ozone with hydroquinone

Hydroquinone reacts relatively fast with ozone ($k = 2.3 \times 10^6 \text{ dm}^3 \text{ mol}^{-1} \text{ s}^{-1}$ at pH 7, and $1.8 \times 10^6 \text{ dm}^3 \text{ mol}^{-1} \text{ s}^{-1}$ at pH 3). Given its dissociation constants of $\text{p}K_1 = 9.91$ and $\text{p}K_2 = 11.56$,⁷⁰ at pH 3 hydroquinone exist mainly in the non-dissociated form, thus the rate constant measured at pH 3 can be regarded as the rate constant of the reaction of ozone with non-dissociated hydroquinone which is three orders of magnitude higher than that of ozone with non-dissociated phenol. It is difficult to experimentally determine the rate constant of the reaction of ozone with hydroquinone at high pH because hydroquinone autoxidises rapidly to 1,4-benzoquinone (*cf.* reaction 5.1).

The ozonation of hydroquinone was carried out at pH 7 where the non-dissociated form of hydroquinone dominates. The analysis of hydroquinone ozonation products proved to be very difficult. The product yields in the reaction of hydroquinone with ozone are given in Table 10. In this work, only two of its major carbon-containing ozonolysis products, namely 1,4-benzoquinone and 2-hydroxy-1,4-benzoquinone were identified, and their yields show a linear relationship with respect to the consumed ozone at low conversion (Figure 32).

Studies on the hydroquinone consumption as function of ozone consumed using 2.5×10^{-4} mol dm⁻³ hydroquinone and 5×10^{-5} to 2×10^{-4} mol dm⁻³ ozone showed that only 0.47 and 0.48 mol of hydroquinone is destroyed per one mole of ozone consumed in the absence of 2-methyl-2-propanol and presence of 2-methyl-2-propanol, respectively (Table 10). This result is similar to that obtained in the reaction of ozone with phenol, under the same conditions and as shown below, similar results were also obtained for the catechol/ozone system. Despite the fact that 0.48 mol of hydroquinone is destroyed per 1 mol of ozone consumed, the yields of the carbon-containing compounds obtained were only 0.24 mol per 1 mol of ozone representing only ~50% of the total hydroquinone destroyed. Some of the products are difficult to separate on the HPLC column, thus making it difficult for their quantitative analysis.

In the presence of 2-methyl-2-propanol and DMSO, the yield of 1,4-benzoquinone was found to be higher than in the absence of •OH scavengers (Figure 33). This phenomenon was also observed in the ozonolysis of phenol in the presence of 2-methyl-2-propanol. A possible explanation as indicated in section 5.1.3, is the peroxy radical induced oxidation of hydroquinone which give rise to benzoquinone [*cf.* reactions (5.22) and (5.23)].

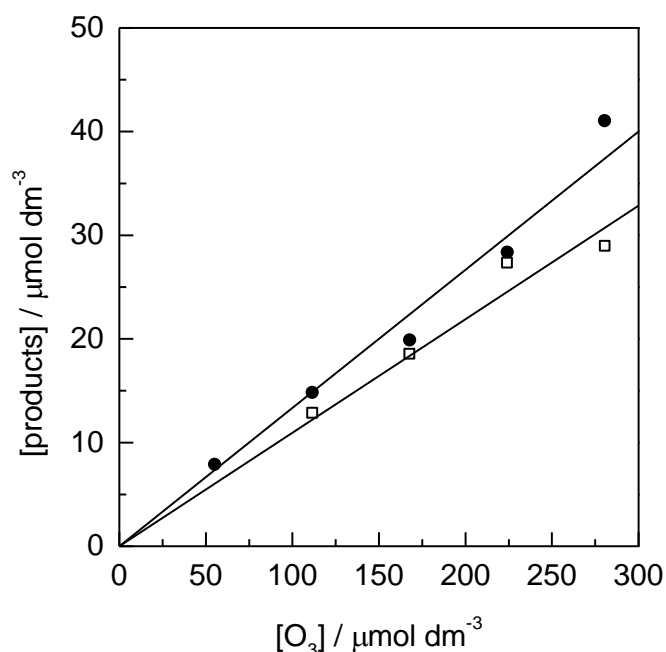


Figure 32 Ozonolysis of hydroquinone (3×10^{-3} mol dm⁻³) in aqueous solution at pH 7. Yields of 2-hydroxy-1,4-benzoquinone (o) and 1,4-benzoquinone (λ) as a function of the ozone concentration.

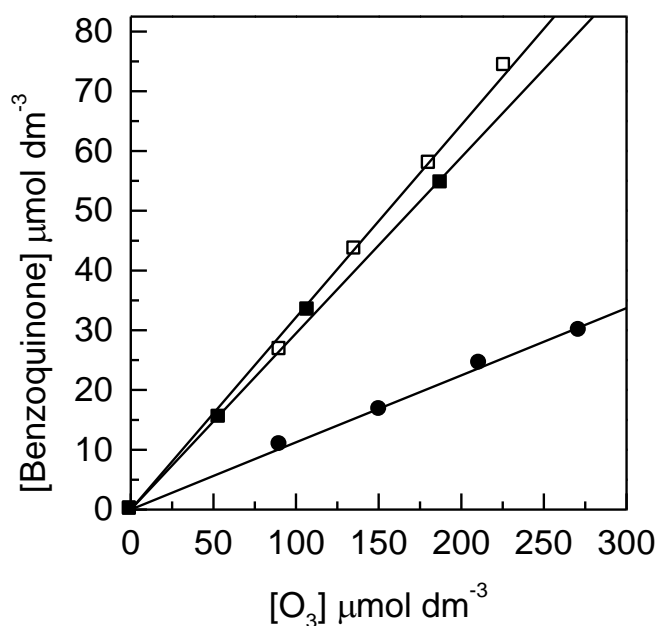


Figure 33 The yield of benzoquinone in the ozonolysis of hydroquinone in aqueous solution (λ), in the presence of 2-methyl-2-propanol (o), and in the presence of DMSO (v).

Table 10 Ozonolysis of hydroquinone ($3 \times 10^{-3} \text{ mol dm}^{-3}$). Products and their yields in % of ozone consumed. 2-Methyl-2-propanol (*t*-BuOH), and DMSO concentrations in these experiments were typically 0.1 mol dm^{-3} and $5 \times 10^{-2} \text{ mol dm}^{-3}$, respectively.

Product	Scavenger	Yield / %
1,4-Benzoquinone	–	13/12
	<i>t</i> -BuOH	36/32
	DMSO	30
2-Hydroxy-1,4-benzoquinone	–	11
	<i>t</i> -BuOH	< 1
	DMSO	< 1
Singlet dioxygen	–	16
Hydrogen peroxide	–	5.6
	<i>t</i> -BuOH	14
	DMSO	10.4
Formaldehyde	–	0
	<i>t</i> -BuOH	21

Table 10 continued

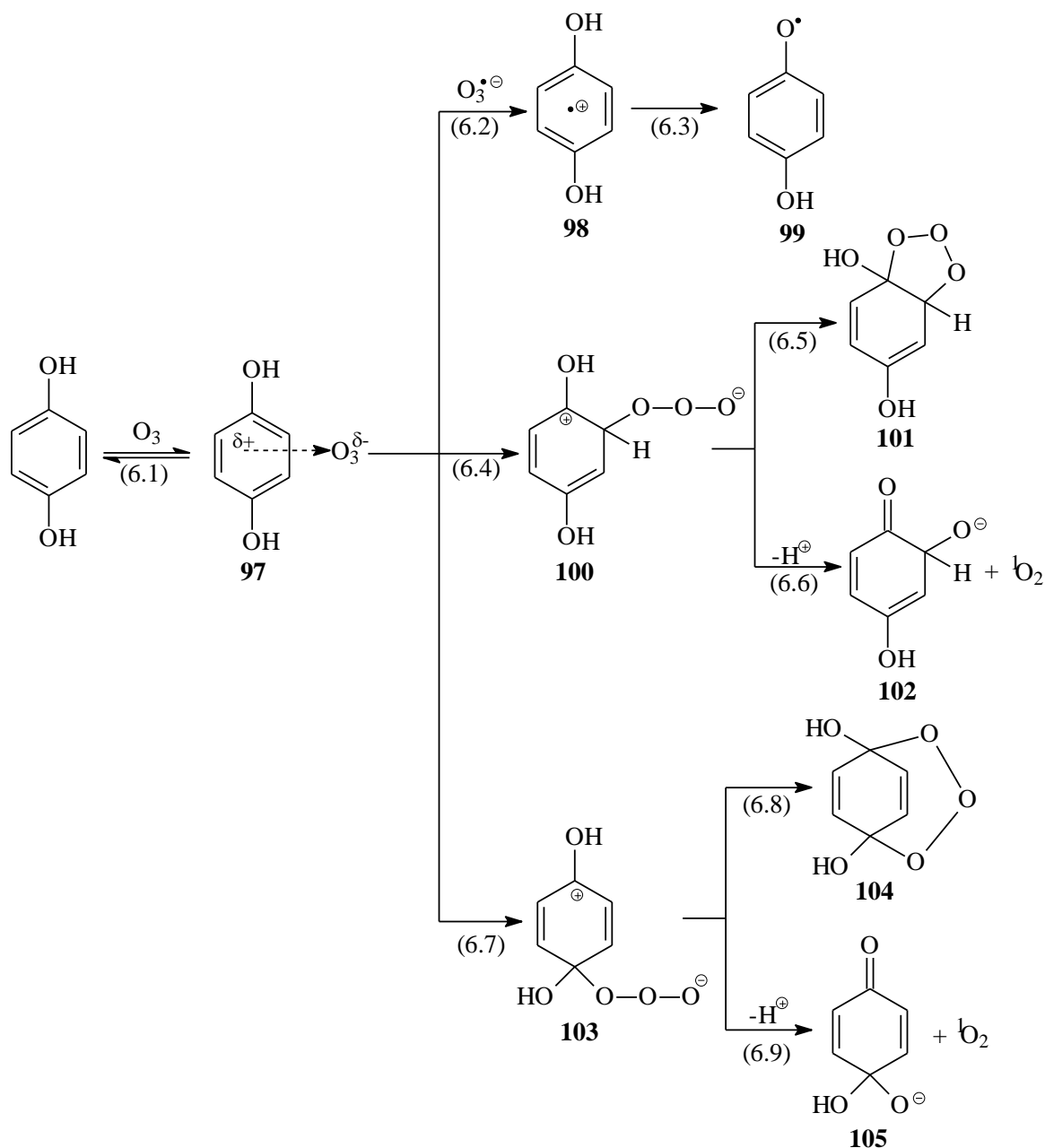
Error! Use the Home tab to apply Überschrift 1 to the text that you want to appear here.

Error! Use the Home tab to apply Überschrift 1 to the text that you want to appear here.

HOC(CH ₃) ₂ CHO	<i>t</i> -BuOH	23
Organic hydroperoxides	–	0
	<i>t</i> -BuOH	1.9
Methanesulfinic acid	DMSO	6.2
Methanesulfonic acid	DMSO	27
Hydroquinone consumption	-	47 ^a
Hydroquinone consumption	<i>t</i> -BuOH	48 ^a

^aat hydroquinone concentration of $2.5 \times 10^{-4} \text{ mol dm}^{-3}$

The ozonolysis of hydroquinone can be explained mechanistically in the same way as for phenol, whereby a π -complex is formed at the initial interaction of ozone with a phenyl ring [equilibrium (6.1) on page 88]. The $\bullet\text{OH}$ yield at pH 7 indicates that 42% of the π -complex **97** decomposes into a radical cation **98** and ozonide (the electron transfer component). The reduction potential of hydroquinone is 0.459 V, much lower than that of ozone. Therefore, the electron transfer reaction is expected to be exothermic.¹⁵

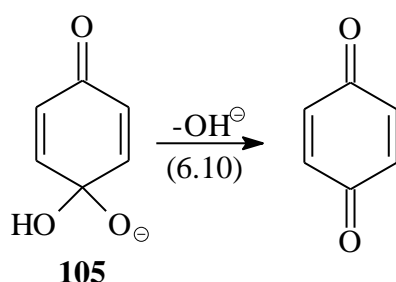


Scheme 11 Mechanism of the ozonolysis of hydroquinone.

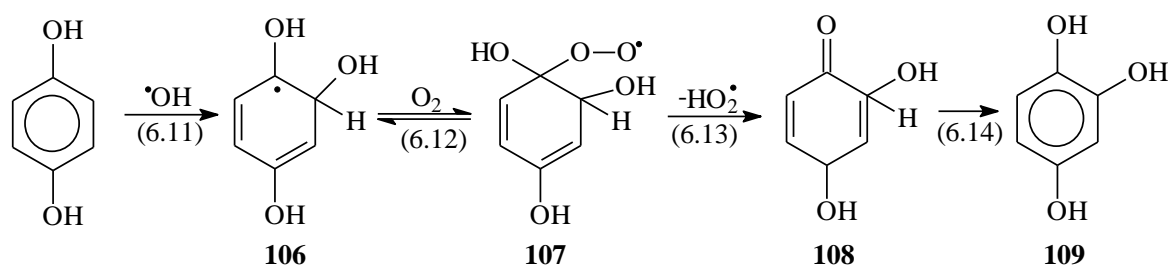
1,4-Benzoquinone, which was detected in the ozonolysis of hydroquinone might be formed from the electron transfer component [reaction (6.2)-(6.3)], whereby the resulting 4-hydroxyphenoxyl radical **99** also known as semiquinone radical undergoes a bimolecular disproportionation [*cf.* reaction (5.23) on page 76]. Another possible pathway leading to the formation of 1,4-benzoquinone are reactions (6.7)-(6.9), in which O₂(¹Δ_g) is released. The elimination of OH⁻ in **105** yields 1,4-benzoquinone [reaction (6.10)].

Error! Use the Home tab to apply Überschrift 1 to the text that you want to appear here.

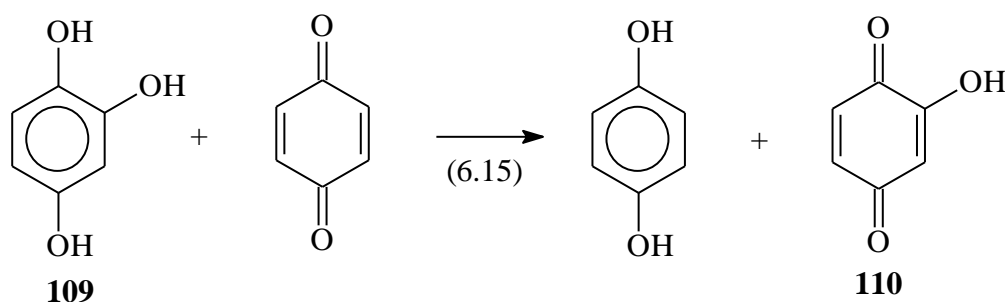
Error! Use the Home tab to apply Überschrift 1 to the text that you want to appear here.



The intermediate **102**, formed in reaction (6.6), rearranges into 1,2,4-trihydroxybenzene **109**. However, this is its only source. In the absence of $\bullet\text{OH}$ scavengers, $\bullet\text{OH}$ which is formed in this system reacts with hydroquinone yielding 1,2,4-trihydroxybenzene **109** [reactions (6.11) to (6.14)].



The yield of 1,2,4-trihydroxybenzene was very low and could not be quantitatively determined. This is not surprising as it is known that 1,2,4-trihydroxybenzene reacts with 1,4-benzoquinone yielding hydroquinone and 2-hydroxy-1,4-benzoquinone **110** [reaction (6.15)].¹⁴⁶ The yields of 2-hydroxy-1,4-benzoquinone was determined as 11% of the ozone consumed.



The rate constant of 1,4-benzoquinone reaction with 1,2,4-trihydroxybenzene depends on the pH. By monitoring the formation of 2-hydroxy-1,4-benzoquinone at 390 - 490 nm using the stopped-flow technique, the rate constants of the reaction of 1,4-benzoquinone with 1,2,4-trihydroxybenzene at pH 3 to 6 (Figure 34) was determined. The rate constants obtained ranged from $28 \text{ dm}^3 \text{ mol}^{-1} \text{ s}^{-1}$ at pH 3 to $1350 \text{ dm}^3 \text{ mol}^{-1} \text{ s}^{-1}$ at pH 6. Due to the fast

autoxidation of 1,2,4-trihydroxybenzene at pH higher than 7, the rate constant could not be measured at high pH.

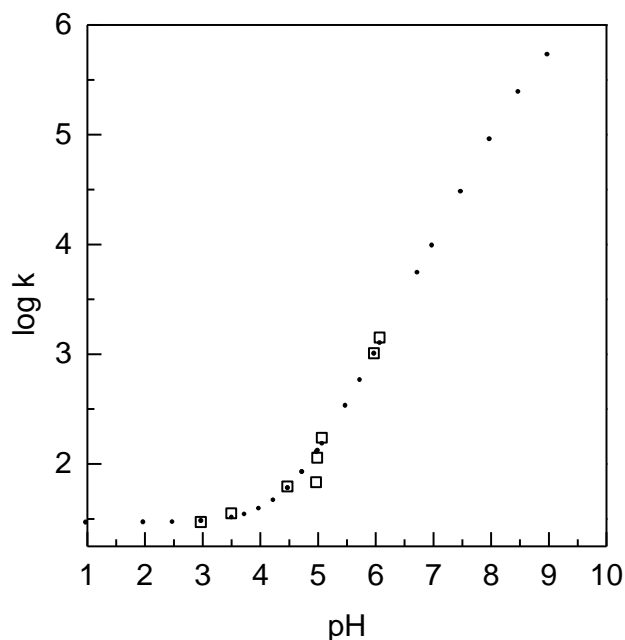


Figure 34 The rate constant of the oxidation of 1,2,4-trihydroxybenzene by 1,4-benzoquinone as a function of pH: experimental(o), calculated (•).

6.2 Reactions of ozone with catechol

As in the case of the ozonolysis of hydroquinone, full material balance was also not achieved in the analysis of catechol ozonation products. The only carbon-containing products identified are *cis,cis*-muconic acid and 2-hydroxy-1,4-benzoquinone. Their yields show a linear dependence on the ozone dose (Figure 35), their sum represent only 17% of the total ozone consumed (Table 11). The amount of catechol destroyed by ozone corresponds only to 47% of ozone consumed. This implies that only 35% of the carbon containing products were accounted for in the ozonolysis of catechol.

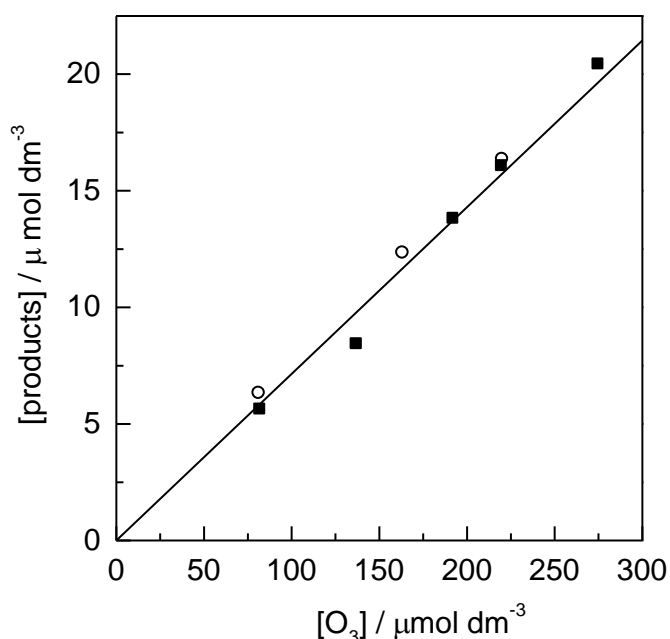


Figure 35 Ozonolysis of catechol ($3 \times 10^{-3} \text{ mol dm}^{-3}$) in aqueous solution at pH 7. Yields of 2-hydroxy-1,4-benzoquinone (μ) and *cis,cis*-muconic acid (ν) as a function of the ozone concentration.

Table 11 Ozonolysis of catechol ($3 \times 10^{-3} \text{ mol dm}^{-3}$). Products and their yields in % of ozone consumed. 2-Methyl-2-propanol (*t*-BuOH) and DMSO concentrations in these experiments were typically 0.1 mol dm^{-3} and $5 \times 10^{-2} \text{ mol dm}^{-3}$, respectively.

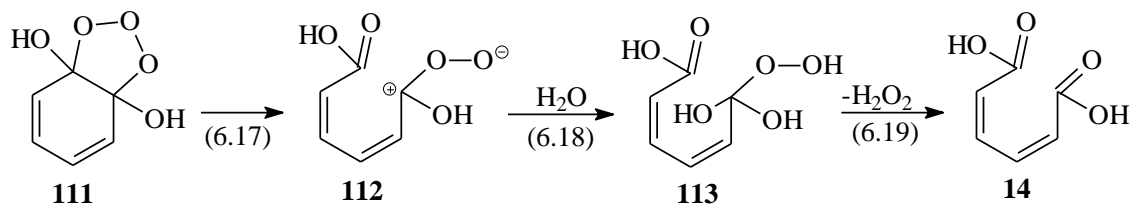
Product	Scavenger	Yield / %
2-Hydroxy-1,4-benzoquinone	–	7.4
Singlet dioxygen	–	14
Hydrogen peroxide	–	5.1
	DMSO	7.2
Formaldehyde	–	0
	<i>t</i> -BuOH	11
<i>cis,cis</i> -Muconic acid		7/10
Organic hydroperoxides	–	0
Methanesulfinic acid	DMSO	0
Methanesulfonic acid	DMSO	22
Catechol consumption		47 ^a

^aat catechol concentration of $2.5 \times 10^{-4} \text{ mol dm}^{-3}$

The mechanism of the reaction of catechol with ozone must be similar to that of hydroquinone with catechol (Scheme 11). Here, the electron transfer component makes up only 22% of the overall reaction since the yield of $\bullet\text{OH}$ measured is only 20% of the ozone consumed (*cf.* Table 11, the yield of formaldehyde and methanesulfonic acid). In this process, the 2-hydroxyphenoxy radical is formed, which react bimolecularly to yield catechol and 1,2-benzoquinone.[*cf.* reaction (5.23) onm page 76, the bimolecular disproportionation of 4-hydroxyphenoxy radical]. However, 1,2-benzoquinone is reported to be highly unstable in water, which might explain why it could not be to identified by HPLC.

Similar to the reaction (6.6) in the ozonolysis of hydroquinone, $\text{O}_2(^1\Delta_g)$ and correspondingly the 1,2,4-trihydroxybenzene **109** are formed in the reaction of catechol with ozone. Another source of 1,2,4-trihydroxybenzene **109** is the $\bullet\text{OH}$ induced oxidation of catechol [*cf.* reactions (6.11)-(6.14), for the $\bullet\text{OH}$ attack on hydroquinone]. The HPLC analysis of the ozonated catechol solution failed to detect 1,2,4-trihydroxybenzene, but its oxidised-derivative 2-hydroxy-1,4-benzoquinone was determined as 7% of the ozone consumed. 1,2,4-Trihydroxybenzene autoxidises very slowly at pH 7, the fact that it was not detected on the times scale of our HPLC analysis indicates that some oxidising agents, which oxidise 1,2,4-trihydroxybenzene into 2-hydroxy-1,4-benzoquinone, are formed in the ozonolysis of catechol. One of such oxidising agent could be 1,2-benzoquinone, which would oxidise 1,2,4-trihydroxybenzene, similar to 1,4-benzoquinone [*cf.* reaction (6.15)] to give rise to catechol and 2-hydroxy-1,4-benzoquinone.

The yield of *cis,cis*-muconic acid was determined to be 10% of the ozone consumed (Table 11). This implies that the Criegee-type reaction pathways [reaction (6.17) – (6.19)] makes up only 10% of the overall reaction.



7 REACTIONS OF OZONE WITH HALOPHENOLS

Halogenated phenols have become wide-spread anthropogenic environmental pollutants. Their major sources are waste incineration, pesticides, fungicides and herbicides. The biological degradation of most of these compounds is slow, and as a result they often remain a persistent problem in many drinking water. A number of investigations have been carried out on chlorinated phenols.³⁵⁻⁴⁰ In this chapter, the kinetic and mechanistic investigation of the reactions of ozone with pentachlorophenol, pentabromophenol and triiodophenol are reported.

7.1 Kinetics of the reactions of ozone with halophenols

Due to the low solubility of the halophenols under investigation (pentachlorophenol, pentabromophenol and 1,3,5-triiodophenol) at pH 7, all experiments were carried out at pH 10. Competition kinetics was used to determine the rate constant of ozone with the above mentioned phenol derivatives (*cf.* section 2.6.2). The reactions were carried out in the presence of DMSO to scavenge the $\bullet\text{OH}$ radical which is produced in these systems. The competition kinetics plot using 3-buten-1-ol as competitor give the slopes of 15.4 for pentachlorophenol, 21.5 for pentabromophenol and 86.1 for 2,4,6-triiodophenol (Figure 36). As described in section 2.6, the rate constants of the reactions of ozone with the pentachlorophenol ($1.2 \times 10^6 \text{ dm}^3 \text{ mol}^{-1} \text{ s}^{-1}$), pentabromophenol ($1.7 \times 10^6 \text{ dm}^3 \text{ mol}^{-1} \text{ s}^{-1}$), and 2,4,6-triiodophenol ($6.8 \times 10^6 \text{ dm}^3 \text{ mol}^{-1} \text{ s}^{-1}$) were obtained from the slope of the competition plots. Since the halophenols are fully dissociated at pH 10, the rate constants mentioned above are those of ozone with the halophenolates.

Rate constants of the reactions of ozone with a series of chlorophenolates (4-chlorophenol, 2,4-dichlorophenol, 2,4,6-trichlorophenol and 2,3,4,6-tetrachlorophenol) have been determined by Benitez et al.³⁶ It was shown in this work that the rate constants of ozone with the chlorophenolates decrease with increasing number of chlorine substituents (*cf.* Table 12). The value obtained for the rate constant of ozone with pentachlorophenolate ($k = 1.2 \times 10^6 \text{ dm}^3 \text{ mol}^{-1} \text{ s}^{-1}$) also follows this trend as determined in this study.

Table 12 Rate constants of ozone reactions with dissociated chlorophenols (chlorophenolates)

Substrate	k ($\text{dm}^3 \text{mol}^{-1} \text{s}^{-1}$)	References
4-Chlorophenolate	3.9×10^9	ref. ³⁵
2,4-Chlorophenolate	6.1×10^8	ref. ³⁵
2,4,6-Trichlorophenolate	5.6×10^7	ref. ³⁵
2,3,4,6-Tetrachlorophenolate	1.9×10^7	ref. ³⁵
Pentachlorophenolate	1.2×10^6	this work
Pentabromophenolate	1.7×10^6	this work
2,4,6-Triiodophenol	6.8×10^6	this work

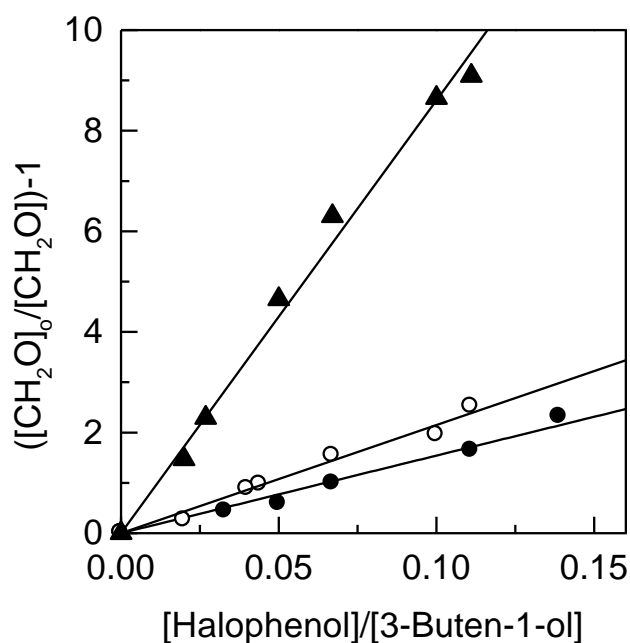


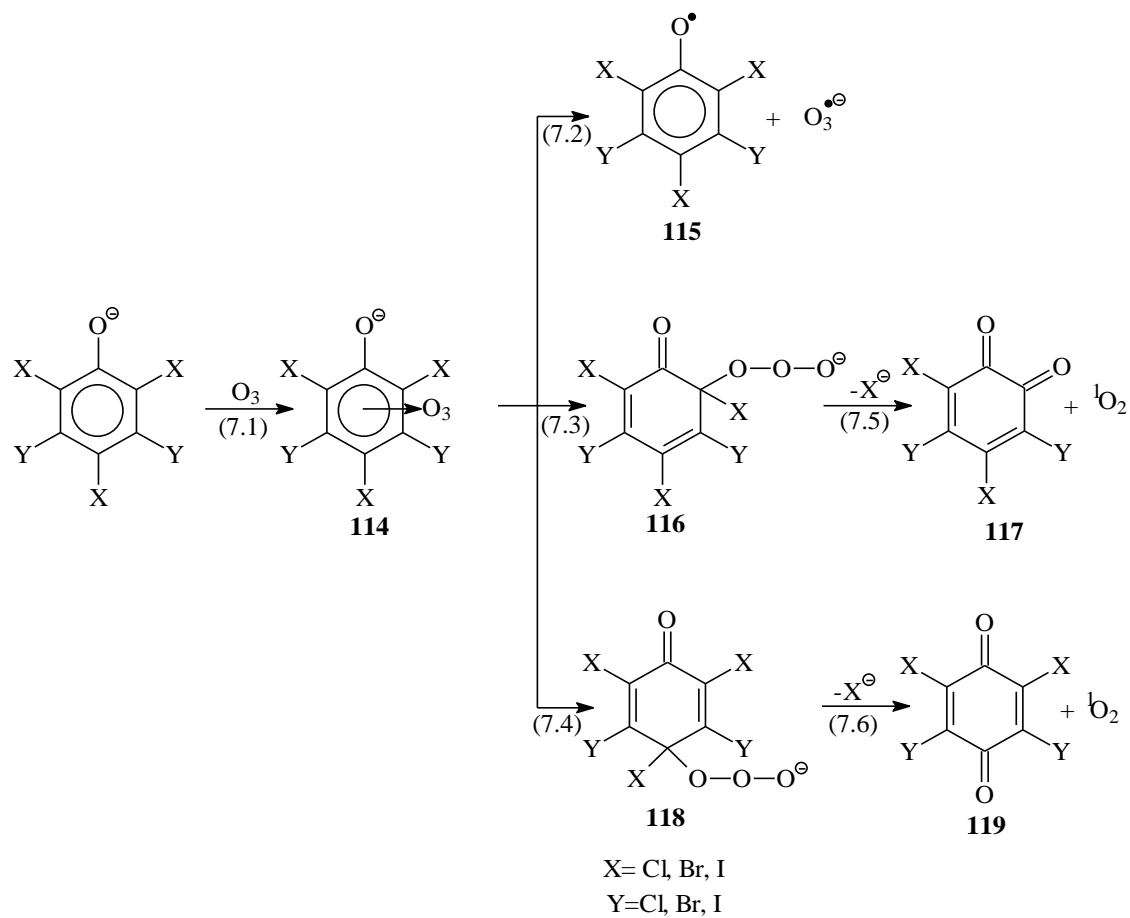
Figure 36 Competition plots for the reactions of ozone with pentachlorophenol (λ), pentabromophenol (μ) and 2,4,6-triiodophenol (σ) at pH 10 using 3-buten-1-ol as competitor. Formaldehyde yields result from the reaction of ozone with 3-buten-1-ol.

7.2 Product studies and mechanism of the reactions of ozone with halophenols

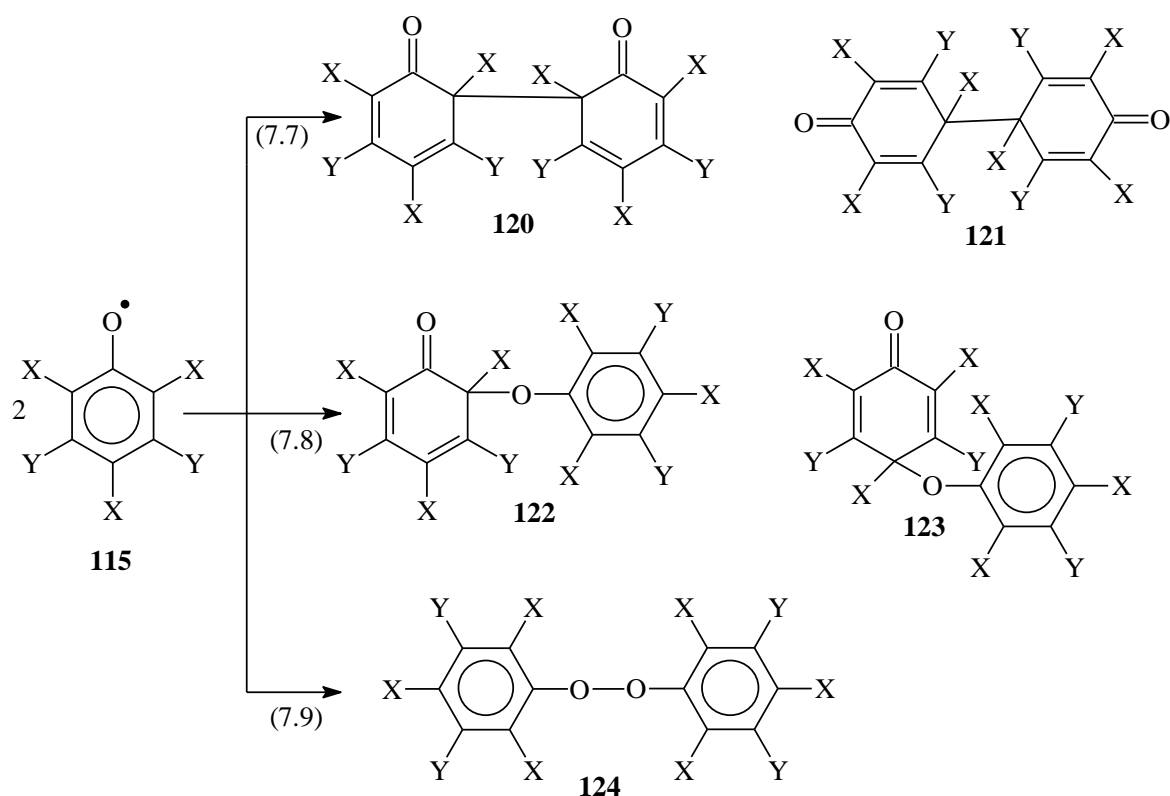
The general mechanism for the ozonolysis of pentachloro-, pentabromo- and 2,4,6-triodophenolate is given in Scheme 12. The determination of $\bullet\text{OH}$ yields in these systems revealed that electron transfer component [reaction (7.2)], take place 22% with pentachlorophenolate, 2% with pentabromophenolate, and 0% with triiodophenolate (*cf.* Table 4). The phenoxy radical formed in reaction (7.2), terminates by recombination at carbon [reaction (7.7)], or by carbon-oxygen coupling [reaction (7.8)] (Scheme 13).⁹⁸ Due to the low O-O binding energy, the termination of the phenoxy radical [reaction (7.9)] at both oxygens will not take place.

Regarding the product studies, it was relatively easy to determine the amount of halide ions released by ion chromatography. In the ozonolysis of pentachlorophenolate, 1 mol of ozone produces 2.5 mol chloride, while 3 mol of bromide and 1 mol of iodide per mol of ozone are formed in the ozonolysis of pentabromophenolate and triiodophenolate, respectively. The initial pathway leading to the halide release are via reactions (7.5) and (7.6). In this pathway, $\text{O}_2(^1\Delta_g)$ is also released and its yields are 58%, 48% and 10% in the reactions of ozone with pentachlorophenol, pentabromophenol and 2,4,6-triiodophenol, respectively [*cf.* Table 3 for the yields of $\text{O}_2(^1\Delta_g)$].

Error! Use the Home tab to apply Überschrift 1 to the text that you want to appear here.
Error! Use the Home tab to apply Überschrift 1 to the text that you want to appear here.

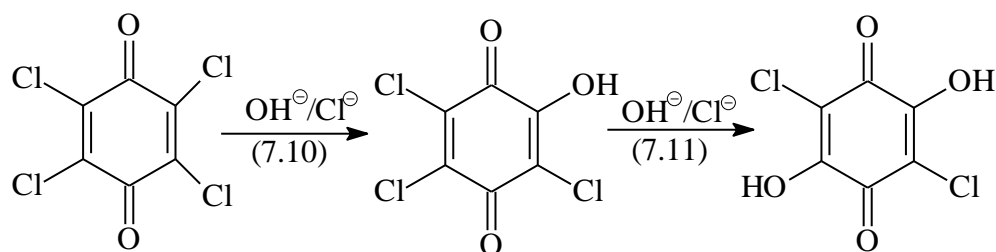


Scheme 12 Mechanism of the ozonolysis of halophenolate.



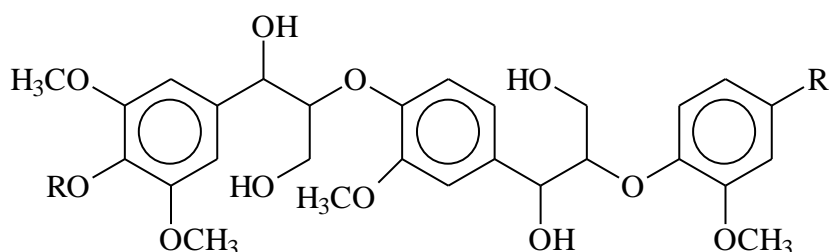
Scheme 13 Bimolecular decay of the halophenoxy radical.

In the ozonolysis of pentachlorophenolate, products corresponding to **117** (*o*-chloranil) and **119** (*p*-chloranil) have been identified by HPLC. It has been shown that *p*-chloranil undergoes a fast hydrolysis [OH^- induced; reaction (7.10), $k = 1.7 \times 10^3 \text{ dm}^3 \text{ mol}^{-1} \text{ s}^{-1}$] into 2,3,5-trichloro-6-hydroxy-1,4-benzoquinone.^{98,147} The second hydrolysis step is much slower [reaction (7.11), $k = 3.9 \text{ dm}^3 \text{ mol}^{-1} \text{ s}^{-1}$]. This hydrolysis is expected to be similar for the 2,3,5,6-tetrabromo-1,4-benzoquinone and 3,4,5,6-tetrabromo-1,2-benzoquinone formed in the ozonolysis of pentabromophenolate. The high yield of the halide ion in these system can be attributed to the above mentioned hydrolysis of the products.



8 REACTIONS OF OZONE WITH METHOXYBENZENES

The study of ozonolysis of methoxybenzenes is important not only for understanding the reactivity of ozone toward aromatic compounds, but also in understanding the degradation of lignin by ozone. Lignin, a complex biopolymer that accounts for 20-30% of dry wood is made up of mainly methoxybenzenes and their derivatives. Lignin is also likely to be found in drinking- and waste-water, especially in the effluents from paper industries as one of the major components. A representation of lignin polymer is given in Scheme 14.



Scheme 14 Schematic representation of typical functional groups of the lignin polymer showing the presence of methoxybenzene groups.

8.1 Product studies

8.1.1 Reactions of ozone with anisole

The only carbon-containing compounds identified in this system are methyl(2*Z*,4*Z*)-6-oxohexa-2,4-dienoate **45** and methyl(2*E*,4*Z*)-3-methoxyhexa-2,4-diendial **47**. However, their yields could not be determined. Hydrogen peroxides, and $\bullet\text{OH}$ were also formed in the ozonolysis of anisole, their yields were measured and are given in Table 8 and 6, respectively. Singlet dioxygen [$\text{O}_2(^1\Delta_g)$] is not formed to any significant extent.

8.1.2 Reactions of ozone with 1,2-dimethoxybenzene

The yields of the products measured in the ozonolysis of 1,2-dimethoxybenzene are given in Table 13. The only carbon-containing compound identified is dimethyl(2*Z*,4*Z*)-hexa-2,4-diendioate **50**. Pure dimethyl(2*Z*,4*Z*)-hexa-2,4-diendioate was not available. Therefore its yield was determined by HPLC after hydrolysis to muconic acid. The muconic acid yield was linear with respect to the ozone dose (*cf.* Figure 37).

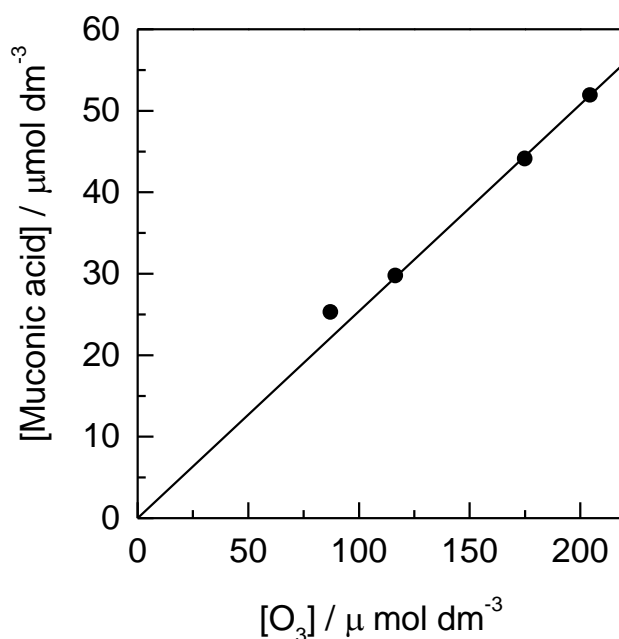


Figure 37 Ozonolysis of 1,2-dimethoxybenzene. The yield of dimethyl(2Z,4Z)-hexa-2,4-diendioate after hydrolysis to muonic acid as a function of the ozone concentration.

Table 13 Ozonolysis of 1,2-dimethoxybenzene. Products and their yields in % of ozone consumed. 2-Methyl-2-propanol (*t*-BuOH) and TNM concentrations in these experiments were typically 0.1 mol dm⁻³ and 1 × 10⁻³ mol dm⁻³, respectively.

Product	Scavenger	Yield / %
Singlet dioxygen	–	9
Hydrogen peroxide	–	27
Formaldehyde	–	0
	<i>t</i> -BuOH	6.4
Nitroform anion	TNM	4
Dimethyl(2Z,4Z)-hexa-2,4-diendioate 50		25

8.1.3 Reactions of ozone with 1,4-dimethoxybenzene

The analysis of carbon-containing products in the ozonolysis of 1,4-dimethoxybenzene was relatively easy, since three different carbon-containing products were identified. These are hydroquinone, 1,4-benzoquinone and methyl(2Z,4E)-4-methoxy-6-oxo-hexa-2,4-dienoate **51**. Their yields were determined by HPLC and show a linear dependence with respect to the ozone dose (Figure 38). The yields of the products measured in this system which account for 62% of ozone consumed are given in Table 14.

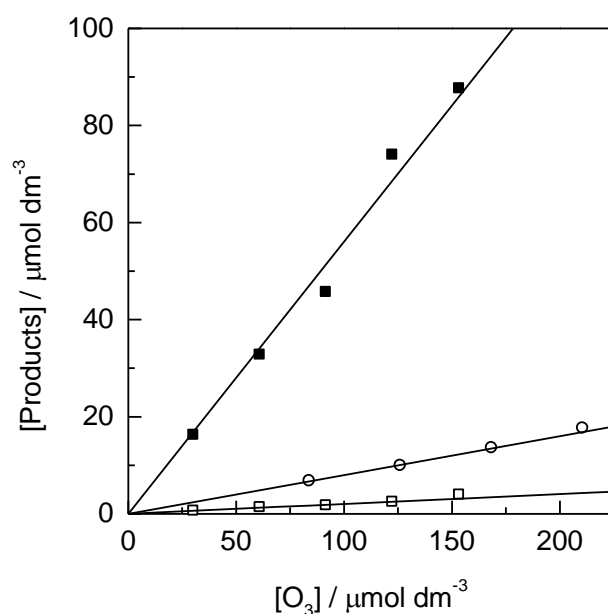


Figure 38 Ozonolysis of 1,4-dimethoxybenzene. The yields of 1,4-benzoquinone (μ), hydroquinone (o) and methyl(2Z,4E)-4-methoxy-6-oxo-hexa-2,4-dienoate (v) as a function of the ozone concentration.

Table 14 Ozonolysis of 1,4-dimethoxybenzene. Products and their yields in % of ozone consumed. 2-Methyl-2-propanol (*t*-BuOH) and TNM concentrations in these experiments were typically 0.1 mol dm^{-3} and $1 \times 10^{-3} \text{ mol dm}^{-3}$, respectively.

Product	Scavenger	Yield / %
1,4-Benzoquinone	–	8
Hydroquinone	–	2
Singlet dioxygen	–	6
Hydrogen peroxide	–	56
Formaldehyde	–	0
	<i>t</i> -BuOH	10
Nitroform anion	TNM	9
Methyl(2Z,4E)-4-methoxy-6-oxo-hexa-2,4-dienoate 51		52

8.1.4 Reactions of ozone with 1,3,5-trimethoxybenzene

By following the reaction of ozone with 1,3,5-trimethoxybenzene using the stopped-flow technique, an interesting spectrum was observed (Figure 39). At $\lambda = 260 \text{ nm}$ and $\lambda = 360 \text{ nm}$, a decay of was observed (Figure 39, inset A and C). The differences in the kinetic of

decay at these two wavelengths indicate that the absorption are due to two different intermediates.⁷¹ Unfortunately, it was not possible to identify them. As shown in Figure 39 inset B, the formation of a species with $\lambda_{\text{max}} = 290 \text{ nm}$ was observed, which reaches a plateau at about 3s and is proportional to the ozone concentration. This product was identified by GC-MS (*cf.* Figure 9 on page 30) and NMR as 2,6-dimethoxy-1,4-benzoquinone **54**.

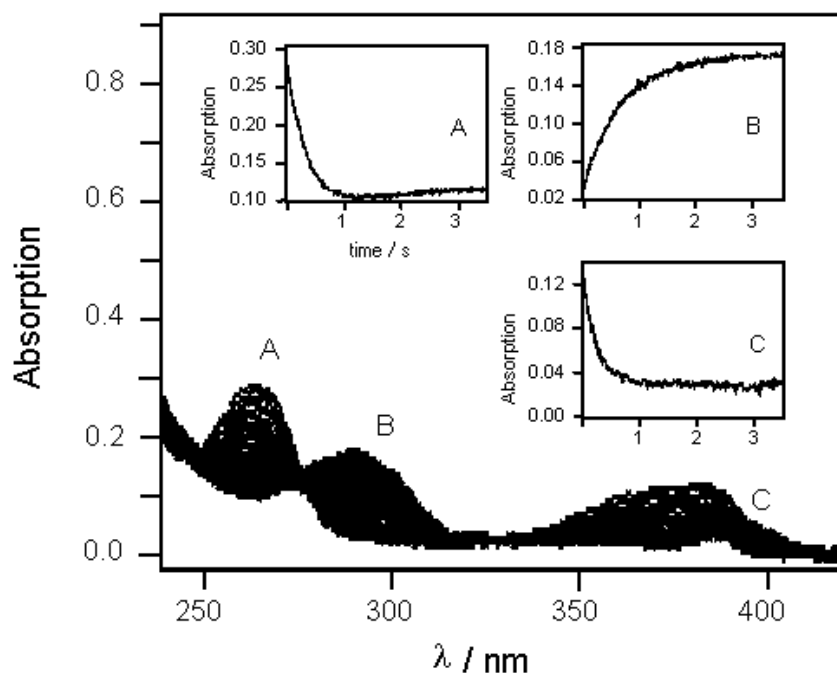


Figure 39 Formation and decay of intermediates in the reaction of ozone with 1,3,5-trimethoxybenzene. Inset A-C: kinetics at 260, 290 and 360 nm respectively.⁷¹

As reference material, **54** was prepared by ozonation of the aqueous solution of 1,3,5-trimethoxybenzene and then separated by preparative HPLC which was used to determine its yield in the ozonolysis of 1,3,5-trimethoxybenzene. The data obtained by HPLC show a linear dependence on the ozone concentration (Figure 40). Yields of other products determined in the reaction of ozone with 1,3,5-trimethoxybenzene are given in Table 15.

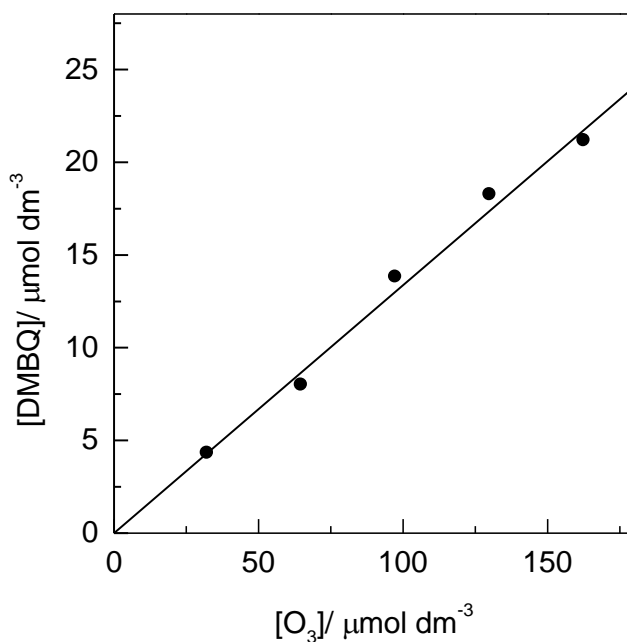


Figure 40 Ozonolysis of 1,3,5-trimethoxybenzene. The yield of 2,6-dimethoxy-1,4-benzoquinone as a function of the ozone concentration.

Table 15 Ozonolysis of 1,3,5-Dimethoxybenzene. Products and their yields in % of ozone consumed. 2-Methyl-2-propanol (*t*-BuOH) and TNM concentrations in these experiments were typically 0.1 mol dm^{-3} and $1 \times 10^{-3} \text{ mol dm}^{-3}$, respectively.

Product	Scavenger	Yield / %
2,6-dimethoxy-1,4-benzoquinone 54	-	20
2,6-dimethoxyhydroquinone 56	-	identified by GC-MS
2,4,6-trimethoxyphenol	-	identified by GC-MS
Singlet dioxygen	-	30
Hydrogen peroxide	-	6.5 (13 at pH 2)
Formaldehyde	-	absent
	<i>t</i> -BuOH	7.4
Nitroform anion	TNM	10
(<i>2E,4E</i>)-2,4,6-trimethoxy-6-oxo-hexa-2,4-dienoic acid 55	-	identified by GC-MS

8.2 Mechanism of the ozonolysis of methoxy benzenes

Due to lack of material balance in these systems, the mechanisms proposed here remain tentative. As in case of all aromatic compound, the ozone reactions proceed via the formation of a π -complex. Unlike in the case of phenol and the dihydroxybenzenes, the reduction potential of methoxybenzene [anisole (1.62 V), 1,2-dimethoxybenzene (1.44 V), 1,4-dimethoxybenzene (1.30 V) and 1,3,5-trimethoxybenzene(1.44 V)]¹²⁴ are higher than that of ozone (1.01 V). Therefore, the electron transfer process is expected to be endothermic.

Without having to draw the mechanism of ozone reactions with each methoxybenzene investigated, Scheme 15 (mechanism of the decay of the 1,4-dimethoxybenzene-ozone π -complex) will be used also to explain product distribution in the reactions of ozone with the other methoxybenzenes studied. The decomposition of the 1,4-dimethoxybenzene-ozone π -complex yields the zwitterion **125** and **126**. The zwitterion **125** may decompose via a reaction pathway in which is $O_2(^1\Delta_g)$ [reactions (8.1) and (8.6)] or HO_2^\bullet [reactions (8.1), (8.5) and (8.7)] is released, or may undergo a 1,3-dipolar cycloaddition reaction [reaction (8.2)]. Both $O_2(^1\Delta_g)$ and HO_2^\bullet have been detected in the reaction of ozone with 1,4-dimethoxybenzene, but in relatively low yields of 6 and 9%, respectively. Another source of $O_2(^1\Delta_g)$ in the reaction of ozone with 1,4-dimethoxybenzene is the decomposition of **126**, whereby 1,4-benzoquinone is formed. The yield of 1,4-benzoquinone was determined as 8% of the ozone consumed which is very close to that of $O_2(^1\Delta_g)$. Similar routes may be responsible for the formation of $O_2(^1\Delta_g)$ and HO_2^\bullet in the reaction of ozone with 1,2-dimethoxybenzene.

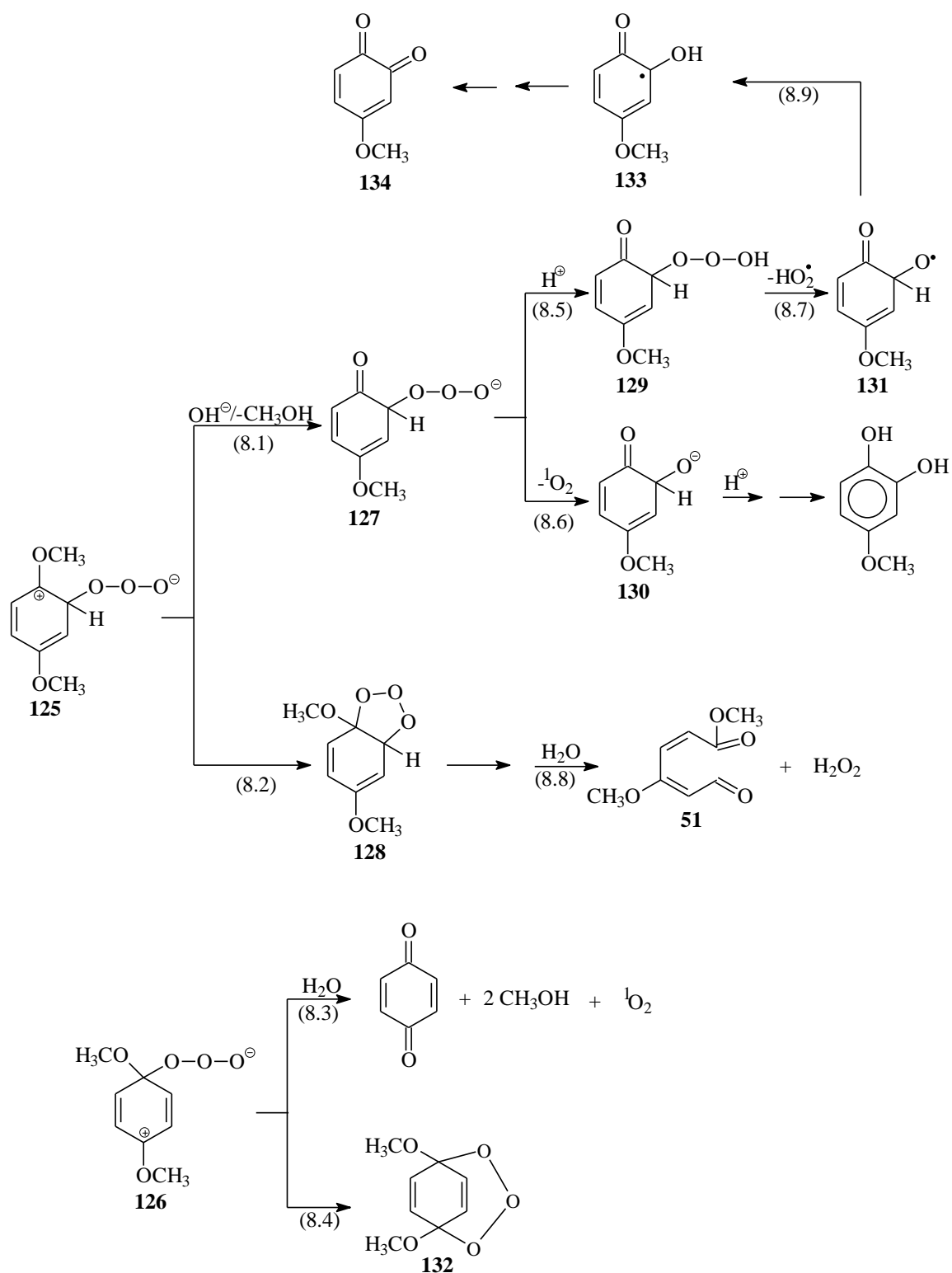
The 1,3-dipolar cycloaddition [*cf.* reaction (8.2)] is a well known reaction pathway in ozone reaction. One of the product formed via this route is H_2O_2 . The H_2O_2 yield in the reaction of ozone with 1,4-dimethoxybenzene agrees very well with that of methyl(2*Z*,4*E*)-4-methoxy-6-oxo-hexa-2,4-dienoate **51** (*cf.* Table 14). This confirms the occurrence of reactions (8.2) and (8.8). A similar reaction pathway was also observed in the reaction of ozone with 1,2-dimethoxybenzene [reactions (4.40) to (4.44)]. Here, the yield of H_2O_2 is 27% and that of the corresponding product dimethyl(2*Z*,4*Z*)-hexa-2,4-diendioate **50** is 25% (*cf.* Table 13). Only 6% H_2O_2 at pH 7 and 13% H_2O_2 at pH 2 are detected in the reaction of

O₃ with 1,3,5-trimethoxybenzene where as its corresponding product 2,6-dimethoxy-1,4-benzoquinone is formed in 20% yield.

It is important to note that the 1,3-dipolar cycloaddition reaction pathway is more pronounced in the reaction of ozone with methoxybenzenes as compared to hydroxybenzenes (*cf.* Table 8 on page 62), on the yield of hydrogen peroxide). This can be attributed to the fact that the zwitterion formed in the reaction of ozone with hydroxybenzenes deprotonate fast preventing the 1,3-cyclisation to occur.

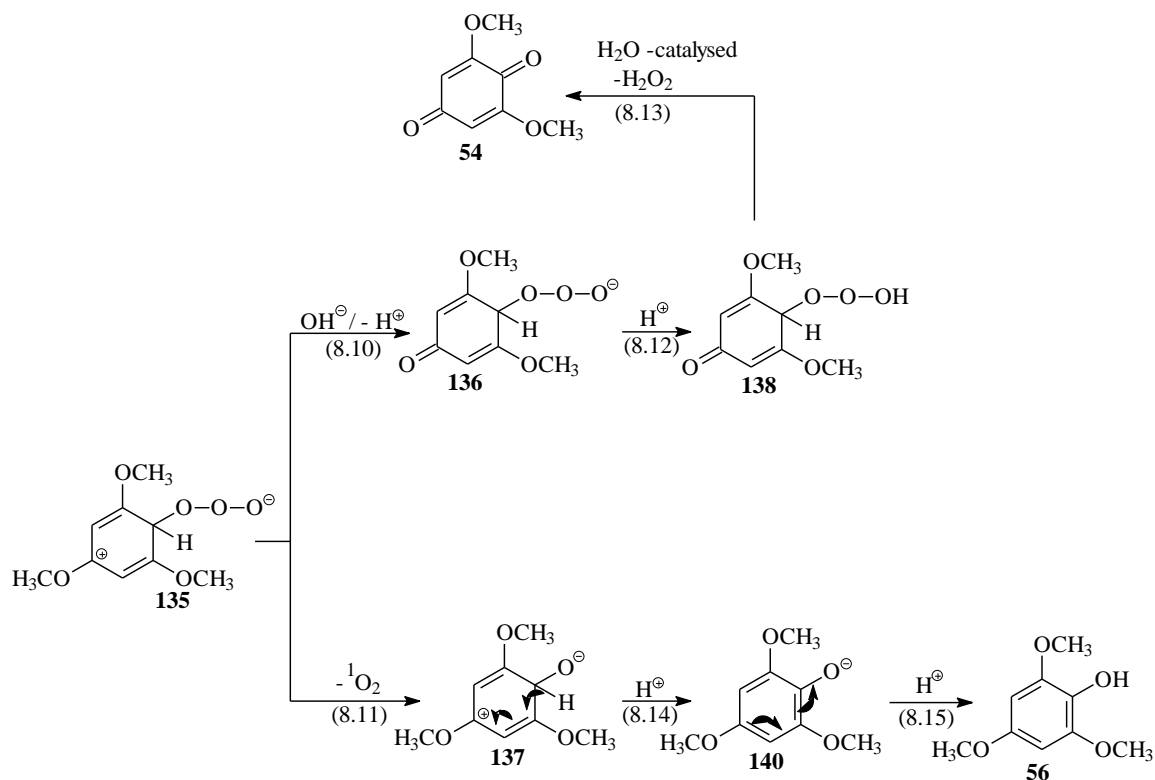
The formation of 2,6-dimethoxy-1,4-benzoquinone in the reaction of ozone with 1,3,5-trimethoxybenzene is very much intriguing. Efforts have been made to find a meaningful reaction mechanism which explains this observation. In Scheme 16, the mechanism leading to the formation of 2,6-dimethoxy-1,4-benzoquinone in the ozonolysis of 1,3,5-trimethoxybenzene is proposed. A possible route is suggested which involves the H⁺ - catalysed elimination of H₂O₂ [reaction (8.10)-(8.13)]. The yield of 2,6-dimethoxy-1,4-benzoquinone was determined as 20% of the ozone consumed (*cf.* Figure 40), corresponding to that of H₂O₂. The route leading to the formation of 2,6-dimethoxy-1,4-benzoquinone [reaction 8.10] competes with the O₂(¹Δ_g) elimination reaction [reaction 8.11]. In the O₂(¹Δ_g) reaction, 2,4,6-trimethoxyphenol is formed. This product was identified by GC-MS (*cf.* section 2.8.6) but its yield could not be determined.

Error! Use the Home tab to apply Überschrift 1 to the text that you want to appear here.
 Error! Use the Home tab to apply Überschrift 1 to the text that you want to appear here.



Scheme 15 Mechanism of the ozonolysis of 1,4-dimethoxybenzene.

Error! Use the Home tab to apply Überschrift 1 to the text that you want to appear here.
Error! Use the Home tab to apply Überschrift 1 to the text that you want to appear here.



Scheme 16 Mechanism leading to the formation of 2,6-dimethoxy-1,4-benzoquinone **54** and 2,4,6-trimethoxyphenol **56** in the ozonolysis of 1,3,5-trimethoxybenzene.

9 SUMMARY AND CONCLUSION

9.1 Review of the methodology

In this work, various techniques were applied in order to help with the elucidation of the mechanism of ozone reactions.

9.1.1 Kinetics of ozone reactions

The competition method (*cf.* section 2.6.2) was successfully employed to determine the rate constant of the reactions of ozone with hydroquinone, catechol, pentachlorophenolate, pentabromophenolate, triiodophenolate, 2,3-dihydroxydithiane and 1,4-dithiothreitol. The results are in good agreement with the literature data, some of which were obtained by other methods e.g. for catechol and hydroquinone.

9.1.2 Detection of singlet dioxygen

As far as the product studies are concerned, it was important to determine the yield of short-lived products which cannot be measured directly by conventional methods. The yields of singlet dioxygen, one of the short-lived products in ozone reactions, were measured (Chapter 3). This method provides unambiguous information on the reaction mechanism, *i.e.* detection of $O_2(^1\Delta_g)$ is an indication that an O-transfer reaction must be involved. The $O_2(^1\Delta_g)$ yield measurements can be used with some confidence within the limitations discussed in Chapter 3, and provides most valuable information as to mechanistic details of ozone reactions in aqueous solution. Thus, the determination of $O_2(^1\Delta_g)$ yields is an indispensable tool in mechanistic studies of ozone reactions in general.

The ease of such experiments and the relatively low equipment cost may stimulate a more abundant use of this technique. In principle, this technique may also be applied to study ozone reactions in non aqueous media.

9.1.3 Detection of $\cdot OH$ and $O_2^{\bullet -}$

Ozone reactions sometimes also involve free-radical pathways. Methods developed in radiation chemistry for the detection of free radicals were successfully employed to ozone chemistry in this work. 2-Methyl-2-propanol and DMSO were used for the detection of

$\bullet\text{OH}$ formation and TNM was applied for $\text{O}_2^{\bullet-}$ formation. Although the free-radical detection methods are well developed and used routinely in radiation chemistry, they could not simply be transferred to ozone chemistry. These radical scavengers (2-methyl-2-propanol, DMSO and TNM) also react with ozone. Fortunately, their reaction rates with ozone are lower ($k = 1 \times 10^3 \text{ dm}^3 \text{ mol}^{-1} \text{ s}^{-1}$, $8.2 \text{ dm}^3 \text{ mol}^{-1} \text{ s}^{-1}$, and $10 \text{ dm}^3 \text{ mol}^{-1} \text{ s}^{-1}$ for 2-methyl-2-propanol, DMSO and TNM, respectively) than that of the substrates studied ($k > 1 \times 10^3 \text{ dm}^3 \text{ mol}^{-1} \text{ s}^{-1}$). Nevertheless, conditions could be established in order to avoid interference of the added scavengers to the ozone reactions with the substrates. By considering the rate constants of the substrate, the radical scavengers and that of the radicals with ozone, optimal scavenger to substrate ratio in terms of their concentrations could be calculated at which radicals can be successfully detected. For the detection of $\bullet\text{OH}$ with 2-methyl-2-propanol, a 2-methyl-2-propanol concentration of about 30 times than that of the substrate was used, i.e., $3 \times 10^{-3} \text{ mol dm}^{-3}$ substrate and 0.1 mol dm^{-3} 2-methyl-2-propanol while keeping the ozone concentration below $2 \times 10^{-4} \text{ mol dm}^{-3}$ to avoid secondary ozone reactions. In some cases, a ratio of 100:1 2-methyl-2-propanol to substrate was used. In the DMSO system, choosing an appropriate substrate to scavenger ratio alone does not suffice as the ensuing product in the reaction of $\bullet\text{OH}$ with DMSO, namely methanesulfinic acid, reacts very fast with ozone yielding methanesulfonic acid ($k = 6 \times 10^6 \text{ dm}^3 \text{ mol}^{-1} \text{ s}^{-1}$). In this case, methanesulfinic acid may compete against the substrate for ozone. The error in the measured $\bullet\text{OH}$ yield can be minimised by measuring both the methanesulfinic and methanesulfonic acid yields.

There are also challenges in using TNM to detect $\text{O}_2^{\bullet-}$ in ozone reactions. The low solubility of TNM in water ($\sim 1 \times 10^{-3} \text{ mol dm}^{-3}$) prevents us to increase the TNM concentration beyond this limit as one might wish. Since the substrates studied do not react with $\text{O}_2^{\bullet-}$, the only other concern is the reaction of ozone with $\text{O}_2^{\bullet-}$ ($k = 1.6 \times 10^9 \text{ dm}^3 \text{ mol}^{-1} \text{ s}^{-1}$) which is about equally fast as TNM ($k = 2 \times 10^9 \text{ dm}^3 \text{ mol}^{-1} \text{ s}^{-1}$). The reaction of ozone with $\text{O}_2^{\bullet-}$, can be prevented by using an ozone concentration ~ 10 -fold lower than that of TNM, i.e. an TNM concentration of $\sim 1 \times 10^{-3} \text{ mol dm}^{-3}$ (the maximum concentration of TNM that can be dissolved in water); ozone concentration must be kept below $1 \times 10^{-4} \text{ mol dm}^{-3}$. In the reaction of TNM with $\text{O}_2^{\bullet-}$, the ensuing product, the nitroform anion ($\text{C}(\text{NO}_2)_3^-$), reacts with ozone yielding 3 mol of nitrite ($k = 1.4 \times 10^4 \text{ dm}^3$

$\text{mol}^{-1} \text{ s}^{-1}$). Measuring both $\text{C}(\text{NO}_2)_3^-$ and nitrite yields gives a reasonable estimate of the $\text{O}_2^{\bullet-}$ yield. It should also be noted that nitrite reacts much faster than $\text{C}(\text{NO}_2)_3^-$ ($k = 6.08 \times 10^5 \text{ dm}^3 \text{ mol}^{-1} \text{ s}^{-1}$).¹⁰³

The detection of $\text{O}_2^{\bullet-}$ and $\bullet\text{OH}$ are important to distinguish between an electron-transfer reaction which gives rise to $\bullet\text{OH}$ and addition/elimination reaction which give rise to $\text{O}_2^{\bullet-}$. A case in point is the reaction of ozone with phenol, where 22% of $\bullet\text{OH}$ and 19.5% of $\text{O}_2^{\bullet-}$ were determined. These data showed that $\bullet\text{OH}$ is formed as result of an electron-transfer reaction [*cf.* reaction (4.16) on page 47] while $\text{HO}_2^{\bullet}/\text{O}_2^{\bullet-}$ is exclusively formed as a result of $\bullet\text{OH}$ attack on phenol and subsequent HO_2^{\bullet} elimination [*cf.* reactions (4.23) - (4.25)].

9.2 General mechanism of the reaction of ozone with phenol and its derivatives

As the general mechanism of the reaction of ozone with aromatic compounds one may consider the formation of a donor-acceptor π -complex. The subsequent decay of such complexes depends on the nature of the ring substituents. Two possible pathways are shown through which the π -complexes decay has been identified, *i.e.* a pathway leading to the formation of a zwitterion complex (σ -complex) and an electron-transfer pathway (*cf.* Scheme 8, 10, 12 and 13).

9.2.1 Reactions of ozone with phenol and dihydroxybenzenes

Electron transfer reactions are more strongly pronounced in the ozone reaction with phenols due to their low reduction potential. This has also been revealed by the $\bullet\text{OH}$ yields in the reactions of ozone with phenol and dihydroxybenzenes which are $27 \pm 4.5\%$ for phenol, $22 \pm 3.8\%$ for catechol, and $42 \pm 7\%$ for hydroquinone. The products in the electron transfer reactions are phenoxy-type radicals and an ozonide radical $\text{O}_3^{\bullet-}$. The phenol-derived phenoxy radicals react bimolecularly forming dimers while hydroquinone derived phenoxy-type radicals disproportionate into hydroquinone and benzoquinone. In the reaction of ozone with phenol, the yields of dimers is only 2% and there is no evidence of polymer formation. This may be pointing to the occurrence of some reactions which

compete against the bimolecular reaction of phenoxyl radicals. In this work it is suggested that the phenoxyl radicals react with ozone. The consumption of phenol, hydroquinone and catechol at the substrate concentration $2.5 \times 10^{-4} \text{ mol dm}^{-3}$ and ozone concentration of up to $2 \times 10^{-4} \text{ mol dm}^{-3}$, is only 0.5 mol per 1 mol of ozone consumed. This observation is attributed to the consumption of ozone by phenoxyl radicals.

In the reaction of ozone with phenol, not only its rate constant is increased upon deprotonation (from $1.3 \times 10^3 \text{ dm}^3 \text{ mol}^{-1} \text{ s}^{-1}$ to $1.4 \times 10^9 \text{ dm}^3 \text{ mol}^{-1} \text{ s}^{-1}$)⁶⁹ but the product distribution is also affected. For the interpretation of product yields, both phenol and phenolate have to be taken into consideration. From the pK_a value of phenol and the rate constant of ozone with phenol and phenolate a “reactivity pK ” was calculated (*cf.* Figure 22 on page 63). This reveals that at $\text{pH} \leq 3$, ozone react primarily with phenol and at $\text{pH} \geq 5$ with the phenolate. Hydroquinone, catechol, 1,4-benzoquinone and *cis,cis*-muconic acid were detected as the major products. At $\text{pH} 3$, the yield of *cis,cis*-muconic acid is higher (4.8%) than at $\text{pH} 7$ (2.8%) and $\text{pH} 10$ (1%), while $\text{O}_2(^1\Delta_g)$ yields show the opposite trend 0%, 5.6% and 8% at $\text{pH} 3$, 7 and 10, respectively. This indicates that 1,3-dipolar cycloaddition reaction competes with $\text{O}_2(^1\Delta_g)$ release, whereby the later dominates at high pH (*cf.* Schemes 8 and 9 on page 73 and 74).

Due to instability of hydroquinone and catechol at high pH , ozone reactions with these substances were only carried out at $\text{pH} 7$. The product yields given in Table 10 (page 87) for hydroquinone and Table 11 (page 92) for catechol has led to the formulation of the reaction mechanisms for these systems (Scheme 11 on page 89).

9.2.2 Reactions of ozone with halophenols

The reactions of ozone with pentachloro- pentabromo- and triiodophenol were investigated. The yield of $\bullet\text{OH}$ radicals was measured using the 2-methyl-2-propanol system as 22%, 2% and 0% in the reactions of ozone with pentachloro- pentabromo- and triiodophenol, respectively. This led to the suggestion that electron transfer only plays a major role in the reaction of ozone with pentachlorophenol and most likely does not occur in the reaction of ozone with triiodophenol. The yields of halide ions released in these reactions were determined and together with the yield of $\text{O}_2(^1\Delta_g)$, the mechanism in Scheme 12 (page 97) is proposed. In the reaction of ozone with pentachlorophenol, *ortho*-

and *para*-chloranil are formed. These compounds hydrolyse in water and even faster in basic media, releasing Cl^- , thereby giving a yield of 2.5 mol of Cl^- per 1 mol of ozone.

9.2.3 Reactions of ozone with methoxybenzenes

Products study in the reaction of ozone with 1,2-dimethoxybenzene, 1,4-dimethoxybenzene and 1,3,5-trimethoxybenzene has allowed us to gain insight into the reactions of ozone with these compounds. Relatively high H_2O_2 yields were measured in the reactions of ozone with 1,2-dimethoxybenzene (27%) and 1,4-dimethoxybenzene (56%) while only 13% and 6.5 % were detected with 1,3,5-dimethoxybenzene at pH 2 and 7, respectively. Ring opening products dimethyl(2*Z*,4*Z*)-hexa-2,4-diendioate **50**, methyl(2*Z*,4*E*)-4-methoxy-6-oxo-hexa-2,4-dienoate **51** were identified and quantified in the reactions of ozone with 1,2-dimethoxybenzene, 1,4-dimethoxybenzene and 1,3,5-trimethoxybenzene, respectively. The yield of **50** (25%) and **51** (52%) are in good agreement with that of H_2O_2 given above, indicating that these products are formed via the 1,3-dipolar cycloaddition reaction (Criegee mechanism) 52%. No ring opening products were identified in the reaction of ozone with 1,3,5-trimethoxybenzene. 2,6-dimethoxy-1,4-benzoquinone **54**, was identified and its yield quantified as 20%. Therefore, it is postulated that **54** is formed as a result of water-catalysed reaction, in which H_2O_2 is formed.

The yields of $\text{O}_2(^1\Delta_g)$ for 1,2-dimethoxybenzene (9%) and 1,4-dimethoxybenzene (6%) are lower than that 1,3,5-trimethoxybenzene (30%), indicating that O-atom transfer occurs only to a less extent in dimethoxybenzenes. This is due to the fact that in the reaction of ozone with 1,3,5-trimethoxybenzene the carbocation in the ozone/1,3,5-trimethoxybenzene zwitterion is strongly stabilised by the three methoxy substituents preventing the 1,3-dipolar cycloaddition to take place thus favouring the elimination of $\text{O}_2(^1\Delta_g)$ while in the case of 1,2-dimethoxybenzene and 1,4-dimethoxybenzene the 1,3-dipolar cycloaddition is favoured. In the reaction of ozone with 1,4-dimethoxybenzene, the corresponding product was identified as 1,4-benzoquinone and its yield measured as 8%.

9.3 Implication of the findings

The experimental results elucidate several important concepts regarding ozone reaction products with phenolic compounds. Before a phenolic compound is fully decomposed, various primary products are formed. In this work, it is shown that some of such primary

products are even more reactive toward ozone than the substrate itself and may compete with the substrate for ozone already at moderate product/substrate ratio.

Although it is generally believed that ozonation products are more polar and more biodegradable than their precursor, our data showed that this is not always correct. The formation of less polar phenol dimers was detected in the ozonolysis of phenol. In the reaction of ozone with phenol, the yields of 1,2-dihydroxybiphenyl and 1,4-dihydroxybiphenyl were determined as ~1% each. It is also important to note that destruction of the phenol, hydroquinone and catechol is only ~50% of the ozone consumed. This implies that the destruction of 1 mol of any of the above mentioned compounds needs more than 2 mol of ozone, and their full mineralisation requires even more ozone.

For the application of ozone in water treatment, it is interesting to note that a high yield of $\bullet\text{OH}$ radicals is formed in the reaction of ozone with phenolic compounds. $\bullet\text{OH}$ radicals are more reactive and non-selective as compared to ozone and are capable of reacting with ozone-refractory compounds. For this reason, many researchers have been advocating the use of advanced oxidation processes (AOP) (where $\bullet\text{OH}$ radicals are produced) in drinking water treatment. We have also observed that hydrogen peroxide is formed in the reaction of ozone with phenolic compounds. If this hydrogen peroxide formed is allowed to react with ozone, *e.g.* by using an excess of ozone in the water treatment plant, $\bullet\text{OH}$ can also be produced in this way. If conditions suitable for the use of H_2O_2 which is a by-product in the reaction of ozone with phenolic compounds, as a source of $\bullet\text{OH}$ radical are achieved, it will have some implications in water treatment especially for the destruction of dissolved substances which do not react with ozone.

10 REFERENCES

- (1) Schönbein, C. F., *C. R. Hebd. Seances Acad. Sci.*, **1840**, 10, 706.
- (2) Floriano, W. B., Blaszkowski, S. R. and Nascimento, M. A. C., *J. Mol. Struct. (Theochem.)*, **1995**, 335.
- (3) Bailey, P. S., *Ozonation in organic chemistry.*; Academic Press: New York, 1978.
- (4) Hoffman, U., Rudorff, W. *Anorganische Chemie*; Vieweg: Braunschweig, 1973.
- (5) Ardon, M., *Oxygen*; Benjamin, W.A, Inc.: New York, 1965.
- (6) Forni, L., Bahnemann, D. and Hart, E. J., *J. Phys. Chem.*, **1982**, 86, 255.
- (7) Hart, E. J., Sehested, K. and Holcman, J., *Anal. Chem.*, **1983**, 55, 46.
- (8) Staehelin, J. and Hoigné, J., *Environ. Sci. Technol.*, **1985**, 19, 1206.
- (9) Staehelin, J. and Hoigné, J., *Vom Wasser*, **1983**, 61, 337.
- (10) Staehelin, J. and Hoigné, J., *Environ. Sci. Technol.*, **1982**, 16, 676.
- (11) Staehelin, J., Bühler, R. E. and Hoigné, J., *J. Phys. Chem.*, **1984**, 88, 5999.
- (12) Kanofsky, J. R. and Sima, P., *J. Biol. Chem.*, **1991**, 266, 9039.
- (13) Maggiolo, A. and Niegowski, S. J., *Adv. Chem. Ser.*, **1959**, 21, 202.
- (14) Muñoz, F. and von Sonntag, C., *J. Chem. Soc., Perkin Trans. 2*, **2000**, 2029.
- (15) Wardman, P., *J. Phys. Chem. Ref. Data*, **1989**, 18, 1637.
- (16) Schank, K., Beck, H., Buschlinger, M., Eder, J., Heisel, T., Pistprious, S. and Wagner, C., *Helv. Chim. Acta*, **2000**, 83, 801.
- (17) Kläning, U. K., Sehested, K. and Holcman, J., *J. Phys. Chem.*, **1985**, 89, 760.
- (18) Dowideit, P., von Sonntag, C. and Leitzke, O., *gmf Wasser-Abwasser*, **1996**, 137, 268.

- (19) Bailey, P. S. and Lane, A. G., *J. Am. Chem. Soc.*, **1967**, *89*, 4473.
- (20) Bailey, P. S., Carter Jr, T. P., Nieh, E., Fischer, C. M. and Khashab, A. Y., *J. Am. Chem. Soc.*, **1974**, *96*, 6136.
- (21) Huie, R. E. and Herron, J. T., *Int. J. Chem. Kinet.*, **1974**, *7*, 165.
- (22) Williamson, D. G. and Cvetanovic, R. J., *J. Am. Chem. Soc.*, **1968**, *90*, 3668.
- (23) Williamson, D. G. and Cvetanovic, R. J., *J. Am. Chem. Soc.*, **1968**, *90*, 4248.
- (24) Dowideit, P. and von Sonntag, C., *Environ. Sci. Technol.*, **1998**, *32*, 1112.
- (25) Criegee, R., *Angew. Chem.*, **1975**, *87*, 765.
- (26) Sander, W., *Angew. Chem.*, **1990**, *102*, 372.
- (27) Anglada, J. M., Crehuet, R. and Bofill, J. P., *Chem. Eur. J.*, **1999**, *5*, 1809.
- (28) Gillies, J. Z., Suenram, R. D. and Lovas, F. J., *J. Am. Chem. Soc.*, **1988**, *110*, 7991.
- (29) Bunnelle, W. H., *Chem. Rev.*, **1991**, *91*, 335.
- (30) Wadt, W. R. and Goddard, I. W. A., *J. Am. Chem. Soc.*, **1975**, *97*, 3004.
- (31) Bailey, P. S., *Ozonation in Organic Chemistry*; Academic Press: New York, 1982.
- (32) Bailey, P. S., *Ozone in water and wastewater treatment*; Ann Arbor Science, Ann Arbor: Michigan, 1972; pp 29-59.
- (33) Hoigné, J. and Bader, H., *Wat. Res.*, **1983**, *17*, 173.
- (34) Gurol, M. D. and Nekoulaini, S., *Ind. Chem. Eng. Fundam.*, **1994**, *23*, 54.
- (35) Beltran, F. J., Kolaczowski, S. T., Crittenden, B. D. and Rivas, F. J., *Trans. IChemE.*, **1993**, *71*, 57.
- (36) Benitez, J. F., Heredia-Beltran, J., Acero, J. L. and Rubio, F. J., *J. Harz. Materials*, **2000**, *B79*, 271.

- (37) Boncz, M. A., Bruning, H., Rulkens, W. H., Sudhölter, E. J. R., Harmsen, G. H. and Bijsterbosch, J. W., *Wat. Sci. Technol.*, **1997**, *35*, 65.
- (38) Davis, R. A., Rinker, R. G. and Sandall, O. C., *J. Harz. Materials*, **1995**, *41*, 65.
- (39) Kuo, C. H. and Huango, C. H., *J. Harz. Materials*, **1995**, *41*, 31.
- (40) Weavers, L. K., Malmstadt, N. and Hoffmann, M. R., *Environ. Sci. Technol.*, **2000**, *34*, 1280.
- (41) Gurol, M. D. and Vatistas, R., *Wat. Res.*, **1987**, *21*, 895.
- (42) Yamamoto, Y., Niki, E., Shiokawa, H. and Kamiya, Y., *J. Org. Chem.*, **1979**, *44*, 2142
- (43) Duguet, J.-P., Dessert, B., Mallevalle, J. and Flessinger, F., *Wat. Sci. Technol.*, **1987**, *19*, 919.
- (44) Duguet, J.-P. and Mallevalle, J., *Symposium on Drinking Water Treatment*, **1987**.
- (45) Fang, W.-H., *J. Chem. Phys.*, **2000**, *112*, 1204.
- (46) Gadosy, T. A., Shukla, D. and Johnston, L. J., *J. Phys. Chem. A*, **1999**, *103*, 8834.
- (47) Gurol, M. D. and Singer, P. C., *Wat. Res.*, **1983**, *17*, 1173.
- (48) Konstantinova, M. L., Razumvskii, S. D. and Zaikov, G. E., *Bull. Acad. Sci USSR, Div. Chem. Sci.*, **1991**, 266.
- (49) Konstantinova, M. L., Razumvskii, S. D. and Zaikov, G. E., *Bull. Acad. Sci USSR, Div. Chem. Sci.*, **1991**, 271.
- (50) Ku, Y., In, R.-J. and Shen, Y.-S., *Toxicol. Environ. Chem.*, **1997**, *64*, 183.
- (51) Lesczynska, D., *Environ. Protect. Eng.*, **1982**, *8*, 105.
- (52) Lundqvist, M. J. and Eriksson, L. A., *J. Phys. Chem. B*, **2000**, *104*, 848.
- (53) Mvula, E., Schuchmann, M. N. and von Sonntag, C., *J. Chem. Soc., Perkin Trans. 2*, **2001**, 264.

- (54) Roder, M., Wojnarovits, L., Földiák, G., Emmi, S. S., Beggiato, G. and Angelantonio, M. D., *Radiat. Phys. Chem.*, **1999**, *54*, 475.
- (55) Singer, P. C. and Gurol, M. D., *Wasser '81*, **1981**, 540.
- (56) Takahashi, N. and Katsuki, O., *Nippon Kagaku Kiashi*, **1987**, 862.
- (57) Verweij, H., Christianse, K. and van Steveninck, J., *Chemosphere*, **1982**, *11*, 721.
- (58) Whitlock, L. R., Siggia, S. and Smala, J. E., *Anal. Chem.*, **1972**, *44*, 532.
- (59) Konstantinova, M. L., Razumovskii, S. D. and Zaikov, G. E., *Bull. Acad. Sci USSR, Div. Chem. Sci.*, **1991**, 266.
- (60) Bailey, P. S., Carter Jr, T. P. and Southwick, L. M., *J. Org. Chem.*, **1972**, *37*, 2997.
- (61) Bailey, P. S. and Keller, J. E., *J. Org. Chem.*, **1968**, 2680.
- (62) Bailey, P. S., Keller, J. E. and Carter Jr, T. P., *J. Org. Chem.*, **1970**, *35*, 2777.
- (63) Bailey, P. S., Lerdal, D. A. and Carter Jr, T. P., *J. Org. Chem.*, **1978**, *43*, 2662.
- (64) Bailey, P. S., Southwick, L. M. and Carter Jr, T. P., *J. Org. Chem.*, **1978**, *43*, 2657.
- (65) Muñoz, F. *Reaktion von Ozon mit EDTA und einigen weiteren Stickstoffverbindungen in wässriger Lösung: Kinetik und Produkte*, 1999. Doctoral Dissertation, Ruhr Universität Bochum.
- (66) Armstrong, D. In *M-Centered Radicals*; Alfassi, Z.B., Ed.; Wiley: Chichester, 1998; pp 685-710.
- (67) Solision, C., Del Bolgi, A. and De Faveri, D. M., *Chem. Biochem. Eng. Q*, **1999**, *16*, 59.
- (68) Overbeck, P. K., *Proc. -Annu. Conf. , Am. Water Works Assoc.*, **1995**, 241.
- (69) Hoigné, J. and Bader, H., *Wat. Res.*, **1983**, *17*, 185.
- (70) Sunkel, J. and Staude, H., *Ber. Bunsenges. Phys. Chem.*, **1968**, *72*, 567.
- (71) Muñoz, F. and von Sonntag, C., *J. Chem. Soc., Perkin Trans. 2*, **2000**, 661.

- (72) Hoigné, J., Bader, H., Haag, W. R. and Staehelin, J., *Wat. Res.*, **1985**, *19*, 993.
- (73) Fricke, H. and Hart, E. J., *J. Chem. Phys.*, **1935**, *3*, 60.
- (74) von Sonntag, C. and Schuchmann, H.-P., *Methods Enzymol.*, **1994**, *233*, 3
- (75) Schuler, R. H., Patterson, L. K. and Janata, E., *J. Phys. Chem.*, **1980**, *84*, 2088
- (76) Allen, a. O., Hochanadel, C. J., Ghormley, J. A. and Davis, T. W., *J. Phys. Chem.*, **1952**, *56*, 1638.
- (77) Nash, T., *Biochem. J.*, **1953**, *55*, 416.
- (78) kakac, B., Vejdelek, Z. D. *Handbuch der photometrischen Analyse, Band1*; Verlag Chemie: Weinheim, 1974.
- (79) Lipari, F. and Swarin, S. L., *J. Chromatogr.*, **1982**, *247*, 297.
- (80) Buxton, G. V., Greenstock, C. L., Halman, W. P. and Ross, A. B., *J. Phys. Chem. Ref. Data*, **1988**, *17*, 513.
- (81) Schuchmann, M. N. and von Sonntag, C., *J. Phys. Chem.*, **1979**, *83*, 780.
- (82) Veltwisch, D., Janata, E. and Asmus, K.-D., *J. Chem. Soc., Perkin Trans. 2*, **1980**, *2*, 146.
- (83) Flyunt, R., Makogon, O., Schuchmann, M. N., Asmus, K.-D. and von Sonntag, C., *J. Chem. Soc., Perkin Trans. 2*, **2001**, 787.
- (84) Muñoz, F., Mvula, E., Braslavsky, S. E. and von Sonntag, C., *J. Chem. Soc., Perkin Trans. 2*, **2001**, 1109.
- (85) Asmus, K.-D., Henglein, A., Ebert, M. and Keene, J. P., *Ber. Bunsenges. Phys. Chem.*, **1964**, *68*, 657.
- (86) Kasha, M.; Brabham, D.E. In *Singlet Oxygen*; Wasserman, H.H., Murray, R.W., Eds.; Academic Press: New York, 1979; pp 1.
- (87) Higuchi, T., Satake, C. and Hirobe, M., *J. Am. Chem. Soc.*, **1995**, *117*, 8879.

- (88) Egorov, S. Y. and Krasnovsky, A. A. J., *Biophysics*, **1983**, 28, 532.
- (89) Losev, A. P., Byteva, I. M. and Gurinovich, G. P., *Chem. Phys. Lett.*, **1988**, 143, 127.
- (90) Merkel, P. B. and Kearns, D. R., *J. Am. Chem. Soc.*, **1972**, 94, 7244.
- (91) Monroe, B. M., *J. Phys. Chem.*, **1977**, 81, 1861.
- (92) Murray, R. W., Lumma, W. C. Jr. and Lin, J. W. P., *J. Am. Chem. Soc.*, **1970**, 92, 3205.
- (93) Schmidt, R. and Afshari, E., *J. Phys. Chem.*, **1990**, 94, 4377.
- (94) Wilkinson, F., Helman, W. P. and Ross, A. B., *J. Phys. Chem. Ref. Data*, **1995**, 24, 663.
- (95) Foote, C. S., *Acc. Chem. Res.*, **1968**, 1, 104.
- (96) Afshari, E. and Schmidt, R., *Chem. Phys. Lett.*, **1991**, 184, 128.
- (97) Atkinson, R. and Carter, W. P. L., *Chem. Rev.*, **1984**, 84, 437.
- (98) Fang, X., Schuchmann, H.-P. and von Sonntag, C., *J. Chem. Soc., Perkin Trans. 2*, **2000**, 1391.
- (99) Haag, W. R. and Hoigné, J., *Environ. Sci. Technol.*, **1983**, 17, 261.
- (100) Haag, W. R., Hoigné, J. and Bader, H., *Vom Wasser*, **1982**, 59, 238.
- (101) von Gunten, U. and Hoigné, J., *Environ. Sci. Technol.*, **1994**, 28, 1234.
- (102) von Gunten, U. and Hoigné, J., *J. Water STR-Aqua*, **1992**, 41, 209.
- (103) Liu, Q., Schurter, L. M., Muller, C. E., Aloiso, S., Francisco, J. S. and Margerum, D. W., *Inorg. Chem.*, **2001**, 40, 4436.
- (104) Byers, D. H. and Saltzman, B. E., *Adv. Chem. Ser.*, **1959**, 21, 93.
- (105) Parry, E. D. and Hern, D. H., *Environ. Sci. Technol.*, **1973**, 7, 65.
- (106) Schmitz, L. R., *Environ. Sci. Technol.*, **1973**, 7, 647.

Error! Use the Home tab to apply Überschrift 1 to the text that you want to appear here.

Error! Use the Home tab to apply Überschrift 1 to the text that you want to appear here.

- (107) Pryor, W. A., Gialmalva, D. H. and Church, D. F., *J. Am. Chem. Soc.*, **1984**, *106*, 7094.
- (108) Mudd, J. B., Leavitt, R., Ongun, A. and McManus, T. T., *Atmos. Environ.*, **1969**, *3*, 669.
- (109) Neta, P., Huie, R. E. and Ross, A. B., *J. Phys. Chem. Ref. Data*, **1988**, *17*, 1027.
- (110) Bielski, B. H. J., Cabelli, D. E. and Arudi, R. L., *J. Phys. Chem. Ref. Data*, **1995**, *14*, 1041.
- (111) Sehested, K., Holcman, J., Bjergbakke, E. and Hart, E. J., *J. Phys. Chem.*, **1987**, *88*, 4144.
- (112) Bielski, B. H. J., Cabelli, D. E., Arudi, R. L. and Ross, A. B., *J. Phys. Chem. Ref. Data*, **1985**, *14*, 1041.
- (113) Henglein, A., Langhoff, J. and Schmidt, G., *J. Phys. Chem.*, **1959**, *63*.
- (114) Greenstock, C. L. and Ruddock, G. W., *Int. J. Radiat. Phys. Chem*, **1976**, *8*, 367.
- (115) Greenstock, C. L., Ross, A. B. and Helman, W. P., *Radiat. Phys. Chem.*, **1981**, *17*, 247.
- (116) Asmus, K.-D., Möckel, H. and Henglein, A., *J. Phys. Chem.*, **1973**, *77*, 1218.
- (117) Erben-Russ, M., Bors, W. and Saran, M., *Int. J. Radiat. Biol.*, **1987**, *1987*, 393.
- (118) von Sonntag, C.; Schuchmann, H.-P. In *Peroxyl Radicals*; Alfassi, Z.B., Ed.; Wiley: Chichester, 1997; pp 173-234.
- (119) Neta, P., Huie, R. E. and Ross, A. B., *J. Phys. Chem. Ref. Data*, **1990**, *19*, 413.
- (120) Bothe, E., Behrens, G. and Schulte-Frohlinde, D., *Z. Naturforsch.*, **1977**, *32b*, 886.
- (121) Zhang, X.-M. and Zhum, Q., *J. Org. Chem.*, **1997**, *62*, 5934.
- (122) Pan, X.-M., Schuchmann, M. N. and von Sonntag, C., *J. Chem. Soc., Perkin Trans. 2*, **1993**, 289.

- (123) Raghavan, N. V. and Steenken, S., *J. Am. Chem. Soc.*, **1980**, *102*, 3495.
- (124) Jonsson, M., Lind, J., Reitberger, T., Eriksen, T. E. and Merenyi, G., *J. Phys. Chem.*, **1993**, *97*, 11278.
- (125) Tripathi, G. N. R., *J. Am. Chem. Soc.*, **1998**, *120*, 4161.
- (126) Steenken, S. and Jovanovic, S. V., *J. Am. Chem. Soc.*, **1997**, *119*, 617.
- (127) Flyunt, R., Leitzke, A., Mvula, E., Reisz, E., Schick, R. and von Sonntag, C., *unpublished results*, **2001**.
- (128) Ragnar, M., Eriksson, T., Reitberger, T. and Brandt, P., *Z. Holzforschung*, **1999**, *53*, 423.
- (129) Ragnar, M., Eriksson, T. and Reitberger, T., *Holzforschung*, **1999**, *53*, 285.
- (130) Ragnar, M., Eriksson, T. and Reitberger, T., *Holzforschung*, **1999**, *53*, 292.
- (131) Barb, W. G., Baxendale, J. H., George, P. and Hargrave, K. R., *J. Chem. Soc., Faraday Trans.*, **1951**, *47*, 462.
- (132) Phulkar, S., Rao, B. S. M., Schuchmann, H.-P. and von Sonntag, C., *Z. Naturforsch.*, **1990**, *45b*, 1425.
- (133) Schuchmann, H.-P. and von Sonntag, C., *J. Photochem.*, **1981**, *16*, 289.
- (134) Ulanski, P., Merenyi, G., Lind, J., Wagner, R. and von Sonntag, C., *J. Chem. Soc., Perkin Trans. 2*, **1999**, 673.
- (135) Brazdil, L. C., Fitch, J. L., Cutler, C. L., Haynik, D. M. and Ace, E. R., *J. Chem. Soc., Perkin Trans. 2*, **1998**, 936.
- (136) Skokov, S. and Wheeler, R. A., *J. Phys. Chem. A*, **1999**, *103*, 4261.
- (137) Morley, J. O. and Roberts, D. W., *J. Org. Chem.*, **1997**, *62*, 7358.
- (138) Koller, J. and Plesnicar, B., *J. Am. Chem. Soc.*, **1996**, *118*, 2470.
- (139) O'Neil, P. and Steenken, S., *Ber. Bunsenges. Phys. Chem.*, **1977**, *81*, 550.

- (140) Khursan, S. L., Teregolova, Y. C., Zimin, Y. C., Faizova, E. I. and Gerchikov, A. Y., *Khim. Fiz.*, **1995**, *14*, 41.
- (141) Anbar, M., Meyerstein, D. and Neta, P., *J. Chem. Soc., Perkin Trans. 2*, **1966**, 742.
- (142) Land, E. J. and Ebert, M., *Trans. Faraday Soc.*, **1967**, *63*, 1181.
- (143) Land, E. J., Porter, G. and Shrachan, E., *Trans. Faraday Soc.*, **1961**, *57*, 1885.
- (144) Pan, X.-M. and von Sonntag, C., *Z. Naturforsch.*, **1990**, *45b*, 1337.
- (145) Fang, X., Pan, X., Rhmann, A., Schuchmann, H.-P. and von Sonntag, C., *Chem. Eur. J.*, **1995**, *1*, 423.
- (146) Kurien, K. C. and Robins, P. A., *J. Chem. Soc. (B)*, **1970**, 855.
- (147) Sarr, D. H., Kazunga, C., Charles, M. J., Pavlovich, J. G. and Aitken, M. D., *Environ. Sci. Technol.*, **1995**, *29*, 2735.
- (148) Bühler, R. E., Staehelin, J. and Hoigné, J., *J. Phys. Chem.*, **1984**, *88*, 2560.

11 APPENDICES

Appendix A Compilation of rate constants (in units of $\text{dm}^3 \text{mol}^{-1} \text{s}^{-1}$) of ozone reactions determined in the present study and related values taken from the literature

Substrate	pH	Rate constant	Reference
Phenol	3	1.3×10^3	ref. ⁶⁹
Phenolate	10	1.4×10^9	ref. ⁶⁹
Catechol	3	3.1×10^5	ref. ³⁴
	3	5.2×10^5	this work
Hydroquinone	3	1.5×10^6	ref. ³⁴
	3	1.7×10^6	this work
	7	2.3×10^6	this work
1,4-Benzoquinone	7	2.5×10^3	this work
$\text{C}(\text{NO}_2)_4$		10	this work
$\text{C}(\text{NO}_2)_3^-$		1.4×10^4	this work
H_2O^-	5-6	5.5×10^6	ref. ¹⁰
OH^-		70	ref. ¹⁰
Superoxide radical ($\text{O}_2^{\bullet-}$)		1.6×10^9	ref. ¹⁴⁸
$\bullet\text{OH}$		1×10^8	ref. ¹¹¹
1,4-Dimethoxybenzene	7	1.3×10^5	ref. ⁷¹
1,3,5-Trimethoxybenzene	7	9.5×10^5	ref. ⁷¹
Pentachlorophenolate	10	1.2×10^6	this work
Pentabromophenolate	10	1.7×10^6	this work
1,3,5-Triiodophenolate	10	6.8×10^6	this work
2,3-Dihydroxydithiane	7	2.1×10^5	this work

Error! Use the Home tab to apply Überschrift 1 to the text that you want to appear here.

Error! Use the Home tab to apply Überschrift 1 to the text that you want to appear here.

Appendix A continued

1,4-Dithiothreitol	7	1.7×10^5	this work
Methionine		4×10^6	ref. ¹⁰⁷
2-Methyl-2-propanol		1×10^{-3}	ref. ⁶³
DMSO		8.2	ref. ¹⁰⁷
Methanesulfinate ion		2×10^6	ref.
3-buten-1-ol		7.9×10^4	ref. ⁷¹

Appendix B Compilation of rate constants (in units of $\text{dm}^3 \text{mol}^{-1} \text{s}^{-1}$) of OH radical reactions determined in the present study and related values taken from the literature.

Reaction		K	Reference
Ozone		1×10^8	ref. ¹¹¹
2-Methyl-2-propanol		6×10^8	ref. ⁸⁰
DMSO		7×10^9	ref. ⁸²

Appendix C Miscellaneous compilation of rate constants (in units of $\text{dm}^3 \text{mol}^{-1} \text{s}^{-1}$) determined in the present study and related values taken from the literature.

Reaction	k	Reference
$\text{C}(\text{NO}_2)_4 + \text{OH}^- \rightarrow \text{Products}$	0.27 (20 °C)	this work
	0.4 (25 °C)	ref.
$\text{C}(\text{NO}_2)_4 + \text{O}_2^{\bullet-} \rightarrow \text{Products}$	2×10^9	ref. ⁸⁵
$\text{Fe}^{2+} + \text{H}_2\text{O}_2 \rightarrow \text{Fe}^{3+} + \bullet\text{OH} + \text{OH}^-$	48 (18 °C)	this work
	60 (25 °C)	ref. ¹³¹
$\text{Fe}^{2+} + \text{HOCH}_2\text{OOH} \rightarrow \text{Fe}^{3+} + \text{HOCH}_2\bullet + \text{OH}^-$	39 (18 °C)	this work
$\text{Fe}^{2+} + t\text{-BuOOH} \rightarrow \text{Fe}^{3+} + t\text{-BuO}\bullet + \text{OH}^-$	13 (18 °C)	this work

Appendix C continued

$\text{HC(O)OOH} + (\text{HOEt})_2\text{S} \rightarrow \text{HC(O)OH} + (\text{HOEt})_2\text{SO}$	220	this work
$\text{HC(O)OOH} + \text{HOEtSSEtOH} \rightarrow \text{HC(O)OH} + \text{HOEtS(O)SetOH}$	10	this work
$\text{HC(O)OOH} + 2 \text{Fe(CN)}_6^{4-} \rightarrow \text{HC(O)OH} + 2 \text{Fe(CN)}_6^{3-} + 2 \text{H}^+$	4.3	this work
$\text{HC(O)OOH} + \text{catalase} \rightarrow \text{Products}$	$(1.3 \times 10^{-3})^a$	this work
$\text{H}_2\text{O}_2 + \text{I}^- / \text{molybdate-activated} \rightarrow \text{I}_3^-$	2.1	ref. ²⁴
$\text{H}_2\text{O}_2 + \text{I}^- \rightarrow \text{I}_3^-$	1.8×10^{-3}	this work
$\text{HC(O)OOH} + \text{I}^- / \text{molybdate-activated} \rightarrow \text{I}_3^-$	1.7×10^3	ref. ²⁴
$\text{HC(O)OOH} + \text{I}^- \rightarrow \text{I}_3^-$	1.7×10^3	this work
$\text{HOCH}_2\text{OOH} + \text{I}^- / \text{molybdate-activated} \rightarrow \text{I}_3^-$	2.6×10^{-2}	ref. ²⁴
$\text{CH}_3\text{CH(OH)OOH} + \text{I}^- / \text{molybdate-activated} \rightarrow \text{I}_3^-$	0.39	ref. ²⁴
$(\text{CH}_3)_2\text{C(OH)OOH} + \text{I}^- / \text{molybdate-activated} \rightarrow \text{I}_3^-$	1.5×10^{-4}	ref. ²⁴
2 dihydroxycyclohexadienyl radicals \rightarrow products	2.0×10^8	this work
1,4-dihydroxycyclohexadienyl radicals \rightarrow phenoxy + H_2O	$1.8 \times 10^3 \text{ s}^{-1}$	this work
1,4-dihydroxycyclohexadienyl radicals \rightarrow phenoxy + H_2O / HPO_4^{2-} -catal.	5.8×10^7	this work
1,2-dihydroxycyclohexadienyl radicals \rightarrow phenoxy + H_2O / H^+ -catal.	2.1×10^8	this work
1,4-dihydroxycyclohexadienyl radicals \rightarrow phenoxy + H_2O / H^+ -catal.	1.7×10^9	this work
1,4-dihydroxycyclohexadienyl radicals + $\text{O}_2 \rightarrow$ product.	1.2×10^9	this work

12 LIST OF SCHEMES

Scheme 1 Resonance structures of the ozone molecule.....	1
Scheme 2 The mechanism of ozone reaction with an olefin ²⁴	6
Scheme 3 Bailey's mechanism for the reaction of ozone with phenol. ³¹	9
Scheme 4 Oxidative coupling in the reaction of ozone with phenol. ⁴⁸	10
Scheme 5 Reaction of ozone with amines ref. ⁶⁵	11
Scheme 6 The reaction of 1,3,5-trimethoxybenzene with ozone leading to the formation of O ₂ (¹ Δ _g).....	38
Scheme 7 The Criegee component in the reaction of ozone with 1,2-dimethoxybenzene	62
Scheme 8 Mechanism of the ozonolysis of phenol at pH ≤ 3.	73
Scheme 9 Mechanism of the ozonolysis of deprotonated phenol (phenolate) at pH ≥ 3. .	74
Scheme 10 Mechanism of the reaction of phenol with •OH.	77
Scheme 11 Mechanism of the ozonolysis of hydroquinone.	89
Scheme 12 Mechanism of the ozonolysis of halophenolate.	97
Scheme 13 Bimolecular decay of the halophenoxy radical.	98
Scheme 14 Schematic representation of typical functional groups of the lignin polymer showing the presence of methoxybenzene groups.....	99
Scheme 15 Mechanism of the ozonolysis of 1,4-dimethoxybenzene.	106
Scheme 16 Mechanism leading to the formation of 2,6-dimethoxy-1,4-benzoquinone 54 and 2,4,6-trimethoxyphenol 56 in the ozonolysis of 1,3,5-trimethoxybenzene.	107

13 LIST OF TABLES

- Table 1** Rate constants of the ozone reactions with various olefins in aqueous solution (taken from ref.²⁴)7
- Table 2** Names, structures, rate constants of ozone reactions and pK_a -values of the compounds investigated in this work. 13
- Table 3** $O_2(^1\Delta_g)$ yields in O_3 reactions in % of O_3 consumed at different pH and at various substrate/ O_3 ratios (in parentheses). The data are average values of at least five individual determinations (scatter less than $\pm 15\%$). The O_3 concentrations in these experiments were typically $(1-2) \times 10^{-4} \text{ mol dm}^{-3}$35
- Table 4** Formaldehyde yields in ozone reactions in % of ozone consumed at different pH in the presence of 2-methyl-2-propanol. The substrate and 2-methyl-2-propanol concentrations in these experiments were typically $1 \times 10^{-3} \text{ mol dm}^{-3}$ and 0.1 mol dm^{-3} respectively.48
- Table 5** Methanesulfinic and methanesulfonic acid yields in ozone reactions in % of ozone consumed at different pH in the presence of DMSO. The substrate and DMSO concentrations in these experiments were typically $1 \times 10^{-3} \text{ mol dm}^{-3}$ and $5 \times 10^{-2} \text{ mol dm}^{-3}$ respectively.....50
- Table 6** Yields of $\bullet OH$ in the reactions of ozone with a number of ozone-reactive substrates and the reduction potential of the substrates at pH 7.52
- Table 7** Nitroform anion yields in ozone reactions in % of ozone consumed at different pH in the presence of TNM. The substrate and TNM concentrations in these experiments were typically both $1 \times 10^{-3} \text{ mol dm}^{-3}$54
- Table 8** Hydrogen peroxide yields in ozone reactions in % of ozone consumed at natural pH. The substrate concentrations in these experiments were typically $1 \times 10^{-3} \text{ mol dm}^{-3}$62
- Table 9** Ozonolysis of phenol ($3 \times 10^{-3} \text{ mol dm}^{-3}$). Products and their yields in % of ozone consumed. When two values are given, a second run at four different ozone concentrations was carried out. 2-Methyl-2-propanol (*t*-BuOH), DMSO and TNM concentrations in these experiments were typically 0.1 mol dm^{-3} , $5 \times 10^{-2} \text{ mol dm}^{-3}$ and $1 \times 10^{-3} \text{ mol dm}^{-3}$, respectively.67
- Table 10** Ozonolysis of hydroquinone ($3 \times 10^{-3} \text{ mol dm}^{-3}$). Products and their yields in % of ozone consumed. 2-Methyl-2-propanol (*t*-BuOH), and DMSO concentrations in these experiments were typically 0.1 mol dm^{-3} and $5 \times 10^{-2} \text{ mol dm}^{-3}$, respectively. ...87

Error! Use the Home tab to apply Überschrift 1 to the text that you want to appear here.

Error! Use the Home tab to apply Überschrift 1 to the text that you want to appear here.

Table 11 Ozonolysis of catechol ($3 \times 10^{-3} \text{ mol dm}^{-3}$). Products and their yields in % of ozone consumed. 2-Methyl-2-propanol (*t*-BuOH) and DMSO concentrations in these experiments were typically 0.1 mol dm^{-3} and $5 \times 10^{-2} \text{ mol dm}^{-3}$, respectively. **92**

Table 12 Rate constants of ozone reactions with dissociated chlorophenols (chlorophenolates) **95**

Table 13 Ozonolysis of 1,2-dimethoxybenzene. Products and their yields in % of ozone consumed. 2-Methyl-2-propanol (*t*-BuOH) and TNM concentrations in these experiments were typically 0.1 mol dm^{-3} and $1 \times 10^{-3} \text{ mol dm}^{-3}$, respectively. **100**

Table 14 Ozonolysis of 1,4-dimethoxybenzene. Products and their yields in % of ozone consumed. 2-Methyl-2-propanol (*t*-BuOH) and TNM concentrations in these experiments were typically 0.1 mol dm^{-3} and $1 \times 10^{-3} \text{ mol dm}^{-3}$, respectively. **101**

Table 15 Ozonolysis of 1,3,5-Dimethoxybenzene. Products and their yields in % of ozone consumed. 2-Methyl-2-propanol (*t*-BuOH) and TNM concentrations in these experiments were typically 0.1 mol dm^{-3} and $1 \times 10^{-3} \text{ mol dm}^{-3}$, respectively. **103**

14 LIST OF FIGURES

Figure 1 A plot of the Hammett-substituent-constants <i>vs.</i> $\log k_i/k_o$ for various aromatic compounds according to ref ³³	8
Figure 2 Schematic diagram of the post-column derivatisation instrument.....	19
Figure 3 Schematic representation of the $O_2(^1\Delta_g)$ detection system.....	22
Figure 4 Schematic representation of the BIOLOGIC SFM3 stopped-flow apparatus. ...	23
Figure 5 Mass spectrum of (2Z,4Z)-hexa-2,4-dienedioic acid.	25
Figure 6 Mass spectrum of 4,4'-bis(trimethylsilyloxy)biphenyl.....	26
Figure 7 Mass spectrum of 2,4'-bis(trimethylsilyloxy)biphenyl.	26
Figure 8 Mass spectrum of methyl(2Z,4E)-4-methoxy-6-oxo-hexa-2,4-dienoate.	28
Figure 9 The mass spectrum of 2,6-dimethoxy- <i>p</i> -benzoquinone.	30
Figure 10 The electron configuration of the O_2 molecule.....	31
Figure 11 Electronic configuration and energy scheme of three states of dioxygen.	32
Figure 12 Reaction of ozone with methionine at pH 3. Consumption of methionine and formation of its sulfoxide as a function of the ozone concentration.....	40
Figure 13 Plot of the competition of 3-buten-1-ol with 2,3-dihydroxydithiane at pH 7 for the reactions of ozone. Formaldehyde yields result from the reaction of ozone with 3-buten-1-ol.....	41
Figure 14 Plot of the competition of 3-buten-1-ol with bis(dihydroxyethyl)sulfide at pH 7 for the reactions of ozone. Formaldehyde yields result from the reaction of ozone with 3-buten-1-ol.	42
Figure 15 Variation of $\log k(O_3 + H_2S)$ with pH. <u>Inset:</u> The pK curve of H_2S , fraction of HS^- in aqueous solution (ν) and the “reactivity pK” curve, the fraction of HS^- reaction with ozone (μ).	43

Error! Use the Home tab to apply Überschrift 1 to the text that you want to appear here.

Error! Use the Home tab to apply Überschrift 1 to the text that you want to appear here.

Figure 16 Formation of formaldehyde in the reaction of ozone with H_2O_2 (5×10^{-4} mol dm^{-3}) in the presence of 2-methyl-2-propanol (1×10^{-2} mol dm^{-3}). Formaldehyde yield determined by the 2,4-dinitrophenylhydrazone method. Inset: Formaldehyde yields determined by the Hantzsch method; determination of the ozone concentration before (o) and after (σ) preparing the samples.....48

Figure 17 Ozonolysis of phenol in the presence of TNM, yields of nitroform anion at pH 3 (λ) and pH 4 (μ).....55

Figure 18 Rate of reaction of Fe^{2+} in 0.1 mol dm^{-3} H_2SO_4 with H_2O_2 (λ) hydroxymethylhydroperoxide (μ) and tertiary butylhydroperoxide (σ) at 18 °C as a function of the Fe^{2+} concentration. The kinetics of the reaction was followed by stopped-flow.58

Figure 19 Reaction of H_2O_2 (varied between 2×10^{-4} and 2×10^{-3} mol dm^{-3}) with Fe^{2+} (6×10^{-3} mol dm^{-3}) in the presence of 2-propanol at pH 1.5. Formation of Fe^{3+} as a function of the 2-propanol concentration.....60

Figure 20 Formation of Fe^{3+} in the reaction of tertiary butylhydroperoxide with Fe^{2+} (3×10^{-3} mol dm^{-3}) at pH 1.5 as a function of the tertiary butylhydroperoxide concentration in the presence of air (λ) and in deoxygenated solution (μ). 61

Figure 21 Rate of reaction of formic peracid with $(\text{HOCH}_2\text{CH}_2)_2\text{S}$ (λ) ($k = 220$ dm^3 mol^{-1} s^{-1}) and $\text{HOCH}_2\text{CH}_2\text{SSCH}_2\text{CH}_2\text{OH}$ (μ) ($k = 10$ dm^3 mol^{-1} s^{-1}) as a function of the sulfide/disulfide concentration. The kinetics were followed by the build-up of conductance due to the formation of formic acid.....63

Figure 22 Variation of $\log k(\text{O}_3 + \text{phenol})$ with pH. Inset: The $\text{p}K$ curve of phenol, fraction of phenolate in aqueous solution (λ) and the “reactivity $\text{p}K$ ” curve, the fraction of phenolate reacting with ozone(o).....64

Figure 23 Ozonolysis of phenol (3×10^{-3} mol dm^{-3}) in aqueous solution at pH 7. Yields of hydroquinone (σ), catechol (Δ), 1,4-benzoquinone (λ) and *cis,cis*-muconic acid (μ) as a function of the ozone concentration.65

Figure 24 Ozonolysis of phenol (2.5×10^{-4} mol dm^{-3}) in aqueous solution. Consumption of phenol as a function of the ozone concentration at pH 3 (σ), 7 (o) and 10 (λ).66

Figure 25 Plot of the competition of 3-buten-1-ol with 1,4-benzoquinone at pH 7 for the reaction of ozone. Formaldehyde yields result from the reaction of ozone with 3-buten-1-ol.....69

Figure 26 Plot of the competition of 3-buten-1-ol with catechol at pH 7 for the reactions of ozone. Formaldehyde yields result from the reaction of ozone with 3-buten-1-ol. 69

Error! Use the Home tab to apply Überschrift 1 to the text that you want to appear here.

Error! Use the Home tab to apply Überschrift 1 to the text that you want to appear here.

Figure 27 Plot of the competition of 3-buten-1-ol with hydroquinone at pH 7 for the reactions of ozone. Inset: Plot of the competition of 3-buten-1-ol with hydroquinone at pH 3 for the reactions of ozone. Formaldehyde yields result from the reaction of ozone with 3-buten-1-ol. **70**

Figure 28 Calculated reduction potentials of phenol (λ) and ozone (o) as a function of pH. **72**

Figure 29 Pulse radiolysis of N₂O-saturated solution of phenol (10⁻³ mol dm³) at pH 6.8. Transient absorption spectra observed 2 μ s (ν), 30 μ s (Δ), and 200 μ s (λ) after the pulse (~4 Gy per pulse). Inset A: k_{obs} of absorbance build-up at 400 nm as function of the HPO₄²⁻ concentration. Inset B: k_{obs} as function of the proton concentration. **78**

Figure 30 Dioxygen concentration dependence of the observed first-order rate constant of absorption decay at 330 nm in the pulse radiolysis of N₂O/O₂ (4:1)-saturated solution of phenol at pH 6.8 (~ 5 Gy/pulse)..... **81**

Figure 31 Proton concentration dependence of the term $G(\text{Product})_o/G(\text{Product}) - 1$ in the γ -radiolysis of N₂O/O₂ (4:1)-saturated solution of phenol, (λ) Product = hydroquinone, (μ), Product = catechol. **83**

Figure 32 Ozonolysis of hydroquinone (3 \times 10⁻³ mol dm⁻³) in aqueous solution at pH 7. Yields of 2-hydroxy-1,4-benzoquinone (o) and 1,4-benzoquinone (λ) as a function of the ozone concentration. **86**

Figure 33 The yield of benzoquinone in the ozonolysis of hydroquinone in aqueous solution (λ), in the presence of 2-methyl-2-propanol (o), and in the presence of DMSO (ν). **87**

Figure 34 The rate constant of the oxidation of 1,2,4-trihydroxybenzene by 1,4-benzoquinone as a function of pH: experimental(o), calculated (\bullet). **91**

Figure 35 Ozonolysis of catechol (3 \times 10⁻³ mol dm⁻³) in aqueous solution at pH 7. Yields of 2-hydroxy-1,4-benzoquinone (μ) and *cis,cis*-muconic acid (ν) as a function of the ozone concentration. **92**

Figure 36 Competition plots for the reactions of ozone with pentachlorophenol (λ), pentabromophenol (μ) and 2,4,6-triidophenol (σ) at pH 10 using 3-buten-1-ol as competitor. Formaldehyde yields result from the reaction of ozone with 3-buten-1-ol. **95**

Figure 37 Ozonolysis of 1,2-dimethoxybenzene. The yield of dimethyl(2Z,4Z)-hexa-2,4-diendioate after hydrolysis to muconic acid as a function of the ozone concentration. **100**

Error! Use the Home tab to apply Überschrift 1 to the text that you want to appear here.

Error! Use the Home tab to apply Überschrift 1 to the text that you want to appear here.

Figure 38 Ozonolysis of 1,4-dimethoxybenzene. The yields of 1,4-benzoquinone (μ), hydroquinone (\circ) and methyl(2*Z*,4*E*)-4-methoxy-6-oxo-hexa-2,4-dienoate (ν) as a function of the ozone concentration.101

Figure 39 Formation and decay of intermediates in the reaction of ozone with 1,3,5-trimethoxybenzene. Inset A-C: kinetics at 260, 290 and 360 nm respectively.⁷¹ 102

Figure 40 Ozonolysis of 1,3,5-trimethoxybenzene. The yield of 2,6-dimethoxy-1,4-benzoquinone as a function of the ozone concentration. 103